PHYSICAL REGULATION OF EPIPHYSEAL CARTILAGE BIOSYNTHESIS: RESPONSES TO ELECTRICAL, MECHANICAL, AND CHEMICAL SIGNALS

by

Martha Lane Gray

B.S., Michigan State University
(1978)

S.M.E.E., Massachusetts Institute of Technology
(1981)

SUBMITTED TO THE HARVARD-MIT DIVISION
OF HEALTH SCIENCES AND TECHNOLOGY
IN PARTIAL FULFILLMENT OF THE
REQUIREMENTS FOR THE DEGREE OF

DOCTOR OF PHILOSOPHY

at the

MASSACHUSETTS INSTITUTE OF TECHNOLOGY

July 1986

Signature of Author _____
Division of Health Sciences and Technology
July, 1986

Certified by _____
Alan J. Grodzinsky
Thesis Supervisor

Certified by _____
Raphael C. Lee
Thesis Supervisor

Accepted by _____
Roger G. Mark
Chairman, Graduate Committee

Certified by _____
William M. Siebert
Thesis Reader

Certified by _____
David A. Swann
Thesis Reader

Certified by _____
Stephen B. Trippel
Thesis Reader

Accepted by _____
Ernest G. Cravalho
Accademic Advisor

PHYSICAL REGULATION OF EPIPHYSEAL CARTILAGE BIOSYNTHESIS: RESPONSES TO ELECTRICAL, MECHANICAL, AND CHEMICAL SIGNALS

Submitted to the Harvard-MIT Division of Health Sciences and Technology in partial fulfillment of the requirements for the degree of Doctor of Philosophy in Medical Engineering.

ABSTRACT

Physiological tissues adapt their structure and composition to functional demands. Since a major function of connective tissues is mechanical support, physical forces are believed to play a significant role in connective tissue growth and development. This thesis focuses on the response of epiphyseal plate chondrocytes to mechanical loading. A basic system theory approach is used as a framework for examining the complex interactions which exist between the applied signal, tissue matrix, cells, and measurable response.

Under physiological loading conditions, many events occur simultaneously within the tissue. These include deformation, streaming currents and potentials, fluid flow, changes in hydrostatic pressure, and physicochemical changes associated with consolidation. Any one or more of these events may act as a modulating signal to the cell. Experimental configurations which decouple these events and which provide a spatially uniform signal were used to probe and characterize the cellular response.

Reserve zone epiphyseal plate cartilage was harvested from newborn calves immediately after slaughter and maintained in organ culture for 2 days. For the next 12 hours tissue was subjected to one of three exposure conditions: (1) sinusoidal currents up to 1 mA/cm^2 at frequencies ranging from 0.1 to 100 Hz, (2) static compressive loads up to 3 MPa, and (3) physicochemical alterations of $[SO_4^{2-}]$ (0.8 mM to 1.6 mM), $[K^+]$ (5.4 mM to 10.4 mM) or pH (5.5 to 7.9). During the exposure period, tissue was bathed in media containing ^{35}S-sulfate and ^{3}H-proline to assess glycosaminoglycan and protein synthesis. In a separate series of experiments the kinetics of the response to mechanical loading was examined for step loading and step unloading.

The applied currents, which were similar to those expected to occur under in vivo loading conditions, did not significantly alter the incorporation of proline and sulfate over the 12 hour period.

Under static loading conditions there was a dose-dependent depression in proline and sulfate incorporation. This depression was strongly dependent on compression for compressions greater than 35%. Proline incorporation was found to decrease under load in less than 1/2 hour, while sulfate incorporation decreases in 2 to 6 hours. The response to unloading following a 12 hour preload was not simply the inverse of the response to loading; proline incorporation exceeded control levels for ~4 hours, while sulfate incorporation remained depressed for over 4 hours.

Because of the high negative fixed charge density of cartilage,

compression leads to increases in interstitial cation concentration (e.g. $[K^+]$, $[H^+]$) and decreases in anion concentration (e.g. $[SO_4^{2-}]$) consistent with Donnan equilibrium. Increasing $[SO_4^{2-}]$ did not alter the incorporation of sulfate under free swelling or loading conditions. When the potassium concentration was increased under unloaded conditions to levels expected to occur at 60% consolidation there was no detectable effect on either sulfate or proline incorporation. In contrast, adjustment of bath pH with bicarbonate led to changes in incorporation consistent with those seen under equivalent loading conditions.

The insensitivity of chondrocytes in organ culture to electric fields (and/or associated fluid flow) suggests that such fields either have a minimal effect on the total biosynthetic behavior of chondrocytes, or result in a very slow response by the chondrocytes. The dose-dependent response to static loads suggests that longitudinal growth rate is modulated, in part, by the time-average load. This response may be accounted for by the decreased interstitial pH which occurs with consolidation. Compression induced changes in $[K^+]$ and $[SO_4^{2-}]$ do not appear to influence the response to compressive loads. The nonlinear response seen when comparing step increases in load to step decreases suggests that the response to dynamic loads may not simply reflect the response to the time-average load.

ACKNOWLEDGEMENTS

To appropriately acknowledge and thank all those who have helped and encouraged me over the years would require a document in itself. This dissertation truly represents the work and ideas of many people; in all honesty, it should not be called mine. I hope that all involved will accept my most sincere thanks.

The members of my committee spent considerable time and effort guiding the research and reading the document. For 7 years Alan Grodzinsky has been my research advisor, patiently encouraging and teaching me, all the while treating me as a colleague rather than as the naive young graduate student that I was. The support and guidance provided by Raphael Lee were instrumental to this project. He helped me to maintain a broad perspective by introducing me to many of the relevant clinical and research issues. David Swann taught me the necessary cell culture and biochemical techniques and was always helpful in analyzing and interpreting the results. Steve Trippel's enthusiasm for the work was a major source of encouragement. He and his co-workers were very helpful in teaching me practical procedures such as harvesting the epiphyseal plate. Bill Siebert has always been very supportive as was demonstrated by his willingness to serve on my committee, despite a very busy schedule.

The success of this project is due in large part to the wonderful people in the Continuum Electromechanics Group. Chapter 6 is dedicated to my dear friend Angelina Pizzanelli, for without her those experiments would not have been possible. In addition, she is responsible for the careful and tedious biochemical analyses. Caroline Wang and Pauline Liu performed most of the electrical experiments. Caroline has been extremely helpful in running control experiments and harvesting the tissue. Lori Tsuruda faithfully hunted down numerous references, patiently calibrated thermistors and load cells, and willingly assisted in preparing samples for counting. I am particularly indebted to Eliot Frank both for his friendship and assistance. In a calm, type B way he revolutionized the production of theses and he provided regular expert consultation on topics ranging from cartilage electrokinetics to circuit design. Linda Bragman was always ready to help out in every way. It would be impossible to list all she has done for me but to name a few: she typed some of these chapters; labeled sample tubes; took data; brought me lunch; and prevented many crises. TOATEOH will be remembered always for the support and friendship and for introducing me to the lore of Continuum Electromechanics. Susan arrived on the scene with a helping hand just as desperation had begun to sink in; no thesis is complete without a figure from Kevin; Laura, Bob and Debbie spent inordinate amounts of time reading and rereading the document. Professor Sol taught me a tremendous amount about cartilage and research and was always ready and willing to listen and offer suggestions. As a colleague and friend, KJ has had a tremendous influence in my life. Working with him was always fun (even though it usually meant getting drenched in the rain) and I am very much looking forward to working together in the coming

years.

Finally, it seems appropriate here to express my appreciation to the faculty and students in HST. Roger Mark convinced me that MIT and MEMP would provide a wonderful and exciting graduate education. As usual, he was right. Ernie Cravalho has been a continuing source of encouragement and friendship. He was instrumental in making MEMP a very special experience in the midst of this institution. The MEMP students comprise a truly remarkable group. The friendship provided by Dave and Linda, Debbie, Jose, and many others deserves my most sincere appreciation.

Table of Contents

List of Figures

List of Tables

Chapter I

MECHANICAL SUPPORT IN PHYSIOLOGIC SYSTEMS

1.1 Overview

Physiological tissues adapt their structure and composition to functional demands by a process referred to as functional adaptation. Since a major function of connective tissues in general and the skeleton in particular is that of mechanical support, it is not surprising that physical forces are believed to play a significant role in connective tissue cell behavior. However, little evidence exists at the clinical or cellular level to quantify this role. Experimental work to date has provided phenomenological evidence that an altered mechanical environment will modify tissue structure or cell behavior in an experimental setting. The first objective of this thesis is to provide a conceptual model with which the relationship between mechanical parameters and tissue cell behavior can be systematically examined. The second objective is to develop an experimental approach based on the conceptual model which can be used to quantitatively study the response of a connective tissue system (specifically the cartilaginous growth plate) to mechanical loading.

The principle of functional adaptation serves as the foundation for this work. Connective tissues subserve a mechanical function and cells are responsible for maintaining a viable functional tissue; therefore, the cells must be capable of modulating their activity in

response to an altered mechanical environment. The proposed conceptual model utilizes a basic system theory approach to direct the study of the interaction between applied mechanical signals and cell behavior. The structure provided by the application of system theory provides a coordinated means for examining the complex interactions which exist between the applied signal, the tissue material, the cells and the measurable response.

This chapter reviews general connective tissue physiology with special emphasis on the means by which mechanical support is achieved in terms of both structural composition and arrangement. The review provides a basis for discussion of how connective tissues might be structurally and compositionally modified in response to altered mechanical loading. Qualitative clinical and experimental evidence demonstrating such modification are provided. Finally, investigations directed at quantifying or characterizing the adaptive response of connective tissues are reviewed.

Chapter 1 provides the general foundation for Chapter 2 which, addressing the fist objective of the thesis, develops the conceptual model. The model serves as a framework for the investigation of cellular responses to mechanical signals, in general, but the development focuses primarily on cartilaginous tissues and, where possible, specifically on epiphyseal plate cartilage. The remaining chapters are devoted to experiments, motivated by the conceptual model, which examine the response of epiphyseal plate cartilage in organ culture to mechanical loading.

1.2 Connective Tissue Constituents

Connective tissues are a class of tissues derived embryologically from mesenchyme with functions ranging from mechanical support to nutrition and cellular immunity. Tissues in this class include cartilage, bone, fascia, dermis, circulating blood cells, fat, and muscle. This discussion focuses on the subclass of connective tissues which function primarily to maintain mechanical homeostasis. Bone provides the support framework in vertebrates; cartilage acts to distribute the load, dampen impact loading and minimize friction between moving joints; the dermis provides the elasticity allowing the skin to accommodate a wide range of motion; tendons translate muscle force without significant deformation maximizing muscle efficiency. Although each of these tissues has a specific role, they are composed of similar biological "ingredients". The variation in distribution and organization of these ingredients is an important indicator of how they function effectively. In this section, the major connective tissue constituents are briefly reviewed, and mechanisms by which they contribute to mechanical homeostasis are highlighted. In the following section the structural organization and its relationship to mechanical properties is described for each of the major tissues.

The constituents comprising any tissue can be separated into three categories: cells, extracellular matrix (ECM), and interstitial fluid. The supporting connective tissues have relatively low cellularity and are high in extracellular matrix. The ability of these tissues to

provide support is a direct function of the extracellular matrix composition and structure. The cells are responsible for maintaining the appropriate ECM environment by directing synthesis and breakdown of the ECM material. Cell/ECM and cell/cell interconnections presumably allow the cell to probe the "status" of its environment. The interstitial fluid provides the pathway for diffusion of nutrients and waste products to and from the cell. In addition, fluid plays an important role in joint lubrication.

1.2.1 Extracellular Matrix

There are two major classes of extracellular matrix constituents[1]: fibrous components (which include the collagens and elastin) and ground substance (composed of proteoglycans or isolated glycosaminoglycans, and glycoproteins). The mechanical properties of each of these components in isolation suggest how the cell uses them to create an appropriate ECM environment.

Collagen is a linear triple helical molecule approximately 300 nm long and 1.5 nm in diameter which associates in a specific way to form fibrils. These fibrils may further aggregate to form the collagen fiber. The fiber form predominates in some tissues (e.g. tendon) while in other tissues only the fibril form is apparent (e.g. cartilage). There exist both inter- and intra- molecular crosslinks which contribute to the

---

[1] There are many reviews of extracellular matrix biochemistry which provide more complete discussions than included here. In particular see Hay [1981a], Piez and Reddi [1984], Comper and Laurent [1978], Grodzinsky [1983].

collagen fiber's substantial tensile strength while retaining flexibility. Investigators have isolated genetically distinct collagens within an organism and have characterized their distribution among tissue types. The functional significance behind the differing types is presumed from the correlation between tissue localization and tissue material properties [Miller, 1984]. (For example, type I collagen predominates in the less extensible tissues such as tendon and bone while type II predominates in tissues such as cartilage which are subjected to compressive forces.) The structure of the fibril makes it very resistant to degradation by nonspecific proteases. Normal turnover of extracellular matrix collagens is difficult to assess but appears to be much slower than other soluble proteins [Gross, 1981]. In the context of functional adaptation, turnover may be rapid, on the order of hours or days [Gross, 1981].

Elastin is a protein polymer similar in physical structure to collagen. Its considerable tensile strength is comparable to that of collagen however it is far more extensible. It is found predominantly in major arterial walls and to some extent in skin.

Proteoglycans (PGs) consist of a protein core with abundant glycosaminoglycan (GAG) sidechains. Glycosaminoglycans are sequences of 20 to 60 repeating disaccharide units formed from two of four monosaccharides (glucuronic acid, iduronic acid, N-acetyl glucosamine, and N-acetyl galactosamine). The GAGs are named according to the predominant disaccharide pair. Chondroitin sulfate, keratan sulfate, dermatan sulfate and hyaluronic acid comprise the GAGs of the supporting

connective tissues. GAGs confer a net negative fixed charge to the tissue because the sulfate and carboxyl groups (each disaccharide unit contains at least one of these groups) are negatively charged at physiologic pH. Electrostatic repulsion between these anionic groups results in a tendency for connective tissues to swell and resist compressive forces. In some tissues the proteoglycans are associated with hyaluronic acid to form a proteoglycan aggregate. There are at least 2 metabolic pools of proteoglycan which appear to be under separate regulation [Heinegard and Paulsson, 1984]. One pool with a turnover rate of 3 days is comprised of smaller PGs than the pool with 2 to 4 month turnover rates. It is unclear which pools contribute to the adaptive response or how the relative kinetics of synthesis and degradation might change under various mechanical loading conditions.

1.2.2 Cells

Residing in the extracellular matrix are the connective tissue cells. The basic functions of a cell are replication, motility, energy conversion, communication, synthesis, export, and import.

The cell membrane is the site of interaction between the external world (ECM and bathing fluids) and the internal (intracellular) world. It thus becomes the site at which many control or mediating factors act. Intramembranous proteins have been shown to be involved in controlling ion fluxes through the membrane and in acting as a receptor for peptide hormones and neurotransmitters.

The interior of the cell contains the apparatus required for synthesis (ribosomes, endoplasmic reticulum and golgi), a system for

energy conversion (mitochondria), templates to direct replication and protein synthesis (nucleus), mechanisms to degrade material taken up from the outside of the cell (lysosomes and peroxisomes), and a cytoskeletal network necessary for maintaining cell shape and organization (microfilaments, microtubules, and intermediate filaments). The cytoskeleton is believed to play an important role in the ECM/cell interaction scheme [Hay, 1981b].

1.2.3 Interconnections

Interconnections between cells and their environment are continually being discovered. Electron microscopic techniques have demonstrated several types of cell-cell junctions, some of which provide direct electrical connection between cells [Alberts et al., 1983]. More recently, investigators [Yamada, 1983; Hook et al., 1984] have discovered connections between the cell and its extracellular matrix which appear to be provided by proteins such as laminin, fibronectin, and chondronectin. In vitro experiments indicate that the ECM can affect the organization of cytoskeletal components [Hay, 1981b]. These findings are particularly relevant as they emphasize the importance of considering both the cells and the matrix in any study of connective tissue physiology.

1.3 Connective Tissue Composition and Organization

Connective tissues rely on the proper content and organization of cells, ECM, and interconnections. By considering a variety of functionally distinct connective tissues, a useful paradigm can be developed to relate form and function. To this end, the structure, composition, and mechanical properties of tendon, skin, cartilage, and bone will be discussed and compared. In each case, the correlation between composition and load bearing function is illustrated.

1.3.1 Tendon

Tendons provide the link between the muscles and their points of action. They are comprised of a highly ordered dense array of parallel collagen fibers, giving tendon a flexible, yet relatively indistensible and strong character. Tendon is sparsely populated by fibroblastic type cells sometimes referred to as tenocytes. In tendon the cells are spindle shaped, oriented parallel to the collagen axis, and may make connections with one another.

While collagen accounts for over 70% of the dry weight of tendon and provides the considerable tensile strength, the proteoglycan content appears to vary directly with the amount of compressive loading experienced by the tendon. Several investigators [Koob et al., 1986, Okuda et al., 1986, Gillard et al., 1979] found that the glycosaminoglycan content was 4 to 7 times greater in regions normally subjected to compressive forces compared to those regions loaded only in tension. Gillard and colleagues [1979] found that when regions of the

rabbit flexor digitorum profundus tendon normally subjected to a compressive load, as around a pulley point, were released and those normally loaded in tension were subjected to a compressive component, the GAG distribution and content was modified to reflect the change in loading pattern.

1.3.2 Dermis

The dermis is the underlying connective tissue of the skin. Dermis serves as an elastic body covering the underlying musculature, and can expand and contract as needed. It further acts to protect against environmental impacts. This fibrous tissue contains collagen, elastin and proteoglycans. While comprised primarily of collagen, dermis does not exhibit the strict organization of tendon. Like tendon, it is populated with fibroblasts with some cell-cell junctions although the cells do not have an obvious preferred orientation.

Based on their finding that the GAG content in dermis obtained from weight bearing regions was significantly greater than in non-load bearing sites, Gillard and coworkers [1977] concluded that mechanical forces influenced dermal fibroblast behavior. Although the mechanism has not been clearly elucidated, surgeons have recognized for many years that the cosmetic quality of a healing dermal wound appears to be related to the tension on the wound. Repeated tensile forces imposed perpendicular to the wound will often result in a grossly bulky (hypertrophic) scar [Ketchum, 1979].

1.3.3 Cartilage

Structurally cartilage can be described as a collagen network filled with proteoglycan aggregates. Cartilage is generally classified according to its composition, which correlates well with its apparent mechanical function. The hyaline cartilages, rich in proteoglycans, must sustain impact compressive loading while the fibrocartilages, which are more collagenous, must sustain more shear loading. The proteoglycans provide the poroelastic and swelling character while the collagen acts to restrict the swelling and to provide tensile and shear strength. Unlike the cells of the other connective tissues, cartilage cells (chondrocytes) are spherically shaped and do not appear to have direct contact with other cells.

A number of investigators have examined cartilage composition as a function of presumed load bearing requirements and as a function of the tissue's ability to bear load. Kempson et al. [1970] found the creep modulus of adult articular cartilage to be strongly correlated to GAG content and uncorrelated with collagen content. Weight bearing cartilage tends to be thicker and have higher GAG and lower collagen content than less weight bearing areas [Venn et al., 1979].

1.3.4 Bone

Bone is a highly organized tissue which serves as a rigid support for weight bearing and muscle attachments. The matrix is a composite of collagen and mineral providing high compressive and tensile strength, together with some elasticity. The predominant cells in bone are osteocytes, osteoblasts, and osteoclasts. The osteoclasts and

osteoblasts resorb and lay down, respectively, the osseous matrix. Osteocytes, derived from osteoblasts, are considered the resting cell and resides "trapped" within the bone matrix. Although they are relatively sparse, the osteocytes have processes which extend into the bone interstices and can make contact with adjacent osteocytes. Thus, they have the apparent capability of sensing the state of a large surrounding area of matrix and of communicating with neighboring cells.

The ability of mechanical stresses to modulate the structure of bone is well known. The loss of bone mass induced by prolonged bed rest, weightlessness, or more sedentary life styles presents a significant clinical problem. In a recent study by E.L. Smith et al. [1984] physical activity (aerobic dance class) was sufficient to reverse the normal -1.1% annual bone mineral loss to a +0.8% annual gain. Woo et al. [1981] subjected one year old Yucatan swine to a 12 month exercise regimen, comparable in intensity to one adhered to by an active athlete. Relative to the sedentary animals, the cortical thickness of the femur of the exercised pigs showed a net 17% increase over the sedentary controls. In contrast to the adaptive responses of the other connective tissues, they found that the material properties and composition were essentially identical. This suggests that the response of mature bone to prolonged exercise is to increase load bearing capacity through an increase in bone quantity, not density, whereas the response to decreased loading involves a decrease in bone density.

1.3.5 Summary

In summary, collagen is flexible and strong in tension. With proper orientation, collagen can confer flexibility, tensile and shear strength to a tissue. Proteoglycans resist compressive loads, particularly dynamic (impact) loading. The content and organization of these two constituents can govern the tensile, compressive, and shear strength, as well as the flexibility and deformability of connective tissues. The various connective tissue cells are responsible for maintaining the proper organization and content of the matrix materials. Their shape, distribution, and relationship with each other must reflect the mechanism by which they sense and respond to the state of the tissue.

1.4 Growth and Development of Bone

Tissues can grow (increase in volume) by several mechanisms. The cells can enlarge (hypertrophy), synthesize more extracellular matrix, or increase in number (divide). The cells of structural connective tissues utilize primarily the latter two mechanisms, achieving growth by cell division and subsequent secretion of matrix by the new cells. This type of growth can occur interstitially where new growth occurs within the tissue and pushes the surrounding tissue further outward, or appositionally where new growth occurs at the boundary. Bone is unique among the connective tissues in that it is formed by the replacement of a preexisting connective tissue, presumably because its rigid structure

makes it relatively incapable of interstitial growth. Patterns of bone formation are classified as either endochondral or intramembranous indicating, respectively, a cartilaginous or noncartilaginous preexisting tissue.

1.4.1 Intramembranous Ossification

Direct bone formation which occurs within a non-specific connective tissue (primitive mesenchymal condensation, periosteum, endosteum) is called intramembranous bone formation. The cells of the precursor tissue apparently are osteoblasts or have the potential to become osteoblasts. These cells secrete collagen and proteoglycan eventually enclosing themselves in an extracellular osseous shell at which point they become osteocytes. In this system interstitial growth is not possible; intramembranous ossification allows for appositional growth only. Most of the flat bones of the skull, referred to as membrane bones, develop by this intramembranous process. Functionally, these bones provide rigid protection and are subjected primarily to shear stresses by attached musculature.

1.4.2 Endochondral Ossification

The majority of bones are initially formed of cartilage which is gradually replaced by bone. The process as it occurs in long bones is well studied and consists of a coordinated sequence as depicted in figure 1.1. The perichondrium along the shaft condenses and becomes ossified forming the periosteal band. The cells internal to this band become hypertrophied and the matrix becomes ossified. The remaining

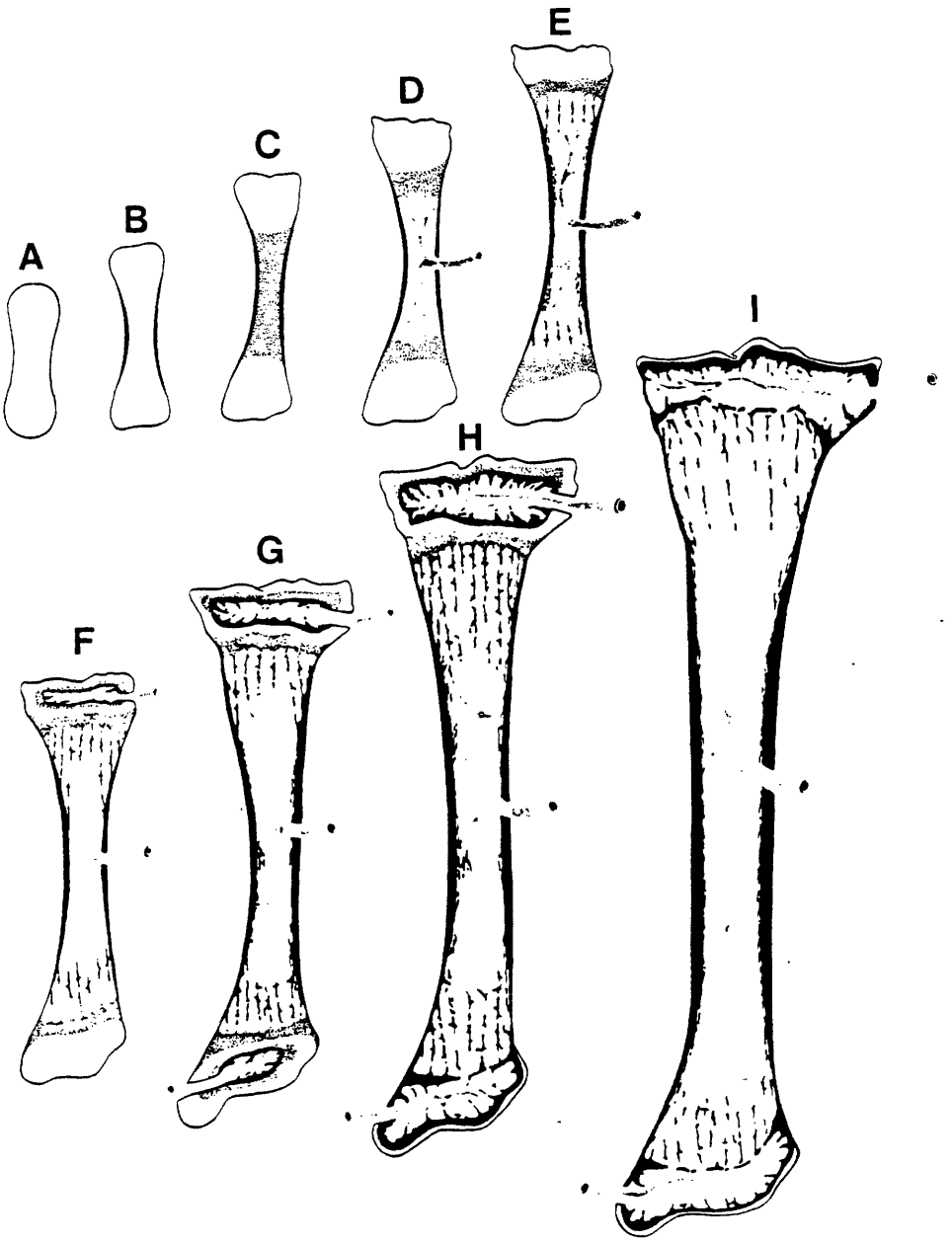

Figure 1.1: Endochondral bone formation for a typical long bone. (a) cartilaginous structure, (b) formation of periosteal band, (c) calcification of the shaft, (d) invasion of blood vessels, (e,f,g) ossification and blood vessel invasion of epiphyses. (Generally, one epiphysis ossifies before the other.) Increase in length occurs at the plate., (h,i) Closure of plates leaving a continuous bony shaft.
From Histology, L. Weiss Ed., Elsevier Biomedical, 1983.

cartilaginous heads attain a more organized structure (see figure 1.2). The region nearest the shaft is comprised of hypertrophied cells in a calcified matrix. Columns of chondrocytes which appear to feed into the hypertrophic zone comprise the proliferative zone which is thought to be responsible for the increase in bone length. The proliferating columns are adjacent to cartilage with an organization typical of hyaline cartilage. Initially this hyaline tissue extends to the articular surface. After this region is invaded by a vascular supply the central portion ossifies to form the epiphysis and effectively separates the articular cartilage of the joint surface from a cartilaginous region called the epiphyseal plate sandwiched between the bony epiphysis and metaphysis. At the cessation of longitudinal growth, the growth plate disappears leaving a continuous long bone.

Some endochondral bones of the skull represent slight deviations from the growth pattern of long bones. The mandibular condyle does not develop an epiphyseal bone, nor does the organized proliferative zone form. Rather, the "articular" surface is composed of a fibrous connective tissue and the underlying cartilage maintains the apparent random orientation typical of hyaline cartilage.

1.4.3 Role of Mechanical Forces in Skeletal Growth

Skeletal growth is primarily under hormonal control. Calcitonin and parathyroid hormone promote bone formation and resorption, respectively, providing a controlling factor in bone turnover and calcium homeostasis. During the period of growth, the pituitary growth hormone accelerates growth both by elongation and apposition. But, in

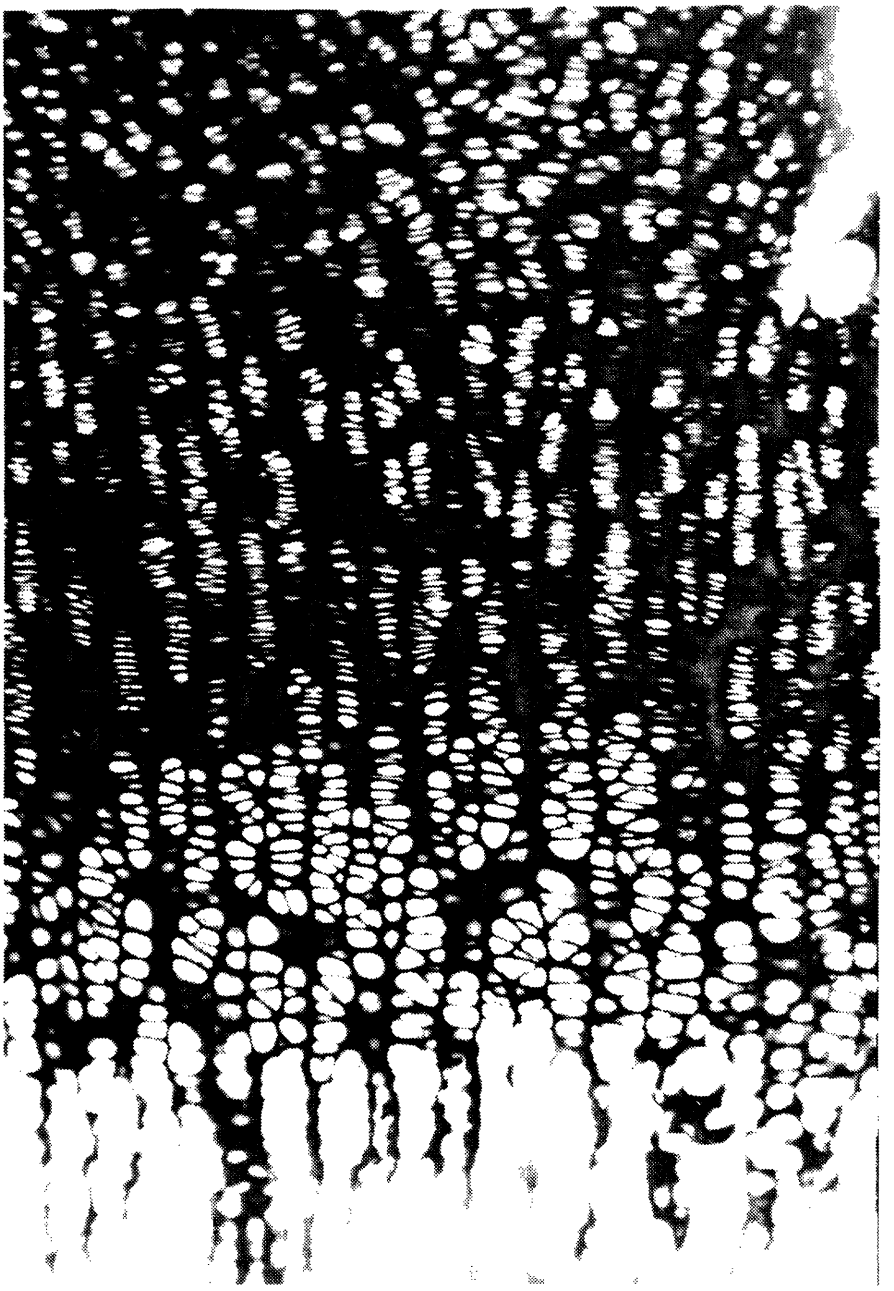

Figure 1.2: Histological section of the epiphyseal plate showing the major zones. The lower region shows the newly calcified primary spongiosa. Prior to calcification, the cells hypertrophy. This region is called the hypertrophic zone. (It can be further subdivided into a maturing and hypertrophic zone.) The cells of the proliferative zone (so called because studies of DNA synthesis indicate a high proliferative rate) are organized into columns. Cells of the resting or reserve zone have an appearance typical of hyaline cartilages.

view of the fact that bones provide mechanical support, it is expected that growth and development of bone will respond to local mechanical factors. Gravity and muscle forces are the primary mechanical factors. The specific influence of these forces on the growth and remodeling behavior of bone is widely conjectured, yet no unifying theory currently exists that explains many of the observed phenomena. Rather than simply listing the plethora of clinical examples believed to represent mechanical influences on growth and remodeling, a working theory will first be proposed to provide a context in which to discuss these clinical examples.

1.4.3.1 Theory for physical regulation of growth

The objective here is to suggest a set of principles which govern skeletal growth. The validity of these principles will be examined using a variety of pathological and experimental situations to highlight salient features and to motivate appropriate experimental tests.

From a design point of view, a growing bone must provide:

1. Stable structural support.
2. Structural adaptation to changes in the mechanical environment.
3. Growth in length and girth while maintaining support.
4. Adequate surfaces in regions where significant motion occurs.

It is convenient and appropriate to separate the growth behavior by cells of bone from those of growth cartilage. It is convenient because growth cartilage seems to be the primary site for increases in length (requirement #3) and, as will be discussed, provides a superior bearing

surface (requirement #4). In contrast, bone is the predominant structural support in mammals (requirement #1) and must be capable of adapting (requirement #2) both during and after growth. It is appropriate to consider the cartilaginous and osseous tissue separately because, although they are derived from the same embryological precursor, the cells and extracellular matrix are quite distinct so that a particular mechanical environment may affect cartilage very differently from bone.

Consider first the expected behavior of bone resulting from a change in its mechanical environment. As with any engineering support material, it should be sufficiently strong while requiring a minimum amount of material. Bone would be expected to increase in mass and therefore in strength in the face of an increased load. Increasing mass by means of periosteal appositional growth will provide the most increase in strength per unit of additional mass. Furthermore, it would be expected that a change in the direction of the mechanical load would eventually result in a change in the oriented architecture of the bone. The premise that bone architecture and mass reflect mechanical loading patterns is a statement of "Wolffs law" as he was the first to propose this relationship in 1884. The simplest application of this law is the assumption that bone mass will be proportional to compressive load. This simple tenet is sufficient to provide an adaptive structural support.

Growth cartilage provides the scaffold for future bone. Unlike bone, it has the capacity for interstitial growth so it is the site of bone elongation. To predict the effect of mechanical loading on bone

elongation, the bone is viewed as a loaded column. The stability of a column is related to the ratio between its length and its diameter. A long thin column is inherently more unstable than a short fat column. So, to maintain stability for a given bone diameter, bone elongation should slow in response to an increase in load, leading to a shorter bone. That increased pressure will inhibit cartilage growth was recognized by Hueter [1862] and Volkmann [1862].

In summary, the working hypothesis will be that an increase in compressive load will result in an increase in bone diameter by periosteal apposition and a decrease in the rate of bone elongation. The net effect on growth depends on the relative kinetics of the two processes. The selected review which follows focuses on clinical and more recent clinical examples. For a review of the earlier experimental literature see Arkin and Katz [1956].

1.4.3.2 Examples consistent with the growth theory

It is well known that the growth plates at either end of long bones exhibit different growth rates. Femoral growth is primarily due to elongation at the distal plate. The proximal tibial plate is responsible for the bulk of tibial elongation. It is difficult to imagine a humoral mechanism other than differential blood supply to account for this difference. As discussed above, a difference in stress would be expected to result in a difference in growth rate. If it is assumed that both epiphyses are subjected to the same loads then the smaller epiphysis would experience more stress (load/area) than the larger and would be

expected to have a slower growth rate. This indeed seems to be the case. The distal femoral plate, where elongation is greatest, is substantially larger than the proximal plate. Similarly, in the tibia the proximal plate is larger and therefore is expected to be subjected to less stress.

Modulation of long bone growth has been achieved through epiphyseal stapling, distraction, and immobilization[2] [Peruchon et al., 1980, and Porter, 1978]. Stapling and distraction respectively reduced and accelerated growth in sheep and rabbit models. In epiphyseal distraction, varus deformities developed which the authors attributed to nonuniformities in the loading systems.

Hall-Craggs and Lawrence [1969] found that when an epiphyseal plate is stapled so as to prevent elongation, the unstapled plate will grow more rapidly than the controls. They suggested that this compensation resulted from physiological communication between plates. An alternative explanation would be that the stapled limb experienced less load allowing the plate that could grow to elongate at a more rapid rate than if it had been normally loaded. If it were to continue growing at the normal rate, the unstapled limb would become longer than the stapled limb. This discrepancy between leg lengths might result in less load to the stapled limb.

---

[2]Stapling: Wire staples are placed across the plate to prevent elongation.
Distraction: Steel pins are placed on either side of the plate and distracted to either reduce the load across the plate or physically separate the plate from the metaphysis.

Another example is provided by the bone and joint formation which occurs with subtalar ankylosis. Normally, medial and lateral rotation (pronation and supination) of the foot occurs at the subtalar joint. If that joint is fused early in childhood, as in subtalar ankylosis, these motions occur at the ankle joint. Presumably as a result of the abnormal mechanical loading, the ankle joint develops a so-called ball and socket appearance which better accommodates the additional movements. The normal ankle joint is rectangular in the mediolateral plane, so medial and lateral rotation would impose an abnormally large load at the corners. If this increase in load acted to limit growth, the joint would attain the rounded appearance seen in such situations.

Gravity or body weight is expected to exert some influence on bone development. Tulloh and Romberg [1963] compared normal lambs to those loaded with saddlebags to maintain their weight at 40% over controls. The loaded bones had an increased diameter but no difference in length. At first this may seem to contradict the theory that increased stress will decrease bone elongation. However, if the plate area were to increase by 40% then it would be subject to the identical stress as the unloaded controls. Measurements made from the photographs provided indicate a 21% increase in plate diameter which corresponds to roughly a 40% increase in area. This suggests that such a system has an elegant control mechanism. If for some reason, limb bones are loaded to a differing degree, the response of the bone and cartilage tissue will provide equal limb lengths while maintaining sufficient strength.

1.4.4 Summary

Clinical and experimental evidence support the theory that increases in stress induce increases in girth by appositional growth and decreases in longitudinal growth rate by the epiphyseal plate. Studies of remodeling in adult tissue where longitudinal growth has ceased provide further corroboration that the response to increasing stress is to increase diameter. This makes the bone structure stronger while maintaining an essentially constant material strength. The evidence that increased stress leads to a decrease in longitudinal growth rate is more circumstantial because the appositional increase in girth increases the area of load distribution, and restores the stress on the plate to normal. The clinical examples do not provide a means of decoupling the appositional from the longitudinal growth responses. Quantification of the magnitude and kinetics of these adaptive responses would be very useful in understanding and predicting growth under normal and pathologic conditions.

1.5 Experimental Quantification of Response to Mechanical Forces

The previous sections described the relationship between mechanical loading and connective tissue composition and structure. The ability of these tissues to adapt their composition when subjected to a change in loading pattern was a recurring theme. This section reviews studies which attempted to quantify or characterize the response to mechanical test conditions, first for *in vivo* then for *in vitro* systems.

In vivo preparations have the advantage of being "physiological".

It is generally difficult, however to impose test conditions in such a way that the relevant controlling parameters (e.g. nutrition, neural activity, stress) can be extracted and quantified. Results from tissue culture preparations have been obtained under more controlled conditions. The disadvantages are that the neurovascular system and normal nutrient supply is absent and in some cases the cells have been isolated from their normal extracellular matrix.

Most in vivo studies examine the response to exercise or immobility. The effect of immobility is most dramatic on bone. A rise in the serum calcium of Skylab astronauts occurred within a day of spaceflight reflecting release from the calcified tissues. Weightlessness or bedrest lead to a continuous drop in calcaneal mineral [Morey-Holton and Arnaud, 1985] which could presumably compromise the ability of the bone's weight-bearing ability. Rubin and Lanyon [1984] have developed an avian model for osteoporosis in which the ulna is "functionally isolated" (i.e. free from normal muscle forces) by parallel epiphyseal osteotomies. They report a 20% reduction in ulnar bone mass after 42 days of functional isolation. Application of only 4 cycles per day of 0.5 Hz ramped square wave loads of physiologic magnitude prevents this loss. (Here, physiologic magnitude means the peak longitudinal strain resulting from the applied load is equivalent to the magnitude of the peak strain which occurs during normal wing flapping.) Application of 36 or more cycles per day resulted in a 40% increase in bone mass. Their group also found that the response exhibited an amplitude dependence for a loading protocol of 100 cycles

per day at 1 Hz over an 8 week period [Rubin and Lanyon, 1985].

This in vivo preparation has demonstrated a magnitude dependent remodeling response to intermittent loading which, above some remarkably small number of consecutive cycles, seems independent of the time the tissue is subjected to the applied load. However, no correlation between the sites of the stimulated remodeling response and the imposed changes in local mechanical environment has been made. Most other attempts to quantify the modulation of cell behavior in response to mechanical stresses use in vitro preparations.

Lippiello et al. [1985] subjected calf articular cartilage to hydrostatic pressures and noted a depression in GAG synthesis over four hours for loads up to 2 MPa. Tissue exposed to a 2.5 MPa pressure, however, synthesized GAGs at control levels. Synthetic behavior following removal of the pressure also differered for pressures under 2 MPa compared to 2.5 MPa. For the conditions inducing a depression in synthesis (under 2 MPa), synthesis was at control levels within 15 minutes of pressure removal. In contrast, removal of a 2.5 MPa pressure led to an increase in synthetic rate which remained after 24 hours.

Kimura et al. [1985] used a similar setup to examine the biosynthetic response of bovine articular cartilage to hydrostatic loading. In contrast to Lippiello's work, they found no difference between experimental and control samples for loads up to 2.75 MPa for up to 4 days.

Rodan and his colleagues [1975] examined the response of embryonic chick tibia model to static compressive loads applied directly to the

tissue. An 8 kPa load resulted in a 15% increase in thymidine incorporation and a 50% depression in glucose utilization over the 3 days examined. Two days after release of the load, glucose utilization had returned to only 75% of control levels. The effect of the load on the diffusion properties was judged to be negligible using ^{22}Na uptake.

Jones et al. [1982] found that GAG synthesis by calf articular cartilage dropped by 50% over six hours for a 2-3 MPa static load. For loads up to approximately 1 MPa synthesis remained unchanged. They noted no change in lactate formation with loading implying that the metabolic capabilities of the cell were not altered. If the tissue was loaded for 2 days and then allowed to recover for 2 days, GAG synthesis was 30% above controls.

Schneiderman, Keret, and Maroudas [1986] examined GAG synthesis by adult human articular cartilage in response to an applied static 4 hour load. They found a dose dependent depression in synthesis over a 200-800 kPa range. Osmotically induced compression gave rise to similar decreases in synthetic rate.

Lee et al. [1982] subjected embryonic chick chondrocytes plated on elastin membranes to 10% cyclical stretching at 1 Hz for 8 hours and found an increase in GAG synthesis.

Dewitt and coworkers [1984] created a tissue-like material by growing chick epiphyseal chondrocytes in high density culture for 14 days. The response to a 5% tensile strain at 0.2 Hz was compared to agitation at 0.2 Hz for 24 hours. An increase was seen in GAG synthesis and cell mitosis doubled, however there was no effect on protein

synthesis.

Palmoski and Brandt [1984] investigated the effects of both static and dynamic loading on dog articular cartilage using a two hour load followed by a two hour label. They compared loads of 1, 5.5 and 11 kPa applied with on:off sequences of either (1) 2 hours on: 0 hours off (static), (2) 60 seconds on:60 seconds off, or (3) 4 seconds on, 11 seconds off. For applied sequences (1) and (2), synthesis was depressed by about 50% for all loads. Synthesis was normal to increased for those loaded according to sequence (3).

Copray et al. [1985a] isolated the condyles from four day old rats and subjected them to static and intermittent strains of up to 20% for 5 days. The strains were imposed by constraining the condyles to be a constant length, thus as the condyles grew, the magnitude of the imposed strain increased. The unloaded controls steadily elongated over the 5 day period. Those subjected to intermittent (0.1 and 0.7 Hz) strains demonstrated a plateau in length while a constant imposed thickness led to initial elongation but eventual decrease in length. Glycosaminoglycan, protein, and DNA synthesis were consistent with the changes in length [Copray et al., 1985b]. The stress magnitudes required for these studies were not known but using the photographs to estimate dimensions and assuming plane parallel specimens the loads were at least 100 kPa. The dynamic loads must have been higher but are difficult to estimate because of the geometry.

In summary, examples exist in the literature for mechanically induced changes in tissue behavior for loads of 1 kPa to 3 MPa at

frequencies from DC to 1 Hz. It is difficult to incorporate all reported results into one theory because the experimental parameters and tissue models vary from one investigator to another. Static loads seem to lead to a dose dependent depression in synthesis however, the minimum dose at which a response is detected seems to vary considerably. Enhancement of synthesis was seen with a few dynamic loading protocols and sometimes for removal of a static load. It appears that the effect of dynamic loading can affect tissues differently than static loading. However, more work remains to define the relevant loading parameters.

In the next chapter, a conceptual model will be developed with which the relationship between mechanical parameters and cell behavior can be systematically examined. The general model is appropriate for any connective tissue, however, discussion will focus on cartilaginous tissues. Chapter 3 describes the organ culture and biochemical techniques used in the experimental studies. In chapters 4,5, and 6 results of experiments designed in accordance with the conceptual model are presented. These experiments provide the first steps in understanding the effect of mechanical loading on the synthetic behavior of cartilaginous tissues.

Chapter II

CONNECTIVE TISSUE SYSTEM

2.1 Introduction

The underlying premise of this work is that connective tissue cells are capable of modulating their activity in response to an altered mechanical environment. This is based on the facts that connective tissues subserve a mechanical function and that it is the cells which are responsible for maintaining a viable functional tissue. One long range goal of connective tissue research which motivates this work is to identify the specific mechanically-induced signals capable of modulating cell activity and to derive the relationship between signal and response. In this chapter a conceptual model based on a system theory approach is proposed as a framework for the investigation of cellular response to mechanical signals. This model suggests experimental approaches which isolate specific signals. Later chapters present the cellular response to these specific signals.

The development of the model incorporates several assumptions. First, connective tissue cells will alter the extracellular matrix if exposed to an altered mechanical environment. The examples cited in the preceding chapter provide experimental evidence that connective tissue cells modify the content or rate of synthesis of ECM material when subjected to change in mechanical loading. This suggests that a physiological mechanism exists by which all connective tissues will be

modulated in the event of an altered mechanical load.

The second assumption is that cells are necessary and fundamentally responsible for this adaptive response to occur. The change in extracellular matrix could be effected by a change in the balance between synthesis and breakdown of the extracellular matrix. The cell is necessary for the synthesis of ECM material and required degradative enzymes. It is conceivable that there is a component of self assembly and disassembly not controlled by the cell which results in an alteration of the ECM in response to mechanical forces, but this process is assumed to be negligible.

Finally, it is assumed that the mechanism by which the response is effected is similar for different types of connective tissue cells and among species. As cell function has become better understood it has been continually confirmed that there are basic principal mechanisms by which cells operate. If the same macroscopically applied load leads to different responses by cells of different tissues, then it is assumed that the local signal seen by the cell must have differed. In fact, such a result would provide important clues as to the mechanism by which cells modulate their behavior.

Currently there is little knowledge relating the tissue response to specific environmental parameters. Furthermore, it is not clear how the cell is able to sense the changing environment or how long it takes to initiate or complete the response. The wide differences in protocol and experimental models found in the literature make it difficult to develop a unifying theory. Because so little is understood about the

response mechanism, the initial choice of experimental parameters is in part arbitrary. The principles of system theory are commonly used as a basis for studying the response of a system to an applied signal. These principles provide guidelines for analyzing and describing a system. Although connective tissues may not represent an ideal causal, time-invariant, linear system, a great deal can be gained by learning to what extent it may deviate from an linear system.

2.2 System Definition

System theory provides a framework in which one may systematically examine system dynamics. A system is comprised of a number of interconnected components, each of which can be acted upon by an input signal and can, in turn, alter the input to another component. Conceptually, the connective tissue-mechanical response system can be represented as in figure 2.1 by three elementary response units: mechanical, cellular, and output conversion. The tissue will exhibit a material response to an applied mechanical load. (e.g. it will deform when loaded.) Some aspect of that material response serves as a trigger or input to the cells. The cells modify their activity according to their input signal. Finally, their response is exhibited in the form of some testable output.

Ignored so far in this discussion is the existence of feedback and feedforward. In general there may exist connections between the output of any unit to the input of any unit and between the applied input

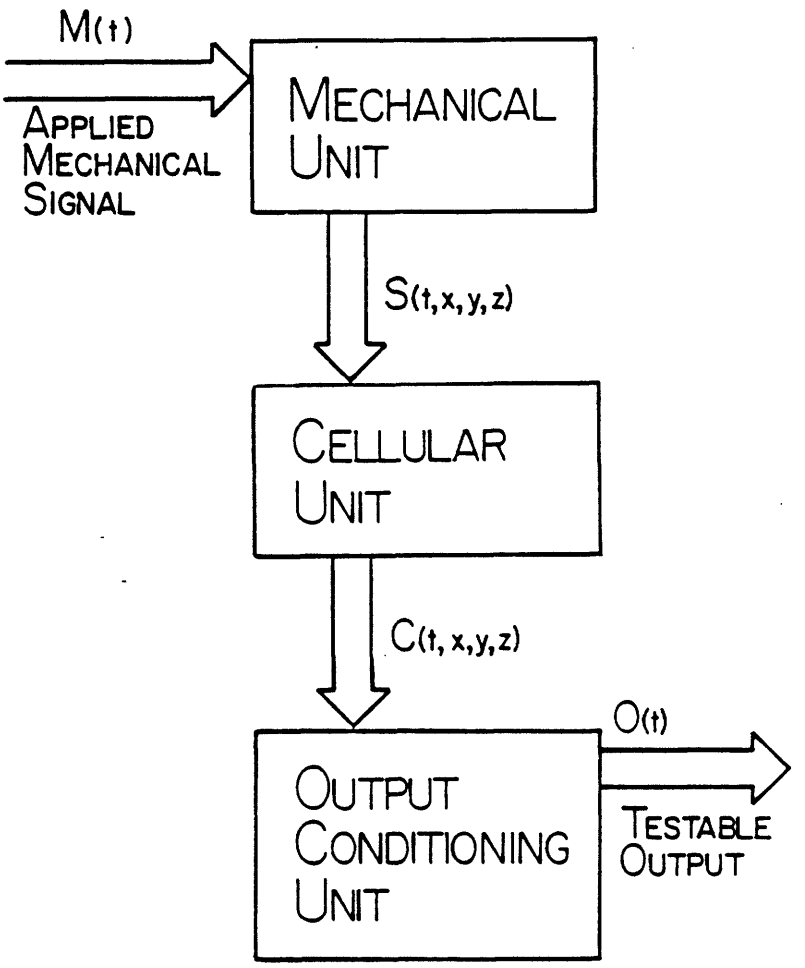

Figure 2.1: The connective tissue-mechanical response system is represented by three elementary response units. The mechanical unit describes the material response ultimately resulting in an input signal to the cell. The cell is represented by the cellular unit whose output can be detected following processing by the output conversion unit.

signal and any input. Feedforward, that is, pathways which bypass any unit in the forward path enhance system response time without sacrificing system stability. It is unlikely that feedforward paths are important to the ability of connective tissues to adapt to mechanical loading.

Feedback provides the means of maintaining a regulated quantity within a desired range despite disturbances (applied inputs) that may act on the system. For connective tissues, where the ECM properties are known to change in the face of an altered mechanical environment, it seems that the feedback is derived from the alteration in material parameters which occur as a result of the cell response as depicted in figure 2.2. The relatively slow turnover rates of collagen and GAG suggests that the time required to achieve regulation is also relatively slow.

The sections which follow discuss each of the elementary response units in detail. Emphasis is placed on a description appropriate for cartilaginous tissues to motivate the experiments of the succeeding chapters.

2.3 The Mechanical Unit

As mentioned in chapter 1, the material properties for the tissues of interest are conferred by the extracellular matrix. Studies of material properties necessarily focus on the macroscopic relationships and attempt to separate tensile, compressive, and shear properties. On a

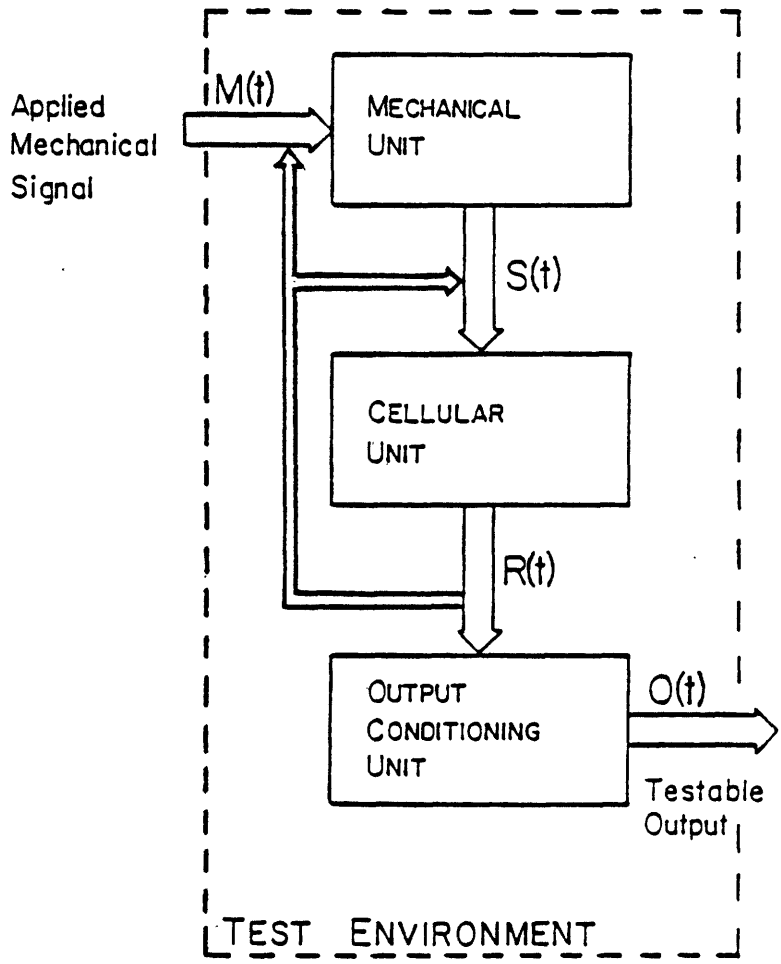

Figure 2.2: Mechanical Response System with Feedback

microscopic level, the local tissue elements may be subjected to compressive, tensile, or shear stresses which may differ from what is occurring at the boundary. Furthermore, the local material response is a function of time and space. Thus, in general, it is difficult to deduce a specific cell's mechanical environment. This section discusses the material response of cartilage to mechanical loading and identifies several aspects of the material response which might constitute the output signals from this component of the system. Section 2.4 will consider these output signals as inputs to the cellular unit.

2.3.1 Material Behavior

Cartilage, like all structural connective tissues, is a porous material comprised of a fibrous collagen network filled with fluid, cells, and proteoglycan. When the tissue is subjected to loading forces, a hydrostatic pressure develops driving fluid from the matrix thereby leading to bulk deformation [Armstrong et al., 1984; Mow et al., 1980; Freeman and Kempson, 1972]. It is generally assumed that under physiologically reasonable loads, the matrix material itself is incompressible and so does not contribute to the bulk deformation [e.g. Mow et al., 1980]. The force required to maintain the tissue in a deformed state balances the elastic recoil of the fibrous network and electrostatic repulsion by the fixed charge groups of the proteoglycan. The required force is dependent on the pH of the bathing medium (to the extent that the number of charge groups is affected) and on the salt concentration (since salt acts to shield the charge groups from each

other) [Sokoloff, 1963; Lee, 1979; Eisenberg, 1983].

The dynamic material behavior of connective tissues is governed primarily by the ease with which fluid can be redistributed [Lee et al., 1981; Armstrong et al., 1984]. Consider, for example, the material behavior in confined uniaxial compression as depicted in figure 2.3. Because fluid flow cannot occur instantaneously, if a step load is applied, fluid will be exuded, leading gradually to a deformation. Alternatively, if a step displacement is applied, a relatively large force will be required and the displacement will be initially restricted to the upper regions of the tissue. With time, the displacement will diffuse through the tissue until the strain profile becomes uniform [Mow and Lai, 1979]. Figure 2.3 diagrams typical creep (response to a step load) and stress-relaxation (response to a step displacement) behavior. If the tissue is subjected to sinusoidal or dynamic loading at frequencies with periods much longer than the mechanical diffusion time, the behavior will be similar to the equilibrium step behavior. As the frequency is increased, the entire specimen will be pressurized but the deformations will not have time to diffuse through the tissue, so a progressively smaller fraction of the specimen will experience displacement. This behavior is important to keep in mind when attempting to understand the cellular behavior. If the mechanical signal is of sufficiently high frequency, the material response will be spatially distributed so that cells will be exposed to signals of different types and magnitude.

In order to ensure that the epiphyseal cartilage used in the

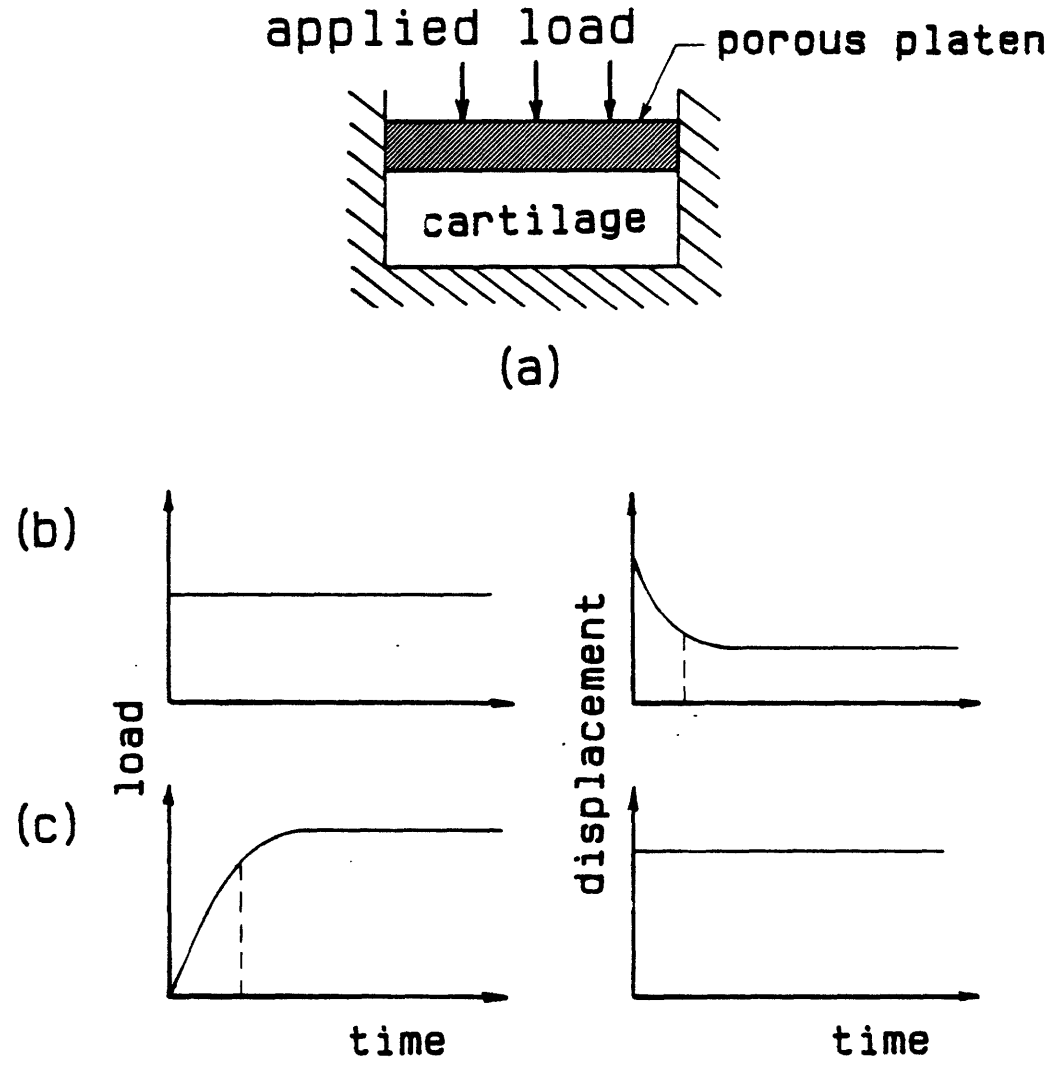

Figure 2.3: (a) Typical experimental configuration for uniaxial confined compression testing. The tissue is confined around the periphery and on the bottom. Compression is applied via a porous platen. Thus all processes are uniaxial. (b) Creep deformation response to an applied step load. (c) Stress relaxation response to an applied deformation.

experimental studies demonstrated material behavior similar to articular cartilage, the compressive electromechanical properties of epiphyseal plate cartilage under physiological salt and pH conditions was examined in confined oscillatory compression. The dynamic stiffness as a function of frequency is shown in figure 2.4 for a typical tissue sample. The response is similar to that described by Lee et al. [1981]; therefore, it is assumed that the theories and methodologies provided by the articular cartilage electromechanical literature are valid for epiphyseal cartilage. Using the theoretical model described by Lee et al., the bulk longitudinal modulus, and hydraulic permeability are estimated to be 1 MPa and 6×10^{-15} $m^2/Pa \cdot s$ respectively.

2.3.2 Mechanical Output Signals

Based on what is known about the material response to loading, we can now consider the physical change in the cellular environment. As the tissue is loaded, a hydrostatic pressure gradient develops driving fluid flow through the matrix, resulting in tissue and perhaps cell deformation. Due to the charged nature of these tissues, the interstitial fluid contains more counterions than coions so that an electrical current will accompany the fluid flow. The tissue consolidation results in changes in the extracellular milieu. (e.g. water content, fixed charge density, and concentration of ionic species.) These induced material responses are considered as an output signals from the mechanical unit.

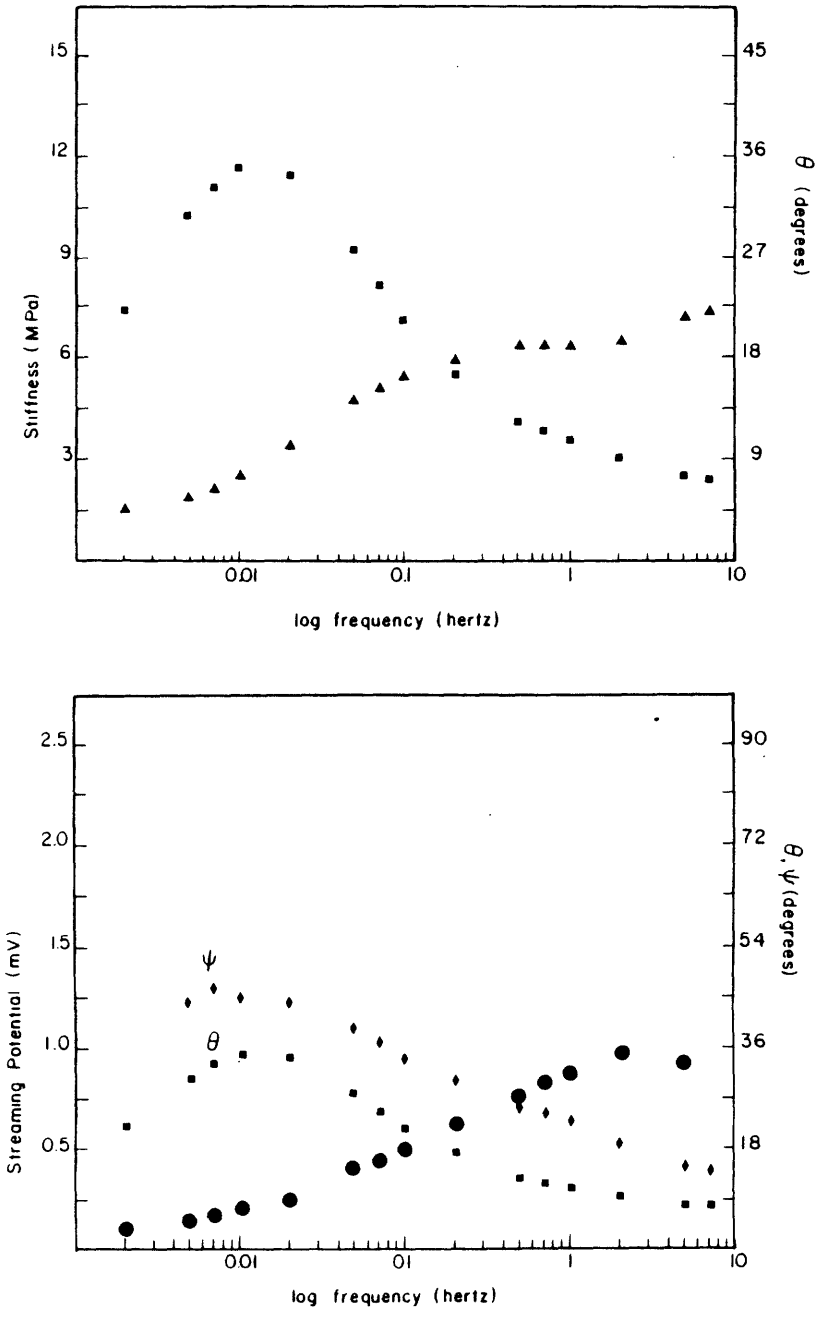

Figure 2.4: Upper panel shows dynamic stiffness (▲) and phase, Θ (■) versus frequency for a confined epiphyseal cartilage sample bathed in physiologic saline and subject to a 15% static and 1% dynamic strain using techniques described by Lee et al. [1981].

Lower panel show the corresponding streaming potential amplitude (●) and phase, ψ (◆) measured simultaneously with the stiffness.

2.3.3 Output Signal: Cell Deformation

Material deformation of the matrix can lead to cell deformation, although the complex material structure and ECM-material interconnections make prediction of the extent of cell deformation in connective tissues difficult. In the noncartilaginous connective tissues, the existence of long cellular processes and the apparent preferred orientation of the cell with respect to collagen lead one to suspect that cell deformation occurs. In cartilage however, cells have an overall spherical morphology which may lessen the possibility of deformation. Broom and Myers [1980] demonstrated compression induced chondrocyte deformation in thin slices of articular cartilage using a Nomarski optical technique. They also noted that the fibrous pericellular material, which is predominantly in tension in free swelling tissue, became progressively more crimped when compression was applied. Although discrete connections between these fibers and the cells were not observed, the authors suggest that this crimping acts as a signal to the chondrocyte either directly or indirectly by changing the local chemical environment.

Using the same compressive device, Poole and co-workers [1984] examined the morphologic response to compression by electron microscopic techniques. They subdivided the matrix into several zones. Immediately surrounding the chondrocyte a fine pericellular matrix was evident and presumed by its appearance to be high in PG content. Territorial and interterritorial matrices surrounding the pericellular zone characterized by organized collagen fibrils were frequently observed.

Under a 250 kPa load, they also noted a crimped collagen pattern in both the territorial and, to a lesser extent, the interterritorial zones. The cells and their pericellular matrices became flattened under compression. In addition, cell processes became flattened against the cell.

Wilsman et al. [1980] observed a single chondrocytic cilium in adult pony articular cartilage using transmission electron microscopy. They proposed that the structure and anisotropic orientation[3] of the cilium are consistent with the hypothesis that these cilia function as a sensory receptor [Wilsman and Farnum, 1986; Wilsman et al., 1980]. Motion of these cilia have been reported but could conceivably occur with material deformation.

It appears that chondrocytes do deform when the tissue is compressed and thus represent an output of the mechanical unit. Section 2.4.1 discusses the cell deformation as an input signal to the cell.

2.3.4 Output Signal: Hydrostatic Pressure

A change in tissue hydrostatic pressure occurs when the tissue is loaded. If fluid is not freely allowed to redistribute, the change in pressure will remain throughout the loading period. Otherwise, it will act as a driving force for fluid flow and be present until the

---

[3]Structure: 9 doublet microtubules, no central tubules, and no dynein arms
Orientation: In the tangential zone (region nearest articular surface) cilia were parallel to articular surface and to cell axis; In the radial zone (deeper articular tissue) cilia were perpendicular to articular surface and parallel to cell axis.

equilibrium deformation has been reached. Hydrostatic pressures may change the state of the fluid itself, but perhaps more importantly, pressure may change the state of the lipid bilayer membrane of the cell and its compartments. Work by R.A. Smith et al. [1984] suggests that pressures of 5-10 MPa can lead to 1/2% changes in equilibrium membrane volume. The kinetics of this change have not been elucidated.

Artificial membranes studied by X-ray diffraction have demonstrated pressure induced changes in the liquid-crystalline state [MacDonald, 1984]. They found that lamellar periodicity decreased by 0.0007%/atm (1 atm ≈ 1 MPa). The compression of water accounted for a quarter of that change. Consolidation of the membrane may alter the distribution or functional properties of the membrane proteins.

2.3.5 Output Signal: Fluid Flow

When the matrix is deformed, fluid is redistributed possibly increasing nutrient supply and waste removal in addition to imposing a shear stress at the cell membrane. The hydraulic permeability of cartilage is reported to be between 10^{-14} $m^2/Pa \cdot s$ and 10^{-15} $m^2/Pa \cdot s$ [Mow and Lai, 1979]. Using the larger value for permeability, to achieve a flow rate of even 10 μm/s through a 1 mm thick specimen, a driving pressure of 10 MPa (1400 psi) is required. In fact, the compression resulting from pressure gradients of that magnitude decreases the permeability by as much as several orders of magnitude [Mansour and Mow, 1976]. From Mansour and Mow's data, a pressure of 1000 MPa would be required to produce flow rates of 10 μm/s.

2.3.6 Output Signal: Streaming Potential

Streaming potentials are related to the charged nature of connective tissues. The flow of ionic species through a charged material will result in streaming currents or potentials. Cartilage tested in oscillatory confined compression has been demonstrated to produce a measurable potential which is a function of the fluid flow relative to the matrix. A 1% dynamic compression at 1 Hz in physiological saline produces a potential of 300 μV. (See data in figure 2.4.) Assuming a conductivity of 1.5 mho/m and a skin depth[4] of 30 μm, a current density of ~1.5 mA/cm² is computed.

2.3.7 Output Signal: Consolidation

The final output signal considered is that of mechanically induced tissue consolidation or swelling. Due to the charged nature of the matrix, hydration changes will alter the concentration of charged solutes in the fluid phase. Consolidation may further act to exclude or impede diffusion of solutes.

2.3.7.1 Concentration Changes

Again, the "concentration" changes expected to occur in cartilage are used to illustrate this output signal resulting from compression.

---

[4] Skin depth refers to the depth to which an applied strain can diffuse and is a function of frequency and material properties. It is given by [Lee et al., 1981] $\sqrt{(2H_A k/\omega)}$ where H_A is bulk modulus (typically 0.5 MPa), k is hydraulic permeability (typically 6×10^{-15} m²/Pa·s), and $\omega = 2\pi f$ is the angular frequency.

Figure 2.5 and table 2.1 summarize the changes in electrolyte concentrations which are predicted to occur as the tissue is compressed assuming that ideal Donnan equilibrium is obeyed.[5] Maroudas and Evans [1972] experimentally confirmed that the partitioning of NaCl obeys ideal Donnan equilibrium over a wide range of bathing salt concentrations.

Maroudas and Evans [1972] also examined the distribution of K^+, Ca^{++}, and SO_4^{--}. They found that a higher concentration of each of these ions was present in cartilage than would be expected by ideal Donnan theory. In addition, they claimed that the distribution coefficient (factor indicating the deviation from Donnan theory) increased with fixed charge density, (although there was insufficient data presented to examine that conclusion). The electrolyte composition expected using their distribution coefficients is also tabulated in table 2.1 for

---

[5] The plots in figure 2.5 are derived from the following:

electroneutrality : $[Na]_i + [H]_i + [K]_i - [Cl]_i - \rho = 0$

thermodynamic equilibrium : $[Na]_i[Cl]_i = [Na]_e[Cl]_e$

$[H]_i[Cl]_i = [H]_e[Cl]_e$

$[K]_i[Cl]_i = [K]_e[Cl]_e$

where the i and e subscripts refer to internal and external concentrations, respectively; ρ is the fixed charge density taken to be 0.15 M for unstrained tissue. The bath concentrations were taken as follows: [NaCl]=0.15 M, pH=7.2, [K+]=4 mM.

The entries in table 2.1 Na^+, Cl^-, K^+, and pH were derived as above. Ca^{++}, and SO_4^{--} were derived from thermodynamic equilibrium only, since their contribution to charge neutrality is negligible compared to NaCl. Explicitly:

$[Ca]_i[Cl]_i^2 = [Ca]_e[Cl]_e^2$

$[Na]_i^2[SO_4]_i = [Na]_e^2[SO_4]_e$

where the bath concentrations were: $[Na_2SO^4]$=0.8 mM, and $[CaCl^2]$=1.5 mM.

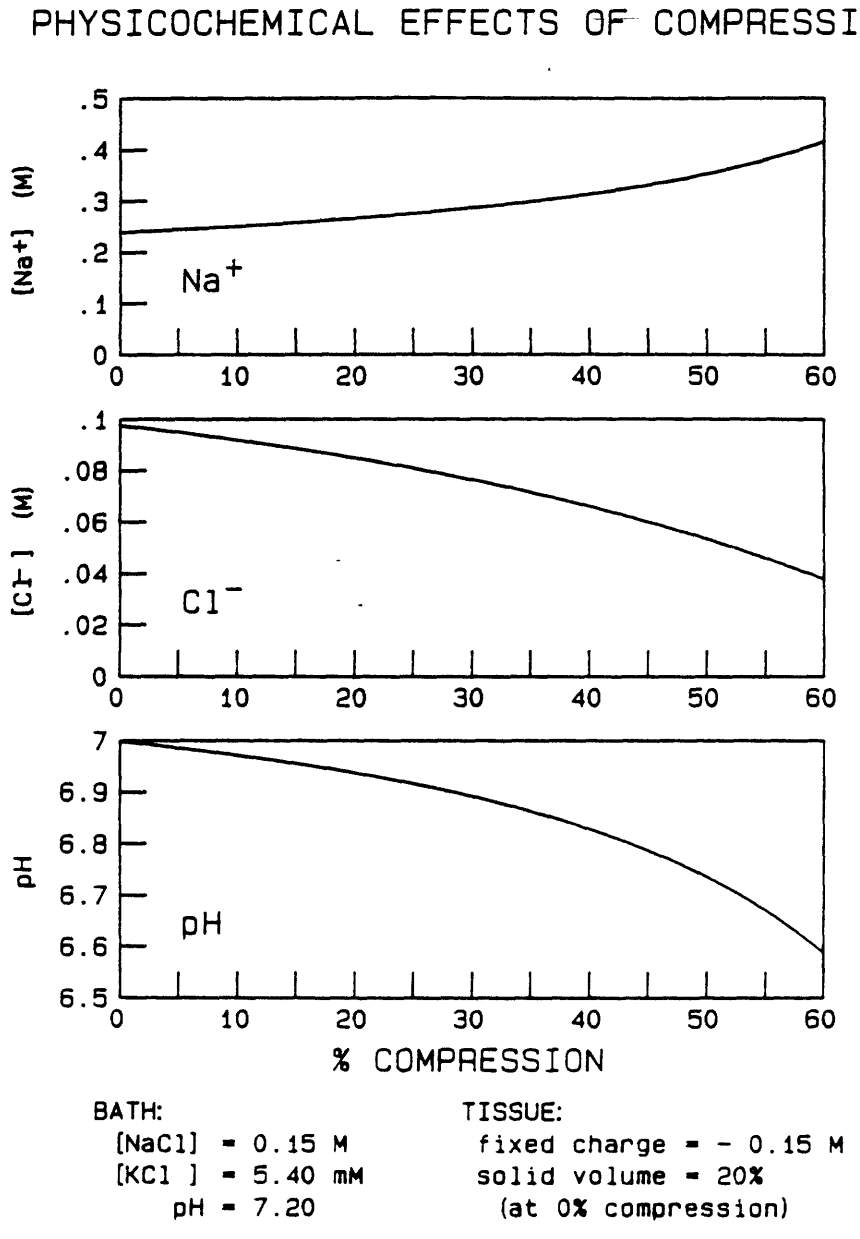

Figure 2.5: Changes in concentration of Na, Cl, and H as a function of compression as predicted by Donnan theory. See text for details.

Effect of tissue compression

bath [NaCl] = 0.150 M
[KCl] = 5.400 mM
pH = 7.200
[CaCl] = 1.800 mM
[NaSO4]= 0.800 mM
fixed charge= -0.150
solid volume = 20 %

Distribution coef: K 1.33, Ca 1.42, SO4 1.37

Internal concentrations

%comp	Na(M)	Cl(M)	K(mM)	pH	Ca(mM)	Ca*(mM)	SO4(mM)	SO4*(mM)
0%	0.239	0.098	8.602	6.998	4.568	6.486	0.315	0.432
5%	0.246	0.095	8.853	6.985	4.839	6.871	0.298	0.408
10%	0.254	0.092	9.145	6.971	5.163	7.331	0.279	0.382
15%	0.264	0.088	9.488	6.955	5.557	7.892	0.259	0.355
20%	0.275	0.085	9.896	6.937	6.046	8.585	0.238	0.326
25%	0.289	0.081	10.389	6.916	6.662	9.460	0.216	0.296
30%	0.305	0.076	10.992	6.891	7.459	10.592	0.193	0.264
35%	0.326	0.071	11.748	6.862	8.520	12.099	0.169	0.232
40%	0.353	0.066	12.718	6.828	9.984	14.177	0.144	0.198
45%	0.389	0.060	13.997	6.786	12.094	17.173	0.119	0.163
50%	0.438	0.053	15.751	6.735	15.314	21.746	0.094	0.129
55%	0.508	0.046	18.275	6.671	20.616	29.275	0.070	0.096
60%	0.616	0.038	22.165	6.587	30.326	43.063	0.047	0.065

Table 2.1: Concentration changes as a function of compression as predicted by donnan theory. Bath concentrations indicated are those of Dulbecco's Modified Eagles culture medium. The starred columns for Ca^{++} and SO_4 take into account the distribution coefficients reported by Maroudas and Evans [1972]. See text for additional details.

comparison with the Donnan predictions.

Donnan theory describes ionic equilibrium in a macroscopic sense, assuming a uniform distribution of fixed charge and electrolyte ions. Since the cells comprise a relatively small and perhaps exclusive region of the tissue, the applicability of Donnan theory to predicting ionic distributions in the immediate vicinity of the cell needs to be addressed.

On a molecular scale, mobile ions will distribute themselves about the fixed charge according to the Poisson-Boltzman relation. This exponential relation has a decay length, known as the debye length, on the order of 1 nm at physiological ionic strength. This implies that the cell must be closely associated with the matrix material if it is to be affected by compression induced ionic changes. This is not unlikely. GAG spacing is on the order of 1 nm allowing electrostatic interaction between adjacent GAG chains and giving the tissue its tendency to swell. A restraining mesh surrounding the cell would be necessary to keep GAGs from being close to the cell.

Both light and electron microscopy show that the molecular environment in the immediate vicinity of the cell appears to be distinct from the rest of the extracellular matrix. Toluidine blue and hematoxylin and eosin staining is most intense pericellularly (figure 2.6), consistent with a relatively high concentration of fixed charge groups. The cells reside in lacunae which appear much larger than the cell. This is generally believed to be a fixation artifact obscuring the extent to which the cell membrane comes in contact with the pericellular

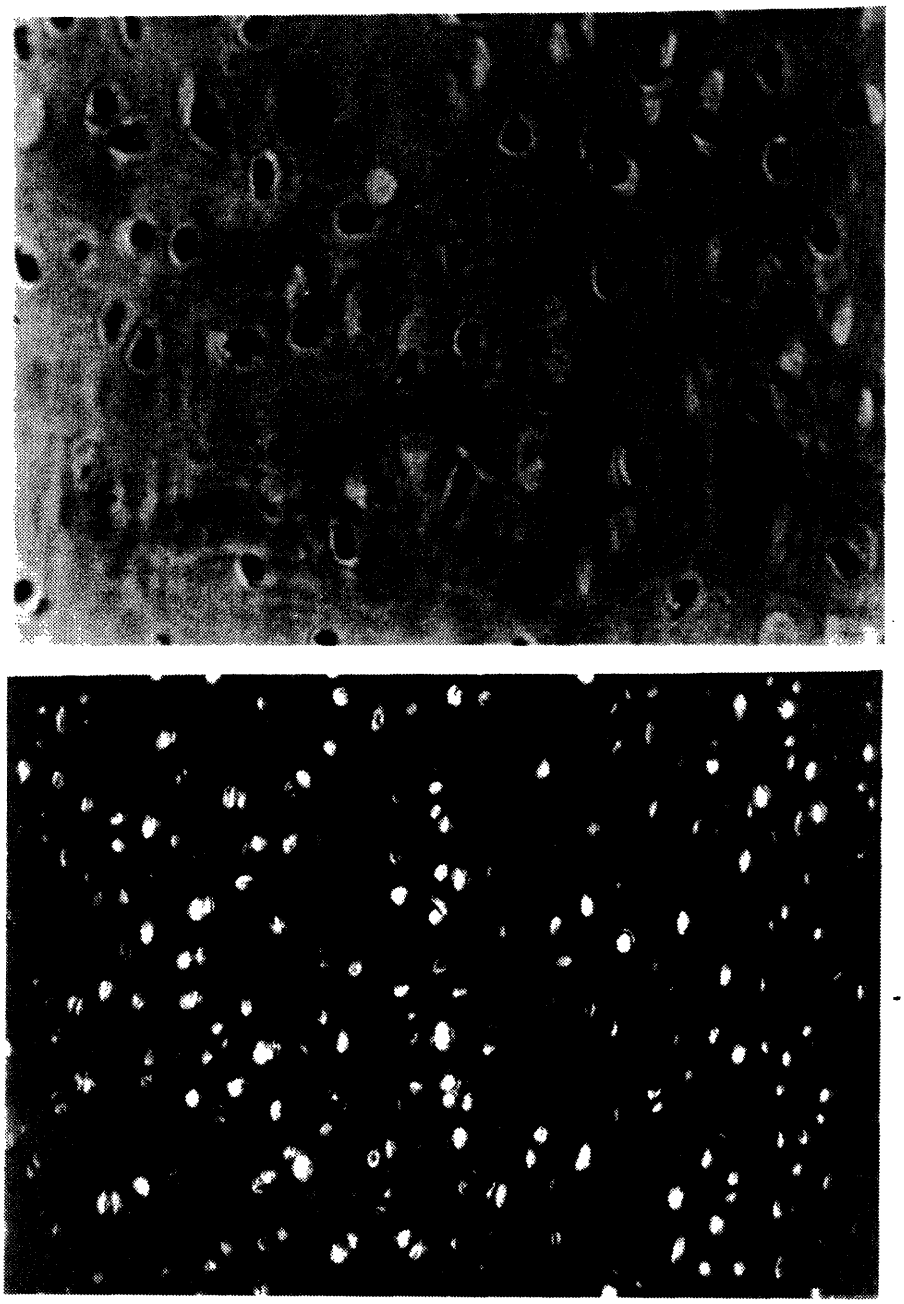

Figure 2.6: Reserve zone epiphyseal plate cartilage sections stained with hematoxylin and eosin (a) and toluidine blue (b). The region immediately surrounding the chondrocytes stains more intensely and has been shown by electron microscopy to by high in GAG content.

shell. Poole et al. [1984] extensively describe the transmission electron microscopic appearance of articular cartilage. The cells are surrounded by a pericellular region, approximately 1 μm thick, which has the granular appearance of GAGs. A concentric collagenous shell encloses this region. This pericellular matrix appears to be intimately associated with the cell. Since the pericellular components are not lost during fixation, it is presumed that they are connected in some way to the tissue structure.

Maroudas and Evans [1972] used an approach based on Donnan theory to determine if there are significant regions of cartilage which have a low fixed charge density (FCD). In a more complete form, equilibrium is given by:

$$\gamma_i^2[Na]_i[Cl]_i = \gamma_e^2[Na]_e[Cl]_e$$

The internal concentrations (denoted by the subscript (i)) were measured experimentally following equilibration of the cartilage in a bathing solution (concentration denoted by subscript (e)). This allowed calculation of the internal activity coefficient, γ_i. For experiments performed at low ionic strength, the activity coefficient is very sensitive to regions of inhomogeneity. If there were regions of low FCD, this bulk experiment would tend to underestimate the activity coefficient. Their data at a bath concentration of 0.01 M is consistent with a region of high FCD comprising 80% of the volume, the remaining 20% being low in FCD. The 1 to 10% of the volume normally occupied by cells [Stockwell and Meachim, 1972] is expected to have no fixed charge. Further increases in charge-free volume are expected from the increased

swelling seen at low ionic strength. Extrapolation of Eisenberg's data [1983] shows that adult bovine articular cartilage will swell between 1 and 10% of its thickness in normal saline when incubated in a 0.01 M bath.

Each of these reports is consistent with the postulate that the cells are in intimate contact with a region of fixed charge so that the dramatic adjustment of electrolyte composition expected as the tissue is compressed will occur in the immediate vicinity of the cell. Therefore, the compression induced changes in interstitial concentration are considered as a possible output signal of the mechanical unit.

2.3.7.2 Solute Exclusion

The effect of consolidation on solute exclusion represents another output of the mechanical unit. Heinegard and Paulsson [1984] state that regulation of diffusion and flow of macromolecules through connective tissues is a function ascribed to proteoglycans. Solute exclusion will occur when the regions of tissue available for solute movement become too small. This exclusion is clearly dependent on solute size, structure, and charge. In free swelling cartilaginous tissues, solutes with radii greater than 6 nm are virtually excluded [Granger, 1978]. If the tissue were compressed by 50%, the theory of Ogston et al. [1973] suggests that solutes over 4 nm in radius would be completely excluded. To put these numbers in perspective, note that albumin and sucrose have effective radii of 3.8 nm and 1 nm, respectively. There are a number of investigators who have suggested, and documented histologically, the

existence of channels in interstitial tissues [Casley-Smith, 1978 and Broom and Myer, 1980]. In fact, Broom and Myer found that these channels remained essentially the same size even after compression by a load sufficient to deform chondrocytes (250 kPa).

While macroscopic measurements suggest substantial solute exclusion by cartilaginous tissues, the presence of channels may minimize the physiological significance.

2.3.7.3 Solute Diffusion

The ability of solutes to diffuse through the matrix is also likely to be affected by consolidation. As exclusion of solute becomes significant, its diffusion rate will be similarly affected. Changes in diffusivity not only affect the rate at which nutrients and waste products are transported to and from the cell, but also determine the time it takes to achieve Donnan equilibrium. Maroudas and Evans [1974] found that the diffusion coefficient for sulfate in free swelling cartilage was identical to that in solution. This suggests that co-ions and water diffuse unhindered, at least in uncompressed tissue. Stambaugh and Brighton [1980] studied the diffusion of sucrose and inulin in rabbit and rat growth plates. Diffusion coefficients for inulin (7000 mw) and sucrose (340 mw) were very similar in the reserve zone, suggesting that diffusion was unhindered by the matrix. Their coefficients were significantly higher than those measured by Maroudas [1970]. Maroudas also found that diffusion of albumin in adult articular cartilage was approximately 20% of that in free solution. Stambough and

Brighton found that diffusion in the hypertrophic and proliferative zones was significantly lower than in reserve zone or hyaline cartilage. These results indicate that for many biological solutes diffusion rates in cartilage are somewhat lower than those in free solution and are likely to be further diminished by consolidation.

There are a number of theoretical approaches one may take to predict the effect of compression on diffusion of solutes. If the solute is small compared to the matrix fibers and the spaces between the matrix components, then the matrix can be considered as a network of obstacles. The relative diffusion constant, $\frac{D}{D_o}$, as a function of solid volume fraction, V_s, is given by [Ogston et al., 1973]:

$$\frac{D}{D_o} = (1 + \alpha V_s)^{-2}$$

where the coefficient, α, depends only on the geometry of the obstacles. In free swelling tissues the diffusion of small solutes is essentially unhindered. Assuming that in this case $\frac{D}{D_o} = 0.99$ and the solid volume fraction $V_s = 0.2$ we conclude that $\alpha = 0.025$. If α remains constant as the tissue is compressed, then for a 50% compression (which leads to an increase in volume fraction to $V_s = 0.4$) $\frac{D}{D_o}$ is computed to be 0.98.

In free swelling tissue the spaces between GAG molecules are on the order of 1 nm and molecules with radii over 6 nm are virtually excluded, so as the tissue is compressed, the assumption that the solute is much smaller than the spaces between the matrix becomes increasingly invalid. Ogston et al. [1973] developed an alternative theoretical model which takes into account the effect of changing pore size. In their

model, the relative diffusion coefficient is:

$$\frac{D}{D_o} = e^{-[(r_s+r_f)/r_f]\cdot(\bar{V}_f C_f)^{\frac{1}{2}}}$$

where r_s and r_f are the solute and fibril radius, respectively, $\bar{V}_f$ is the partial specific volume of fiber, and C_f is the mass concentration of fiber ($V_s = \bar{V}_f C_f$). In the limit of $r_f >> r_s$ then $\frac{D}{D_o} = e^{-\sqrt{V_s}}$. This predicts that the ratio of D to D_o ranges from 0.6 to 0.5 for V_s ranging from 0.2 (free swelling) to 0.4 (50% compression).

Mackie and Meares [1955] considered the effect of a change in hydration on the average path length taken by a diffusing solute. They argued that the average path length in a homogeneous swollen gel was increased by a tortuosity factor $\theta = \frac{(1+V_s)}{(1-V_s)}$. The apparent diffusivity is decreased by an amount proportional to the square of the increased path length. Thus, from their model:

$$\frac{D}{D_o} = \theta^{-2} = \frac{(1-V_s)^2}{(1+V_s)^2}$$

In free swelling cartilage with a solid fraction of 20%, this model would predict the diffusivity of small solutes to be decreased to 44% of the value in infinitely dilute solutions. When the solid fraction is increased to 40%, the diffusivity would drop to 18% of the free solution value.

Experimentally, the diffusivity of small solutes in free swelling epiphyseal plate cartilage seems to be near its value in infinite dilute solution [Stambaugh and Brighton, 1980]. This is inconsistent with the predictions of either the Mackie and Meares or Ogston model. Maroudas [1970], however, reports that diffusivity of small solutes in adult articular cartilage is 40% to 50% of D_o as would be predicted from the

Mackie and Meares model. Maroudas [1970] determined experimentally that the the diffusion coefficient for albumin in cartilage is 0.2 times that in free solution. Mackie and Meares predict a 60% reduction. If albumin has an effective radius twice that of the fibrils and maintains a solid volume fraction of 0.2, then the Ogston model would predict a 74% reduction in diffusivity.

In summary, for the large solutes (greater than 1 nm) it is likely that diffusivity is a strong function of the degree of compression. It is considerably less clear how the diffusivity of the smaller solutes will be affected. If there are channels which are unaffected by compression, the diffusivity changes may be minimal.

2.3.8 Summary

In summary, when cartilage (or any connective tissue) is subjected to a load, a hydrostatic pressure is developed which drives the redistribution of fluid, thereby allowing the matrix and cells to deform. The fluid will entrain counter-ions establishing an electric field. The increased charge density will cause ions to redistribute, changing the concentration of salts, pH, etc. Furthermore, nutrients may be redistributed, excluded, or hindered in diffusion. Any one or more of these tightly coupled events have been suggested as output signals. In the next section, they will be considered as input signals to the cellular unit. In terms of the kinetics, tissue deformation in response to a step occurs with a characteristic mechanical diffusion time τ_m. The concentration changes which occur with consolidation require a diffusion

time τ_d. Chemical equilibrium will occur at a rate dominated by the longer of the two time constants.

2.4 The Cellular Unit

Next consider the response of the cells to the output signals of the mechanical unit. The output of the cellular unit is presumed to be an alteration in one or more of the major functions of a cell: replication, energy production, motility, synthesis, communication, and import and export. Since the extracellular matrix is known to adapt to a change in the mechanical loading, the synthetic activities are very likely altered and so much of the experimentation in this area has been directed toward detecting an alteration in the processes of matrix synthesis.

In the following sections, each of the output signals discused in section 2.3 is treated as an input signal to the cell, citing relevant examples from the literature.

2.4.1 Input Signal: Cell Deformation

Cell deformation could be detected by a number of mechanisms including motion of a specialized appendage which acts as a "mechanoreceptor", a generalized change in membrane tension, or motion of the cytoskeleton.

The hair cells of the auditory system provide a physiological precedent for "mechanoreceptors". These specialized cells release

neurotransmitter in response to motion of the hair bundle residing on the cell membrane. In humans, these cells are able to detect frequencies in the range of 20 - 20000 Hz. A proposed mechanism is that the hair motion leads to tension in cell membrane proteins, thereby altering ion channel characteristics which in turn initiate a response [Holton and Hudspeth, 1983]. Using patch clamping techniques, Corey et al. [1984] have demonstrated changes in Ca^{++} channel activity in response to changes in membrane tension.

The stretch receptors associated with skeletal muscle provide one other example of mechanoreception. The receptor structure, also known as a muscle spindle, is made up of an encapsulated complex of afferent nerve endings wrapped around a spindle fiber (modified muscle cell). This class of receptors provide information regarding the magnitude and speed of muscle stretch and are necessary for the control of muscle activity [Vander et al., 1975].

Some evidence from the literature suggests that cell deformation modulates connective tissue cell activity. The method used in these studies was to plate cells on a deformable substrate and then subject the substrate to cyclic stretching. Rabbit aortic smooth muscle cells (SM) [Leung et al., 1977] and embryonic chick chondrocytes (CH) [Lee et al., 1982] plated on purified elastin membranes increased synthesis of proteins (SM and CH), GAGs (CH), and DNA (SM) during an 8 hour exposure to a 10% cyclical stretch at 1 Hz. Yeh and Rodan [1984] found that prostaglandin E synthesis by fetal rat calvarial cells cultured on collagen tape was enhanced 3.5-fold when the tape was stretched only 8

to 10 times in a 2 hour period. A stretch of 5-10% was imposed over 15 minutes, and the collagen was then allowed to quickly relax. They postulate that the response mechanism involves opening of ion channels and activation of adenylate cyclase. This hypothesis is consistent with the results of the patch clamping studies which show an increase in channel conduction under tension.

2.4.2 Input Signal: Hydrostatic Pressure

The biologic response to hydrostatic pressure has been under study for many decades, typically in the context of deep sea physiology and mechanisms of anesthetic activity. As reviewed by Winter and Miller [1985], pressure can be directly correlated with anesthetic effect (or cellular excitability). R.A. Smith et al. [1984] have advanced the hypothesis (known as the critical volume hypothesis) that the potency of a given anesthetic is related to the increase in membrane volume resulting from dissolution of anesthetic in the membrane. Compression of the membrane by pressure will decrease the membrane volume and thereby nullify the anesthetic effect. When the membrane volume is reduced from normal, a state of excitability is reached. Mice exposed to pressures of approximately 5 MPa exhibited coarse tremors, while those exposed to 10 MPa experienced tonic convulsions often leading to death.

At a cellular level, hydrostatic pressure is believed to affect the the organization of lipid bilayer by bulk compression and changes in protein hydration [MacDonald, 1984]. Changes in passive and active transport, membrane excitability, and synaptic transmission have been

demonstrated in response to increased hydrostatic pressures. [For review, see MacDonald, 1984.] For example in erythrocytes with active transport blocked, a 10 MPa pressure increased K^+ influx by 20%. Pressure generally decreases action potential kinetics and inhibits synaptic transmission.

Pacinian corpuscles represent specific pressure receptors which are found in dermis, muscle connective tissue, periosteum and gut mesentery. The corpuscle has been shown to act like a bandpass filter, with a peak sensitivity at around 200 Hz [Shepherd, 1983].

An example of sensitivity to pressure in non-excitable cells has been reported by Tilney [1979]. The microvilli of the intestinal mucosa of the salamander will retract when exposed to a hydrostatic pressure of 47 MPa. The physiologic significance of this response is unclear; however, the fact that the microvilli reformed upon removal of the pressure suggests that it was a physiological rather than pathological response.

Evidence for a response to pressure by the chondrocyte is conflicting. Subjecting calf articular cartilage to hydrostatic pressures, Lippiello et al. [1985] found that GAG synthesis over four hours was depressed by pressures between 0.5 and 2 MPa and returned to normal within 15 minutes of load removal. When the pressure was increased to 2.5 MPa, synthesis was essentially normal but after pressure removal, synthesis exceeded control levels for at least 24 hours.

Kimura et al. [1985] used a similar preparation to examine the

biosynthetic response of bovine articular cartilage to hydrostatic loading. In contrast to Lippello's work, they found no difference in synthetic activity between experimental and control samples for loads up to 2.75 MPa applied for up to 4 days.

Van Kampen et al. [1985] compressed the gas phase (5% CO_2 in air) over embryonic chick explant and high density chondrocyte cultures using a 0.3 Hz, 13 kPa square wave. GAG synthesis assessed during a 12 hour loading period was increased to 1.4 to 2 times control levels. Because pressures were achieved by compression of the gas phase, the concentration of dissolved gasses also changed and may have accounted for the synthetic response.

2.4.3 Input Signal: Fluid Flow

There are systems in which fluid flow has been shown to modulate synthesis, although the flow rates used are significantly greater than the less than μm/s rates expected to occur in deforming cartilage. Both smooth muscle cells [Leung et al., 1977] and chondrocytes [Lee et al., 1982] cultured on elastin membranes demonstrate enhanced synthesis when agitated. Leung et al. [1977] report a consistent increase in 8 hour ^{14}C-proline and ^{3}H-thymidine incorporation over up to 2 days of repetitive linear agitation with peak flow rates of 3 cm/s. Lee et al. [1982] found that 8 hours of agitation enhanced chondrocyte protein and GAG synthesis, using a similar preparation.

2.4.4 Input Signal: Streaming Potential

The presence of mechanically induced currents or potentials has led several investigators to study the response of tissues to applied electrical forces both *in vivo* and *in vitro*. There is no specific "electroreceptor" known in mammals; however, some aquatic species are able to navigate on the basis of such a receptor [e.g. marine elasmobranch, Kalmijn, 1982]. Studies of connective tissue preparations have focused on the mitogenic and biosynthetic response to applied electrical fields over a wide frequency and amplitude range with varying results. A few are summarized here to illustrate the diversity of systems and results.

In a study using fibroblast populated collagen gels, McLeod [1986] induced a depression in protein synthesis during a 12 hour exposure to currents well within the range of those produced by streaming mechanisms (1 $\mu A/cm^2$, 0.1 - 1000 Hz). In this system, the response exhibited a frequency dependence (peak sensitivity around 10 Hz), but the response was independent of amplitude above a threshold stimulus,

Rodan et al. [1978] observed enhanced DNA synthesis by chick chondrocytes in suspension using a capacitively coupled field pulsed at 5 Hz. In a similar preparation [Norton et al., 1977] these investigators had previously demonstrated increased cyclic AMP content in chick tibiae exposed to fields. The induced current densities are calculated to be well under 1 $\mu A/cm^2$. using provided and estimated values for dimensions.

Brighton et al. [1982] found that protein synthesis was enhanced and GAG synthesis depressed in chondrocyte pellet cultures exposed to a

37 $\mu A/cm^2$, 60 kHz current.

In contrast, chondrocytes cultured on elastin membranes demonstrated enhanced GAG synthesis when exposed to 1 $\mu A/cm^2$ at 60 Hz [Lee et al., 1982].

2.4.5 Input Signal: Consolidation

Consolidation was shown in section 2.3.7 to lead to changes in interstitial ion concentrations, and to possible exclusion and decreased diffusibility of solutes. This section addresses the possible consequences these changes may have on cell behavior in tissues experiencing consolidation.

2.4.5.1 Cell Volume

The first consequence considered is that the increase in ionic concentration could result in a decrease in cell volume. From the concentration changes predicted as described in table 2.1, a 50% compression is seen to cause a 25% increase in osmolarity. This would lead to an 20% decrease in cell volume assuming only water traverses the cell membrane to establish balance in osmolarity.[4] The mechanisms of cell volume regulation are not well understood, but Macknight and Leaf

---

[4] From table 2.1 the ratio between total extracellular ionic concentration at 50% compression and that at 0% compression is:

$$\frac{([Na]+[Cl])_{50\%}}{([Na]+[Cl])_{0\%}} = 1.25$$

If the cell loses 20% of its water, intracellular ionic concentration will also rise to 1.25 times the original concentration.

[1980] suggest that there are processes which counteract the purely osmotic flow. Among those processes suggested are variations in the properties and contents of intracellular constituents and alterations in passive membrane permeability and active transport. For example, duck erythrocytes incubated in hyperosmotic media will shrink. However, if the potassium concentration is increased, cell volume will increase towards normal [Kregenow, 1971].

2.4.5.2 Membrane Potential

The membrane potential is believed to be of prime importance in cell physiology. Two output signals from the mechanical unit are capable of modifying this potential. The electric fields produced by the fluid streaming discussed above are excluded by the insulating cell membrane resulting in an alteration of the cell membrane potential. This perturbation in transmembrane potential is proportional to $E_o L/2$ where E_o is the external field and L is the cell diameter. For 10 μm diameter chondrocytes exposed to 1.5 mA/cm^2 currents in a media of conductivity 1.5 mho/m the change in transmembrane potential is calculated to be on the order of 50 μV. This additional potential would be imposed on the normal membrane potential of approximately -70 mV.

The cell potential in many cell types approaches the potassium diffusion potential, and so a change in extracellular potassium concentration should also result in a change in the membrane potential. Assuming that cells in unstrained tissue have a typical potassium diffusion potential of -98 mV [Hille, 1984] and extracellular potassium

is 8.6 mM (table 2.1) then the intracellular potassium concentration is calculated from the Nernst equation to be approximately 250 mM[5]. When a 50% compression is induced, extracellular potassium rises to 15.8 mM. If the intracellular potassium has not changed, the the change in extracellular potassium will depolarize the cell membrane by 18 mV. A depolarization of this magnitude is sufficient to modify membrane protein activity in excitable cells [Hille, 1984]. If chondrocyte membranes contain Na-K-ATPase ion exchange pumps similar in character to nerve, muscle, and red blood cells, then this rise in extracellular potassium will result in increased pump activity and a subsequent repolarization of the cells.

2.4.5.3 pH

The tight control of pH maintained *in vivo* lends credence to the view that pH is critical for normal cell behavior. Furthermore, most chemical processes of importance in biology exhibit a significant pH dependence. Therefore, the drop in pH which is predicted by Donnan theory to occur upon tissue consolidation could conceivably regulate cell behavior either directly or indirectly by altering enzyme activity. The synthesis of GAG by human chondrocytes in monolayer culture as a

---

[5]This and the following calculation were done using the Nernst equation [Hille, 1984]:

$$E_k = \frac{RT}{F} \ln \frac{[K]_o}{[K]_i}$$

where E_k is the potential resulting from potassium gradients, and the subscripts (o) and (i) indicate, respectively, the potassium concentration outside and inside the cell.

function of pH has been reported by Schwartz et al. [1976]. They found that ^{35}S-sulfate incorporation increased three fold when the pH of the medium was raised from 7 to 8.

2.4.5.4 Nutrient concentration

In addition to electrolytic changes, compression may dramatically alter the concentration of nutrients. Amino acids, for example, will be excluded or concentrated depending on their charge. Sulfate, an essential constituent for sulfated GAG synthesis, is largely excluded because of its divalent negative charge. Ito et al. [1982] investigated PG production by embryonic chick epiphyseal cartilage under various concentrations of sulfate. They found that one specific type of sulfated PG (PG-H) required a minimum sulfate concentration of 300 μM to achieve full sulfation. They previously reported [Sobue et al., 1978] that fully sulfated chondroitin sulfate synthesis by chick embryonic sternal cartilage required a minimum of 30 μM sulfate. Below these minima, sulfation was proportional to sulfate concentration above a threshold of 3 μM, where the synthesized GAGs were essentially unsulfated.

Maroudas and Evans [1974] also studied the dependence of sulfate incorporation on bath sulfate concentration. They found that incorporation was independent of the sulfate concentration in the bathing medium above 300 μM and 500 μM for adult human and cow, respectively. (Compare this result to the 500 μM sulfate concentration found in human serum and synovial fluid [Diem and Lentner, 1970].) A critical internal sulfate concentration can be estimated from Donnan

theory and the sulfate distribution coefficient of 1.37 reported by Maroudas and Evans [1972]. An internal sulfate concentration of 270 μM would be expected for cartilage with .15 M fixed charge bathed in normal saline with 500 μM SO_4. If the bath contained 800 μM sulfate (the concentration in most culture media preparations), a compression of over 35% would result in internal concentrations below the critical level (see table 2.1).

2.4.5.5 GAG concentration

The final "concentration" change considered as a consolidation-induced input signal to the cell is that of changing the GAG concentration directly. Many authors believe that GAG plays a regulatory role in chondrocyte behavior. Investigators study this role in one of two ways: (1) by adding exogenous GAG to the bathing medium and (2) by enzymatic removal of tissue GAGs. The GAGs of rabbit articular cartilage will leach out of the tissue relatively easily when maintained in culture. Sandy et al. [1980] found that this loss was accompanied by an increase in the rate of GAG synthesis. When exogenous GAG was added to the culture medium, or when the tissue was cultured inside dialysis tubing, the synthetic rate remained constant, suggesting that the concentration of GAGs was a major determinant in chondrocyte synthetic behavior.

Huang [1974] treated chondrocytes in monolayer culture with testicular hyaluronidase or chondroitinase AC. While overall synthesis of DNA and protein were not affected, GAG synthesis dropped to 30% of

controls. In a later publication Huang [1977] noted that synthesis returned to normal after 48 hours, suggesting that the response may have been due to removal of cellular coat proteins.

The synthetic behavior of chick embryonic cartilage explants in response to testicular hyaluronidase was investigated by Hardingham et al. [1972]. In contrast to Huang's results in monolayer, they found that GAG synthesis was enhanced following enzymatic treatment.

These studies are not sufficient to demonstrate that the chondrocyte is able to sense GAG concentration directly. Heinegard and Paulsson [1984] point out that the polyanionic character of GAGs may lead to binding of cationic amines, and proteins essential for regulation of cell function. Furthermore, a change in GAG concentration is necessarily accompanied by changes in tissue deformation and intra-tissue electrolyte composition. If GAGs are physically excluded, the addition of exogenous GAGs will constrain the ionic distribution (according to Donnan), tending to equalize the mobile ion concentrations within and outside of the tissue. Schneiderman et al. [1986] recently reported that sulfate incorporation varied inversely with the osmolarity of the medium. Their bathing solution contained polyethelyne glycol and chondroitin sulfate, which were excluded from the articular cartilage specimen by means of a dialysis bag. The tissue was equilibrated under free swelling conditions so that the fixed charge density as well as ionic concentrations changed as the osmolarity was varied.

2.4.6 Bandpass description of cellular unit

Physiologically, connective tissues appear to adapt over a period of weeks to years. Because the kinetics of the instigating signal are unknown, the slow tissue adaptation provides no clues as to the kinetics of the cell response. If the "signal" is present throughout the remodeling period, then perhaps the cells are capable of "tracking" its input. The fact that the change in serum Ca^{++} occurs soon after weightlessness and soon after return to normal gravity supports this [Morey-Holton and Arnaud, 1985]. Alternatively, there could be instigating events from which the cells do not return to their unstimulated state for many hours or days. Rubin and Lanyon [1982] see remarkable increases in bone mass resulting from only 18 seconds per day of stimulation. Clearly this response did not occur only during the exposure period.

If we attempt to look at a more cellular level, many of the signals discussed in the preceding sections could directly alter a membrane process, such as channel permeability. The direct effect of this would be immediate. However, it is unclear how and how fast that event would lead to an alteration in the extracellular matrix. The concept of a moving setpoint or tolerance is a physiologic baseline correcting behavior exhibited by many systems. Existence of baseline correction implies that the response to a static input will eventually die away as is seen, for example, with the response by Pacinian corpuscles [Shephard, 1983] to a step in pressure. Certainly, there exists some frequency above which the cell can not sense and will

therefore ignore. The cellular unit, therefore is presumed to have bandpass characteristics. An example of the frequency and step response of a bandpass filter is depicted in figure 2.7 for a system with different rise and decay time constants. Conceptually the rise time, τ_{c_on} of the step response is associated with the rate at which a cell can alter its output in response to the signal while the apparent delay and fall rate, τ_{adapt} is associated with adaptation.

2.5 The Output Conditioning Unit

This element is in part an experimentally defined unit which describes the relationship between the actual cell output and the experimental detection capability. For example, in the case of in vivo studies, growth is commonly measured. Growth represents the accumulation and organization of cells and extracellular material, so in a sense, the output conditioning unit could be considered an integrator where the integration constant depends on the degree of organization. Particularly in multicellular systems, sufficiently sensitive techniques do not exist to measure many biological outputs directly. So the testable output is generally represented by an accumulation of a product.

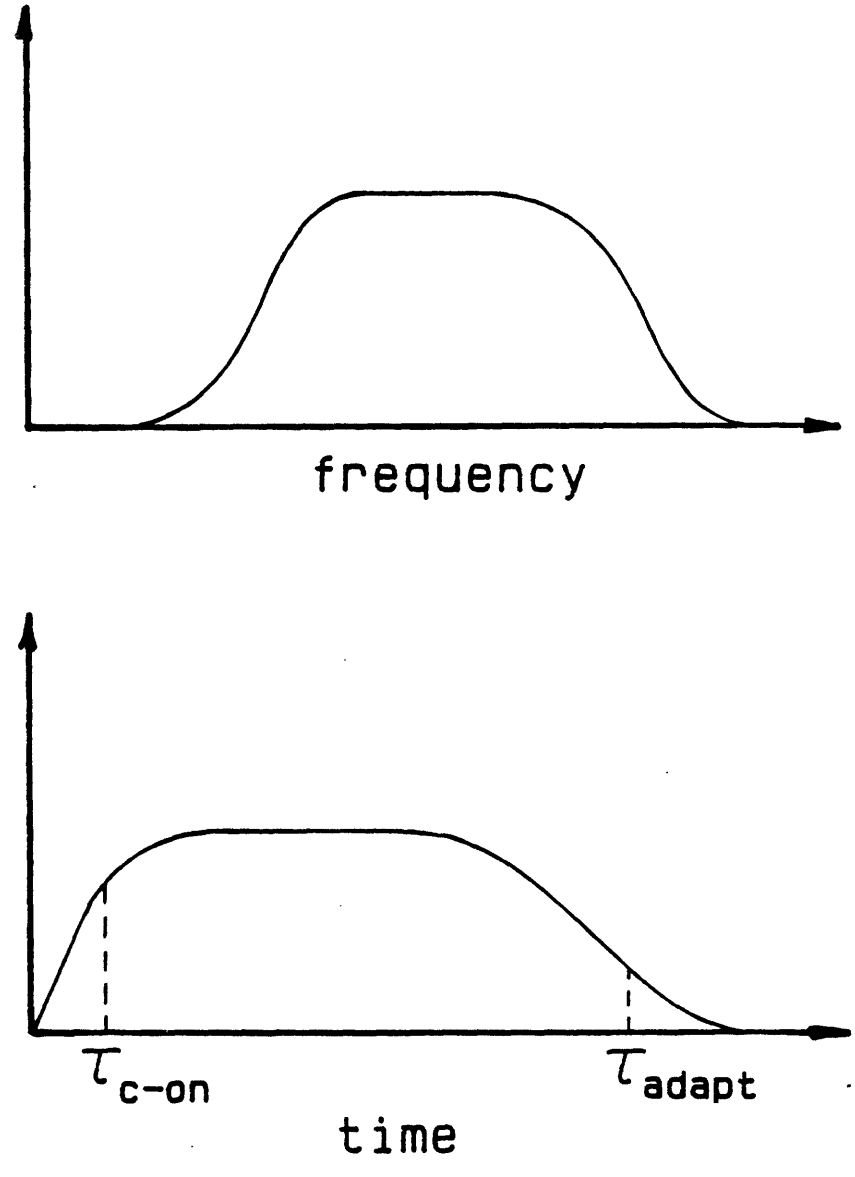

Figure 2.7: The cellular unit is presumed to have bandpass characteristics. The upper graph show the typical frequency response of a bandpass filter. The lower graph shows the step response of a bandpass filter which requires a turn-on time τ_{t-on} and which eventually dies away with a characteristic time τ_{adapt}.

2.6 Experimental Configurations

Sections 2.3.3 through 2.3.7 proposed several outputs signals of the mechanical unit S(t,x,y,z) which may be recognized as input signals by the cellular unit. This identification of signals suggests several experimental configurations which might elucidate mechanisms by which cells sense deformation. In this section possible experimental configurations are discussed in terms of the associated output signals of the mechanical unit, feasibility, relevant time parameters, and potential for interpretation. The discussion focuses on equilibrium tissue behavior in response to a static applied signal in a uniaxial geometry. While physiologic signals are undoubtedly nonuniform, dynamic, and non uniaxial, this presentation can more clearly illustrate the types of behavior possible.

2.6.1 Bulk equations of motion

The experimental configurations involve changing boundary conditions on electromechanical behavior in uniaxial (confined) compression. Therefore, the general stress and constitutive laws are first presented. For a more general formulation, see Frank and Grodzinsky [1986b].

In one dimension, the compressive stress σ can be written in terms of the compressive strain, ε, bulk longitudinal modulus, H_A, and fluid pressure, P_f:

$$\sigma = H_A \varepsilon + P_f \qquad (1)$$

The tissue displacement, u(z) is related to the strain by:

$$\varepsilon(z) = - \frac{\partial}{\partial z} u(z) \tag{2}$$

In the absence of inertial effects, the divergence of the stress is zero, so that:

$$\frac{\partial \sigma}{\partial z} = 0 = - H_A \frac{\partial^2}{\partial z^2} u(z) + \frac{\partial}{\partial z} P_f \tag{3}$$

The flow of fluid relative to the matrix can be written as:

$$U(z) = U_o - \frac{\partial}{\partial t} u(z) \tag{4}$$

Incompressibility requires that the divergence of U be zero. In one dimension:

$$\frac{\partial}{\partial z} U = 0 \tag{5}$$

Likewise, for conservation of charge:

$$\frac{\partial}{\partial z} J = 0 \tag{6}$$

The relationship between fluid flow, U, current density, J, fluid pressure. gradient, $\frac{\partial}{\partial z} P_f(z)$, and voltage gradient, $\frac{\partial}{\partial z} V(z)$ can be expressed by a set of first order, linear equations [DeGroot and Mazur, 1969] :

$$\begin{bmatrix} U(z) \\ J(z) \end{bmatrix} = \begin{bmatrix} -k_{11} & k_{12} \\ k_{21} & -k_{22} \end{bmatrix} \frac{\partial}{\partial z} \begin{bmatrix} P_f(z) \\ V(z) \end{bmatrix} \tag{7}$$

where k_{11} is the "short circuit" hydraulic permeability, k_{22} is the electrical conductivity, and k_{12} and k_{21} are the electrokinetic coupling coefficients.

For a number of the experimental configurations, it is useful to solve the matrix equation (7) for U in terms of the pressure gradient

and current density.

$$U = - k\frac{\partial}{\partial z} P_f - k_i J \tag{8}$$

where $k = k_{11} - \frac{k_{12}k_{21}}{k_{22}}$ is the Darcy ("open circuit" permeability), and $k_i = \frac{k_{12}}{k_{22}}$. The equation of motion (3) can then be written as:

$$0 = H_A k \frac{\partial^2}{\partial z^2} u(z) + k_i J + U \tag{9}$$

For each experimental configuration, the equilibrium solution to the following set of equations subject to the appropriate boundary conditions provide expressions for the resulting "hypothetical signals". Specifically, strain ($\varepsilon(z)$), fluid flow (U), current density (J), and pressure (P_f) are of interest.

$$\sigma = H_A \varepsilon(z) + P_f(z) \tag{1}$$

$$\varepsilon(z) = - \frac{\partial}{\partial z} u(z) \tag{2}$$

$$0 = - H_A \frac{\partial^2}{\partial z^2} u(z) + \frac{\partial}{\partial z} P_f(z) \tag{3}$$

$$0 = H_A k \frac{\partial^2}{\partial z^2} u(z) + k_i J + U \tag{9}$$

$$U = - k\frac{\partial}{\partial z} P_f(z) - k_i J \tag{8}$$

$$U = U_o + \frac{\partial}{\partial t} u = U_o \tag{4}$$

$$0 = \frac{\partial}{\partial z} J \tag{6}$$

In the uniaxial configuration one electrical and two mechanical boundary conditions are required at each surface. To emphasize that at equilibrium fluid flow, U, and current density J be independent of z (see equations (4) and (5)), these quantities U(z) and J(z) are consistently written as U and J, respectively.

2.6.2 Experimental Configuration: Applied Static Load

A configuration commonly used for studying the material response is that of confined compression shown previously in figure 2.3. The bottom surface is pinned and fluid flow can occur only in the z direction through the top surface. Thus the mechanical boundary conditions are no displacement and no fluid flow at the bottom, atmospheric pressure and applied stress at the top. The electrical boundary conditions are no current at either the top or bottom (open circuit). Specifically:

Mechanical B.C.: $u(z=0) = 0$

$U(z=0) = 0$

$P_f(z=\delta) = 0$

$\sigma(z=\delta) = \sigma$

Electrical B.C.: $J(z=0,\delta) = 0$

Using (1) and (2) we find that:

$$u(z) = -\frac{\sigma}{H_A} z$$

$$\varepsilon(z) = \frac{\sigma}{H_A}$$

$$P_f(z) = \sigma - H_A \varepsilon(z) = 0$$

$$U = 0$$

$$J = 0$$

The signals resulting from an applied step load were discussed in section 2.3.1. and are summarized here in figure 2.8. Note that for a step load, after the mechanical relaxation time, τ_m, strain (cell deformation and consolidation) is uniformly distributed throughout the tissue, thereby eliminating the spatial dependence of $S(t,x,y,z)$. If

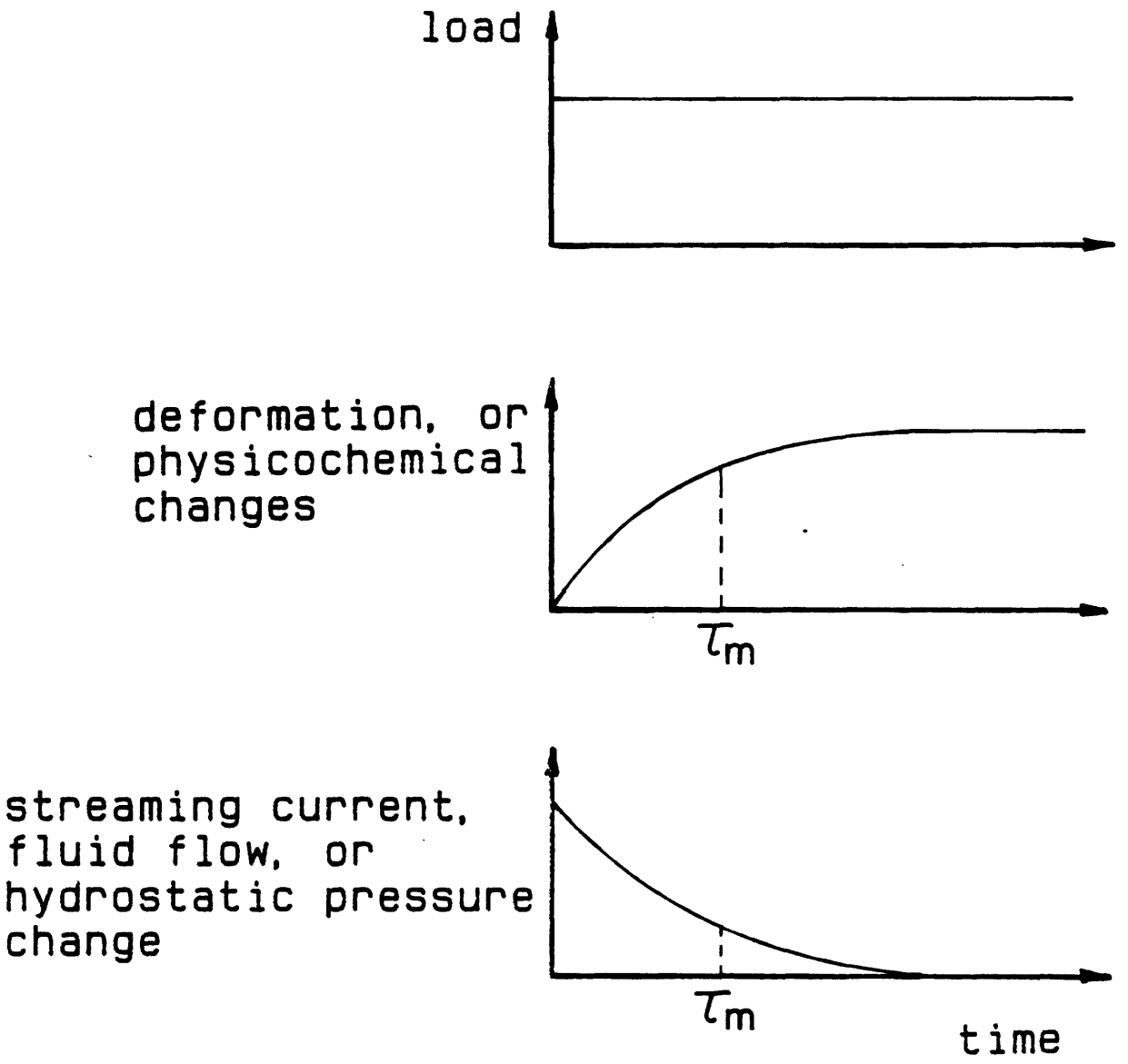

Figure 2.8: A step load is applied under open circuited, uniaxial confined compression conditions. Output signals are shown as a function of time. Note that until equilibrium has been reached, consolidation, fluid flow, and streaming potential vary spatially within the tissue. τ_m represents the time required to reach equilibrium.

fluid flow, streaming potential, or hydrostatic pressure is important to the cellular response, then the response kinetics are likely to be very different than if deformation or consolidation signals dominate.

For cyclical applied loads, fluid flow, streaming potential, and hydrostatic pressure are present. In practice, a cyclical mechanical stimulus must be superimposed on is required to have a net constant stimulus. As discussed in section 2.3.1, in this configuration, frequencies in the physiologic realm result in oscillatory displacements that are confined to the upper regions of the tissue. This indicates that it takes a finite time for the deformation to diffuse through the tissue. Similarly, fluid flow and streaming potential are greatest in the upper region. Thus, interpretation of the response to a dynamic mechanical load requires both an understanding of the response to the static component and a means for dealing with the spatial variations.

2.6.3 Experimental Configuration: Applied D.C. Current

If streaming potential governs the cellular response to loading, then this can be tested in a configuration in which one controls the potential. However, just as compression can lead to electrical currents, electrical currents can lead to tissue deformation. Thus, it is important to examine the relevant boundary conditions for this experimental configuration. Two possible configurations are considered. First, a current density J is imposed under the same mechanical boundary conditions as for section 2.6.2 with zero applied stress:

Mechanical B.C.: $u(z=0) = 0$

$$U(z=0) = 0$$

$$P_f(z=\delta) = 0$$

$$\sigma(z=\delta) = 0$$

Electrical B.C.: $J(z=0,\delta) = J_o$

Using equation (9), (1), and (2) the following are obtained:

$$u(z) = -\frac{u_j}{2H_A k}(z^2 - 2\delta z)$$

$$\varepsilon(z) = -\frac{u_j}{H_A k}(\delta - z)$$

$$P_f(z) = \frac{u_j}{k}(\delta - z)$$

$$U = 0$$

where $u_j = k_i J_o + U = k_i J_o$

Thus a uniform applied current density will result in a linearly varying strain and hydrostatic pressure. Frank and Grodzinsky have examined the material behavior in response to an oscillatory signal imposed together with an offset load both experimentally [1986a] and theoretically [1986b]. As expected, with increasing frequency the induced strain becomes more and more localized to the bottom boundary (bottom and top if there is an additional applied offset strain), and fluid flow is maximal in those regions not undergoing strain.

A very different result is obtained if one allows fluid to flow freely from both boundaries. In this case, the boundary conditions are:

Mechanical B.C.: $u(z=0) = 0$

$$P_f(z=0,\delta) = 0$$

$$\sigma(z=\delta) = 0$$

Electrical B.C.: $J(z=0,\delta) = J_o$

The bulk relations are then:

$$\varepsilon(z) = 0$$
$$u(z) = 0$$
$$P_f = 0$$
$$U^f = -k_i J_o$$

Thus it is possible to apply an electric field in the absence of any mechanical deformation. In this configuration potential and fluid flow will be uniformly distributed throughout the tissue. The fluid flow can be considered a classical example of electroosmotic flow through a nondeforming, porous, charged matrix.

2.6.4 Experimental Configuration: Hydrostatic Pressure

Application of hydrostatic pressure alone is conceptually straightforward. Since the matrix is considered incompressible at pressures of interest, there will be no deformation, fluid flow, or current:

Mechanical B.C.: $P_f(z=0,\delta) = P_a$

$\sigma(z=0,\delta) = 0$

Electrical B.C.: $J(z=0,\delta) = 0$

Bulk Relations: $u(z) = 0$

$\varepsilon(z) = 0$

$P_f(z) = P_a$

$U = 0$

$J = 0$

If this type of experiment is to be interpreted as physiologically relevant, it is essential that the fluid phase, rather than the gas

phase, be compressed so that the concentration of disolved gasses remains constant.

2.6.5 Experimental Configuration: Fluid Flow

One way to induce fluid flow is using by applying a pressure gradient. The experiment could be done either open or close circuited. The example here imposes the open circuit condition:

Mechanical B.C.: $u(z=0) = 0$

$P_f(z=0) = 0$

$P_f(z=\delta) = P_a$

$\sigma(z=\delta) = 0$

Electrical B.C.: $J(z=0,\delta) = 0$

Solution to equation (3) yields:

$$\varepsilon(z) = -\frac{P_a}{H_A \delta} z$$

$$u(z) = \frac{P_a}{2H_A \delta} z^2$$

$$P_f(z) = \frac{P_a}{\delta} z$$

$$U = -\frac{k}{\delta} P_a$$

$$J = 0$$

$$\frac{\partial V}{\partial z} = \frac{k_{21}}{k_{22}} \frac{P_a}{\delta}$$

As expected, the imposed pressure gradient results in fluid flow. In turn, this results in an induced voltage gradient and a linearly varying strain. Lai and Mow [1980] have examined both linear and nonlinear models of fluid drag induced compression of cartilage. The nonlinearity

arises because the permeability is a function of strain which itself is nonuniform. This linear model is sufficient for applied pressures under 100 kPa.

2.6.6 Experimental Configuration: Concentration Changes

The last experimental configuration considered is one in which the availability of nutrients and electrolytes is altered in the absence of tissue deformation, fluid flow, pressure changes, or electrical potential. In section 2.3.7 it was shown that pH and K^+ concentrations change markedly upon tissue compression. A similar change could be induced by changing the concentrations in the bathing medium. The pK of the sulfate and carboxyl charge groups in cartilage are in the range of 2 to 4 [Grodzinsky,1983]. Therefore, the charge density is relatively constant over a pH range from 6 to 8 [Phillips, 1984]. Both potassium and hydrogen are present in very small quantities compared to sodium and chloride, so alterations in these concentrations would not appreciably affect the total ionic concentration in the tissue. One could alter the bath concentrations of these minority carriers without inducing changes in tissue swelling.

The effects of exclusion can be addressed by incubating the tissue in a membrane which is capable of excluding molecules above a specified molecular weight.

2.7 Summary

The connective tissue system, modeled as three conceptual elementary response units: mechanical, cellular, and output conversion, has been described. Events occurring within the material as a result of an applied mechanical signal were suggested as possible outputs of the mechanical unit, $S(t,x,y,z)$, which could induce a cellular response, $C(t,x,y,z)$, and, following some processing, be detected as the output.

The signals, $S(t,x,y,z)$, which may influence cell behavior included cell deformation, hydrostatic pressure, streaming potential, fluid flow, and a variety of direct results of consolidation. Examination of practical experimental configurations reveals that static loads, applied hydrostatic pressure, applied electric fields, and certain imposed concentration changes result in a uniform distribution of "signal" and are likely to be the most straightforward to interpret. Chapter 4 describes the response of epiphyseal plate cartilage to applied fields to examine the effects of a uniform fluid flow and current, in the absence of deformation and hydrostatic pressure. Chapter 5 describes a sequence of experiments investigating the response to applied static loads, in terms of its magnitude dependence and kinetics. An applied step load leads to a uniformly distributed strain profile within a time, τ_m. Consolidation of the matrix will cause adjustments in the ionic and nutrient environment which occur by diffusion. Equilibrium will thus be governed by the longer of τ_m and τ_d. Experiments discussed in chapter 6 examine the response to applied concentration changes for

comparison to the responses seen to applied loads in chapter 5. The next chapter discusses the biochemical and culture methods used in the experiments along with the relevant control studies needed to verify and characterize the experimental preparation.

Chapter III

MATERIALS, METHODS, and CONTROL STUDIES

This chapter discusses the rationale behind the use of an epiphyseal plate organ culture preparation. Details regarding the culture conditions, and analytical procedures and relevant controls are described.

3.1 Tissue model

The choice of a tissue model involves consideration of the relative merits of an *in vivo* and *in vitro* system as they pertain to the connective tissue of interest and to the output measurement constraints. Each connective tissue imposes certain restrictions in terms of the test environment. Although it has been hypothesized that all tissues will exhibit mechanically modulated behavior, the anticipated interplay between system elements and the economic, analytical, and experimental limitations determine the practical usefulness of a given tissue preparation.

Possible test systems can be separated into *in vivo* and *in vitro* environments. The desire for a physiologically relevant response makes an *in vivo* system attractive. However, the mechanical unit and the output conditioning unit in such systems are difficult to define. *In vitro* systems often trade off the true physiological environment for experimental control and improved measurement capabilities. The

extracellular matrix environment is believed to be essential for normal connective tissue behavior so an *in vitro* organ culture environment might satisfy that major physiological requirement while affording us more control of the testing regimen.

Reserve zone epiphyseal plate cartilage (EPC) in organ culture was selected as the connective tissue preparation. From a material standpoint, EPC is relatively isotropic when compared to bone, tendon, and dermis, so a uniform applied mechanical force should represent the same deviation from the physiologic norm for all cells concerned. EPC is relatively cellular so that measurements of the biosynthetic rate can be made on reasonably sized samples. Assuming a composition typical of hyaline cartilages, 90% of the constituents of EPC are accounted for by collagen and proteoglycan [Grodzinsky, 1983], so a synthetic response is likely to involve one of those macromolecules. Cartilage is typically aneural and avascular so that the tissue culture environment may be nearer to the physiological environment than for other connective tissues. Finally, the behavior of EPC has physiological relevance to skeletal growth since it is the developmental precursor to bone and therefore important for growth and it is sometimes involved in the initial stages of bone repair. Furthermore, while the EPC (the reserve zone of the epiphyseal plate) is homogeneous, other areas (the proliferative and hypertrophic zones) show directed organization (see figure 1.2). The potential to compare the response of these regions to the reserve zone region is attractive.

The variety of cellular output signals one could measure was

discussed in section 2.4. Since connective tissues are known to adapt their ECM in response to loading, and since protein and GAG are the predominant ECM material, the cellular output assayed was the biosynthesis of glycosaminoglycans (GAGs), and protein,

The sections which follow discuss the epiphyseal plate explant procedures, tissue culture maintenance techniques, and biochemical assays employed. Studies which characterize the organ culture preparation and which verify of the culture and biochemical techniques are presented.

3.2 Explant Procedure

Intact foreleg "knee" joints from one to two week old calves were obtained with hours of slaughter (Trelegan's, Cambridge). Joints from an animal were paired and right-left designation noted. Superficial tissue was wiped clean of gross dirt and hair, then thoroughly scrubbed with a 10% povidone-iodine solution. From this point on the tissue was treated as sterile. The joint capsule was opened and the radius and ulna stripped clean of muscle and connective tissue. The ulnar periosteum was then dissected from the ulnar surface and the ulna separated from the radius. Generally, the excised ulnar segment was comprised of epiphysis and plate, as the bone had a tendency to fracture at the metaphyseal-epiphyseal plate margin.

The bony epiphysis was mounted in a cylindrical holder in a sledge microtome so that the surface was approximately parallel to the blade.

The plate was observed visually to consist of a transition region less than 1 mm thick and an obviously cartilaginous region 5 to 10 mm thick. The transition region, shown histologically to be comprised of hypertrophic and proliferative zone tissue, was typically removed. 800 μm sections were taken sequentially until the bony epiphysis was reached. These sections were numbered, beginning with the section nearest the metaphysis. Finally a cylindrical cutter was used in cookie cutter fashion to obtain plane parallel 800 μm thick cartilage plugs. Plug diameters were either 1/4 inch (for electrical experiments), 1.8 mm, or 2 mm (for mechanical experiments). Usually, six 1/4 inch plugs or 80 2 mm disks could be obtained from a single joint. The tissue was maintained in primary tissue culture conditions (see below) for at least 2 days prior to testing.

3.3 Culture Conditions

Typically, tissue was incubated at 37°C under an atmosphere of 5% CO_2 in air. Several media formulations were used. Each is discussed here and summarized again in appendix A for convenience. The base medium was Dulbecco's Modified Eagles Medium (DMEM)(Gibco, Grand Island NY). Unless otherwise specified, the medium was supplemented with 0.1% NuSerum (Collaborative Research, Waltham MA). NuSerum is a partially defined serum formulation and therefore considered to be less variable from lot to lot than serum derived entirely from an animal.

Immediately following primary explant, antibiotics were added to

the medium at 2x concentrations (1000 U/ml penicillin, 1000 µg/ml streptomycin (Gibco, Grand Island NY)). After 2 days in culture, antibiotics were omitted from the medium.

During periods in which synthesis of GAGs and proteins were assessed, the media was supplemented with radioactive precursors obtained from New England Nuclear (Boston MA). Sulfate was supplied as Na_2SO_4 at typically 500 mCi/mmol (NEX-041). ^{3}H-proline (NET-573) specific activity was typically 10 - 15 Ci/mmol. For 1/4 inch diameter plugs, the labeling medium contained 10 µCi/ml ^{35}S-sulfate, 5 µCi/ml ^{3}H-proline, and 0.5 mM proline (Sigma, St. Louis MO). The 2 mm diameter plugs were provided with twice the concentration of radiolabel. In DMEM, a proline free medium, the cells can synthesize proline as needed. 0.5 mM proline was added to ensure that specific activity of proline remained constant during the labeling period.[8] Throughout the text, media formulations are referred to as explant medium, standard medium, or labeling medium. These formulations are summarized in appendix A.

3.4 Biochemical Processing

In this section the biochemical procedures used to assess proline

[8] McLeod [1986] found that this was sufficient for a bovine fibroblast cell line which incorporated approximately the same amount of proline per cell as the chondrocytes. Therefore, it was assumed that the 0.5 mM was sufficient for chondrocytes.

and sulfate incorporation are described.

Immediately following the labeling period, the tissue was washed 6 times for at least ten minutes each time in 1-2 ml cold Hanks buffered salt solution (HBSS) to remove unincorporated label. Experiments in which radioactivity of the wash was measured indicated that removal was essentially complete by the 4th wash. This was further confirmed by sephadex G50 chromatography of the papain digest in which the radioactivity was found to be confined to the high molecular weight fractions (figure 3.1). Wet and dry weights were obtained for most samples. Tissue was digested with papain (see appendix A for formulation), and aliquots were then taken in duplicate for scintillation counting.

In general, only the tissue sample was analyzed to assay for biosynthesis. The presence of labeled macromolecules in the media and washes was determined on several occasions following extensive dialysis against sulfate and water to remove unincorporated label. From these studies it was estimated that the amount of newly synthesized material which leaches out into the medium during culture or subsequent washes was under 5% of the total incorporation.

Since glycosaminoglycans are left intact after papain digestion, a characterization of the GAGs could be performed. GAGs were identified by co-electrophoresis with standards containing the cartilage GAGs on cellulose acetate plates. The discontinuous technique described by Cappelletti et. al. [1979] separates GAGs according to their mobility in a barium acetate buffer and their differential sensitivity to ethanol

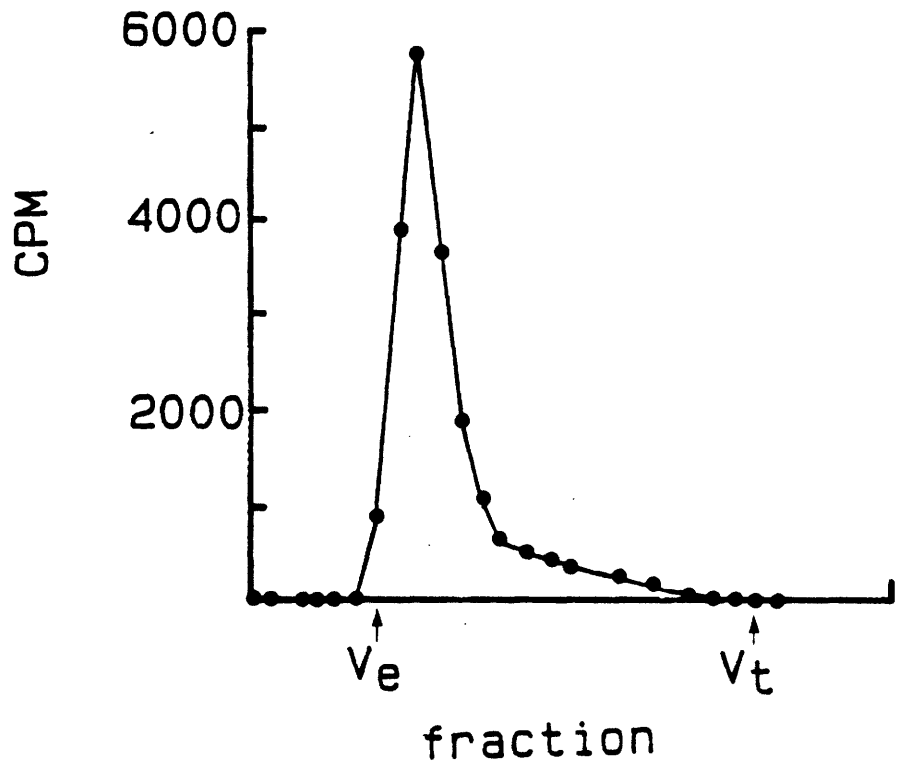

Figure 3.1: Sephadex G50 chromatography of papain digested tissue. Papain digest should leave GAG chains intact. GAGs will elute near the excluded volume (V_e=7) while small molecular weight constituents will elute near the total volume (V_t=22). Digest in this chromatagraph had radioactivity confined to the excluded peak.

precipitation. The bands were stained with alcian blue to assess relative content. They were then cut out and immersed in scintillation fluid to measure synthesis of individual GAGs. The predominant band seen from a typical tissue digest coelectrophoresed with the chondroitin sulfate/keratan sulfate standards. Hyaluronic acid was also observed to a lesser extent. Sulfate incorporation was seen only with the chondroitin sulfate/keratan sulfate band, consistent with the overall content. These results indicate that the sulfate was being incorporated primarily into GAGs.

3.5 Biosynthetic Behavior

Several control studies were performed to characterize the biosynthetic behavior as a function of tissue culture parameters. The overall goal was to establish that the synthetic behavior had reached a steady state by the time of testing and to provide culture conditions in which the cell was capable of modifying the synthetic rate.

3.5.1 Effect of Serum Concentration

Synthetic behavior by many cell lines depends on serum concentration. The objective was to provide sufficient serum for the cells to be able to synthesize normally, but not to maximally stimulate them. The series described here examined serum concentrations ranging from 0% to 5% over a 6 day period.

Tissue from several joints was combined and minced into approximately 1 mm pieces and randomly separated into 72 groups. The groups were divided into 4 sets which were maintained in 6-well dishes in DMEM with 0%, 0.1%, 1.0%, or 5% NuSerum. Media was changed daily. On days 1 through 6 after explant, three groups from each serum set were incubated for 12 hours in ^{35}S-sulfate labeling medium containing the appropriate serum concentration.

Sulfate incorporation by each group was normalized to the dry tissue weight. The mean and standard deviation of incorporation are plotted in figure 3.2. In this study GAG synthesis by epiphyseal chondrocytes in organ culture appears to be relatively insensitive to serum concentration. A separate study, not shown, indicated that the sensitivity to serum became more apparent, particularly to the absence of serum as the time between media changes increased. The rate of sulfate incorporation in this preparation were comparable to those reported by Hascall et al. [1983]. Unless otherwise stated, media was routinely supplemented with 0.1% NuSerum for all further studies.

3.5.2 Synthesis as a function of time after explant

It was important to ensure that the tissue had achieved steady state biosynthetic behavior by the time of testing. Several investigators [Lane and Brighton, 1974, McKenzie et al., 1977] have observed an initial lag in biosynthesis in the first few days following explant which may represent recovery from specimen preparation [McKenzie et al., 1977]. Minced tissue from several joints was divided into 12

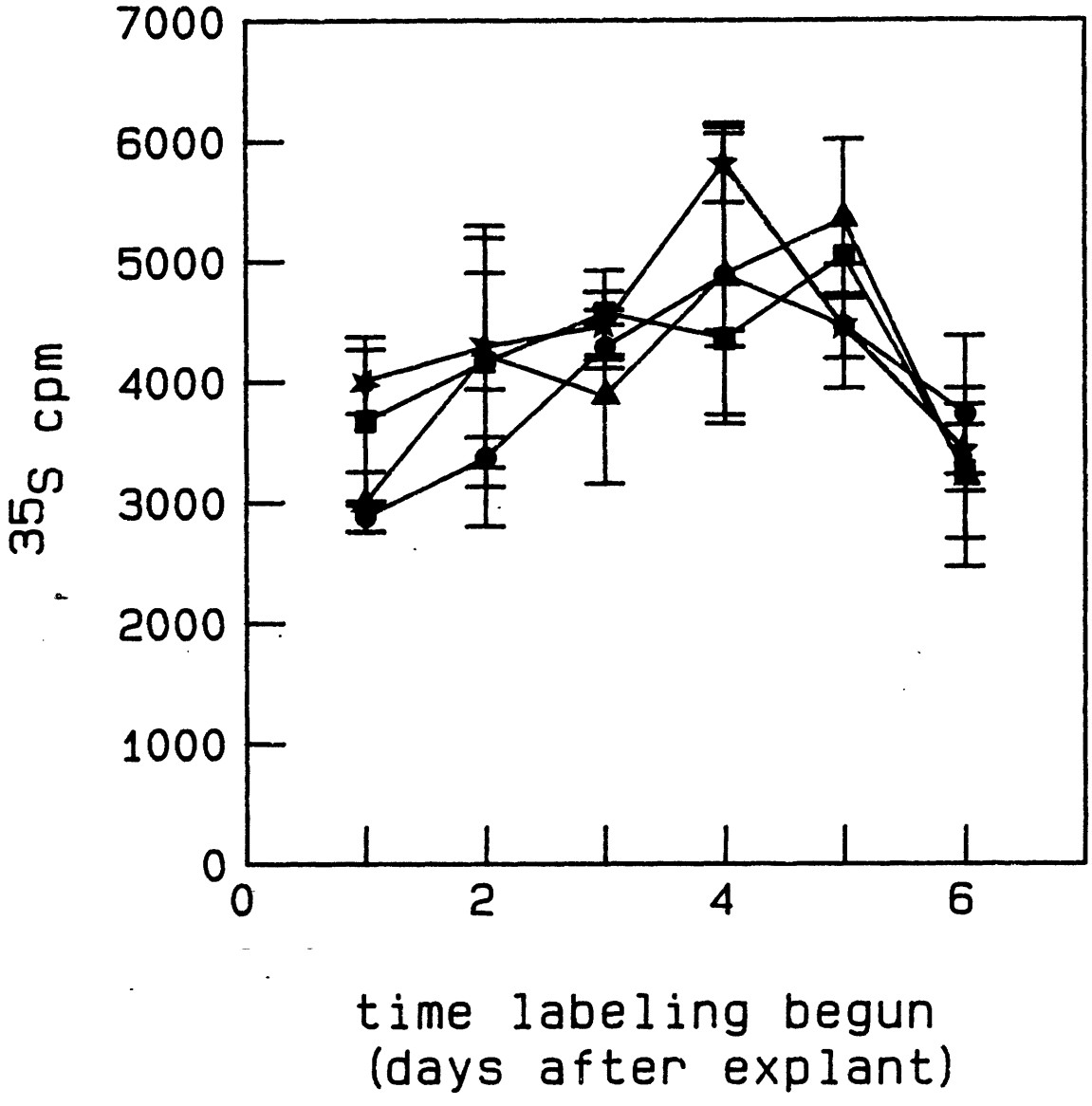

Figure 3.2: Sulfate incorporation during a 12 hour labeling period by minced epiphyseal cartilage maintained for the indicated number of days in DMEM with 0%(●), 0.1%(▲), 1%(■), or 5%(★) NuSerum. Data represents the mean and standard deviation of the mean of three groups, each normalized to the tissue dry weight.

sets, each comprised of three groups. On a specified day, beginning immediately following explant, and ranging up to 2 weeks, 12 hour incorporation of ^{35}S-sulfate was measured for one set. Serum concentration was 0.1% throughout. Tissue was incubated in 6 well dishes with daily changes of 3 ml of medium per well.

The incorporation by each group was normalized to dry weight, then averaged within each set. Figure 3.3 demonstrates a relatively constant 12 hour incorporation of sulfate from day 0 to day 14. These results indicate that tests could be performed any time within a two week period.

3.5.3 Effect of frequency of media changes

While daily media changes appeared sufficient to maintain a steady rate of GAG synthesis, daily changes not only were inconvenient, but also increased the probability of contamination. Therefore, a companion series of experiments was performed in conjunction with those described in the previous section in which media changes were done every other day. Figure 3.4 plots these results together with the results of figure 3.3. There is no significant difference between the two sets. Therefore, media changes were henceforth performed every two days.

3.5.4 Dependency on media volume

Due to the expense of media and radiolabel it is desirable to minimize usage of these materials. Furthermore, cells are believed to

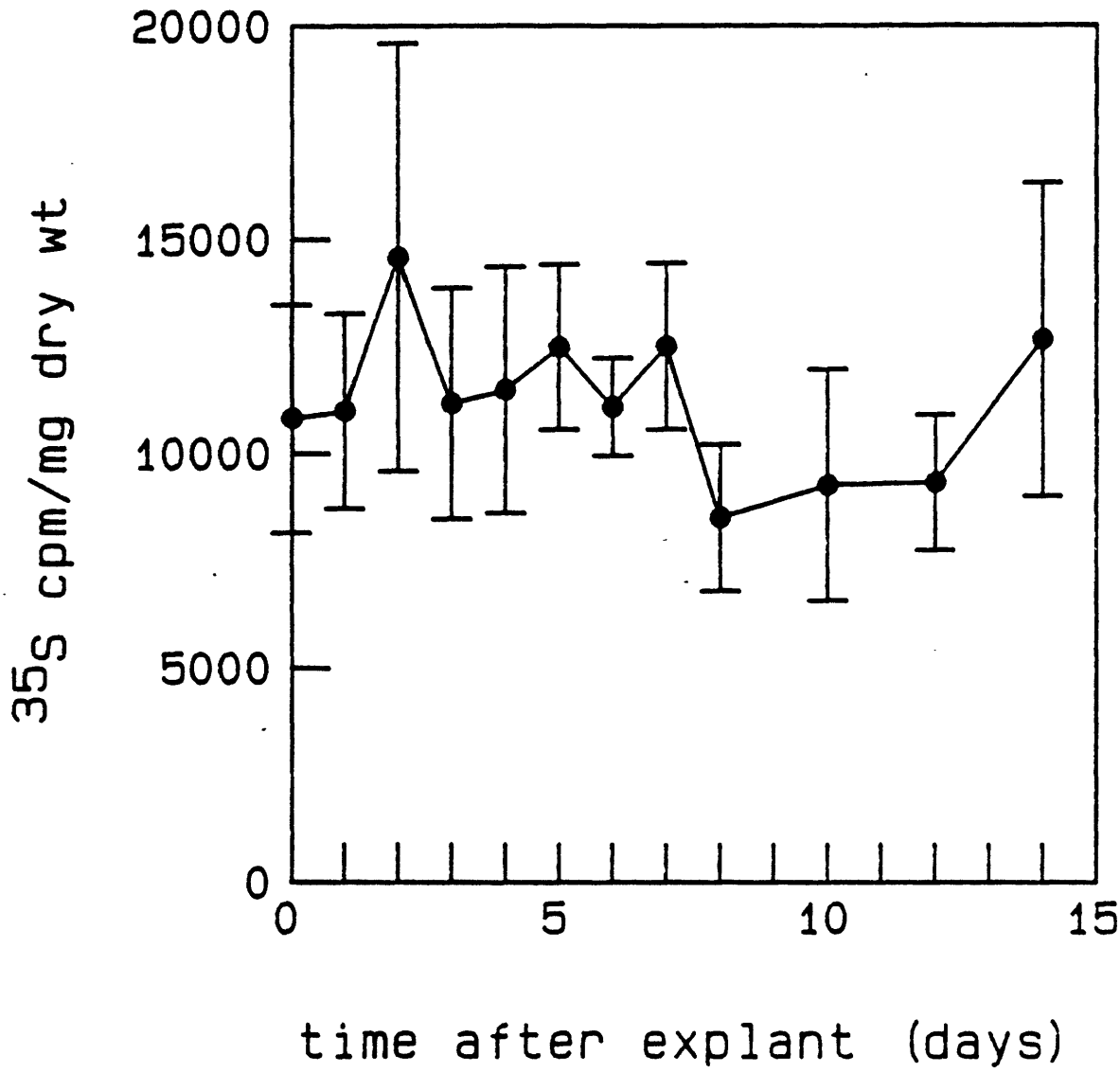

Figure 3.3: Sulfate incorporation during a 12 hour labeling period by minced epiphyseal cartilage maintained for the indicated number of days in DMEM with 0.1% NuSerum changed daily. Data represents the mean and standard deviation of the mean of three groups, each normalized to the tissue dry weight.

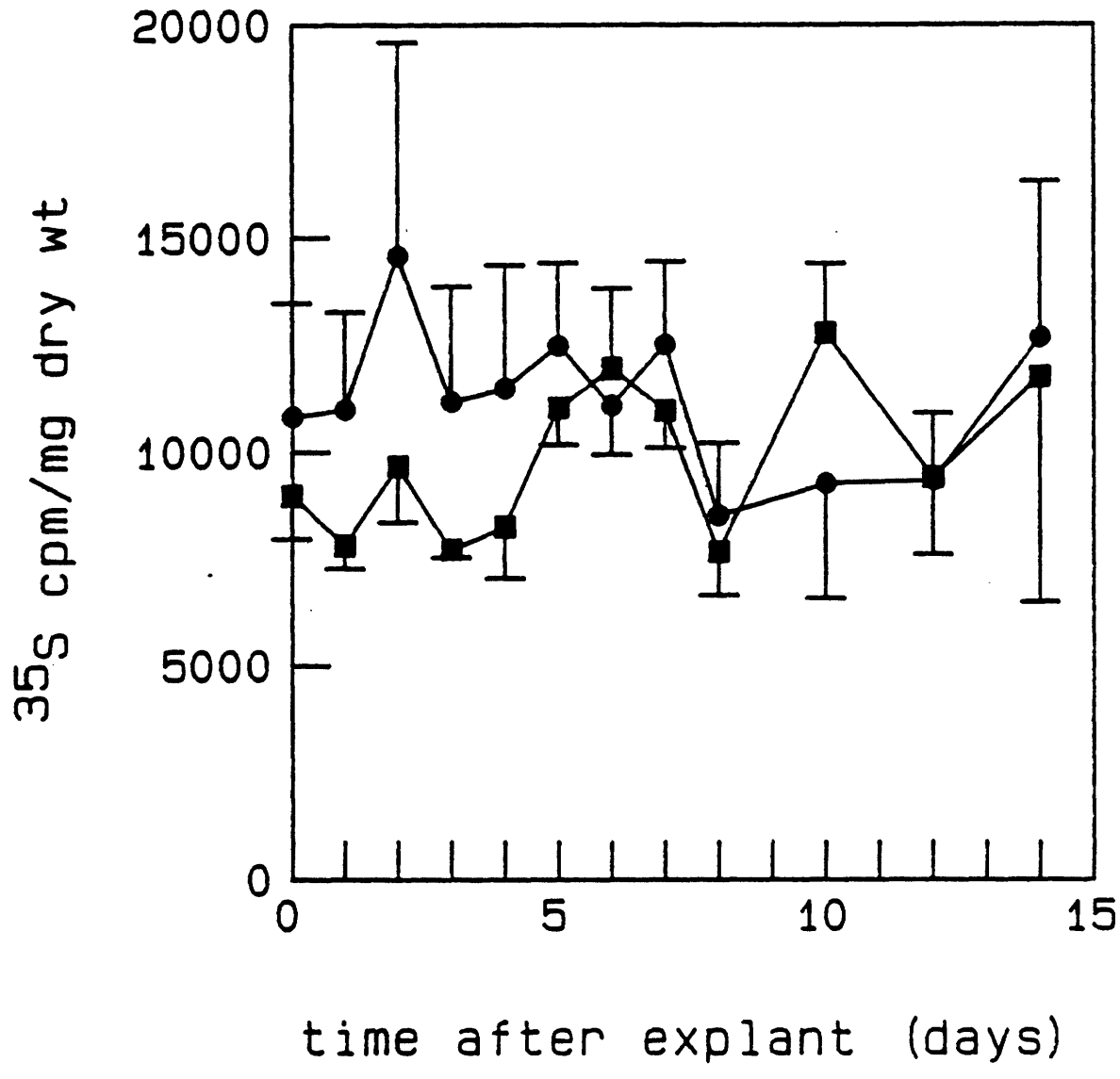

Figure 3.4: Sulfate incorporation during a 12 hour labeling period by minced epiphyseal cartilage maintained for the indicated number of days in DMEM with 0.1% NuSerum changed daily (●) or every other day (■). Daily change data is that shown in figure 3.3. Data represents the mean and standard deviation of the mean of four groups, each normalized to the tissue dry weight.

condition their media. For these reasons, a series was performed to test the effect of media volume on biosynthesis. Minced tissue was divided into groups of increasing amounts of tissue ranging from 3 mg dry weight to 38 mg dry weight. All groups were maintained in 6-well dishes in 2 ml of medium per well. 12 hour incorporation, normalized to dry weight, was approximately constant indicating there was no dependence on tissue volume to media ratios from under 1 to 20 mg/ml. Typically, tissue was maintained at less than 6 mg/ml.

3.5.5 Incorporation as a function of labeling time

Interpretation of studies using radiolabel incorporation as an assay of biosynthesis is aided by an understanding of the kinetics of incorporation. Several series of incorporation versus labeling time were performed to determine the extent to which synthetic rate can be considered constant and to check for initial delays in incorporation due to either cellular or diffusion processes.

After 2 days in culture 2 mm diameter plugs were allowed to incubate for various time durations in 96-well dishes with 300 µl of ^{35}S-sulfate, ^{3}H-proline labeling medium. The study shown in figure 3.5 tracks incorporation for up to 64 hours. As expected, there is a general increase in accumulation with time. The plateau in accumulation of radiolabeled protein and GAG after 36 - 48 hours is probably a result of nutrient depletion and confirms the previous conclusion that media changes every 2 days are necessary.

Figure 3.6 expands the results of figure 3.5 to demonstrate

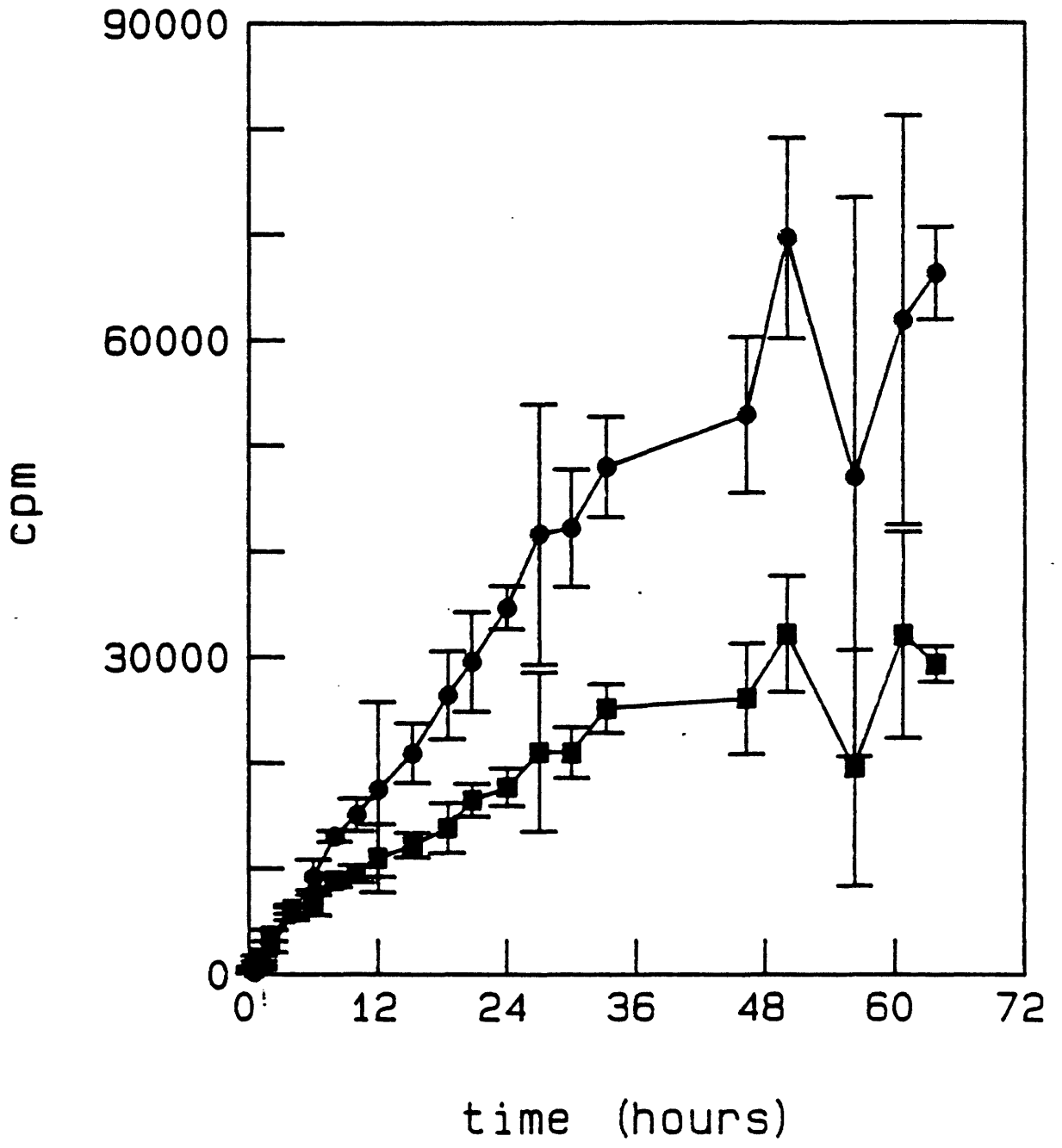

Figure 3.5: Proline (■) and sulfate (●) incorporation by tissue incubated in labeling medium for the time indicated by the x axis. Data represents the mean and standard deviation of four 2 mm diameter plugs.

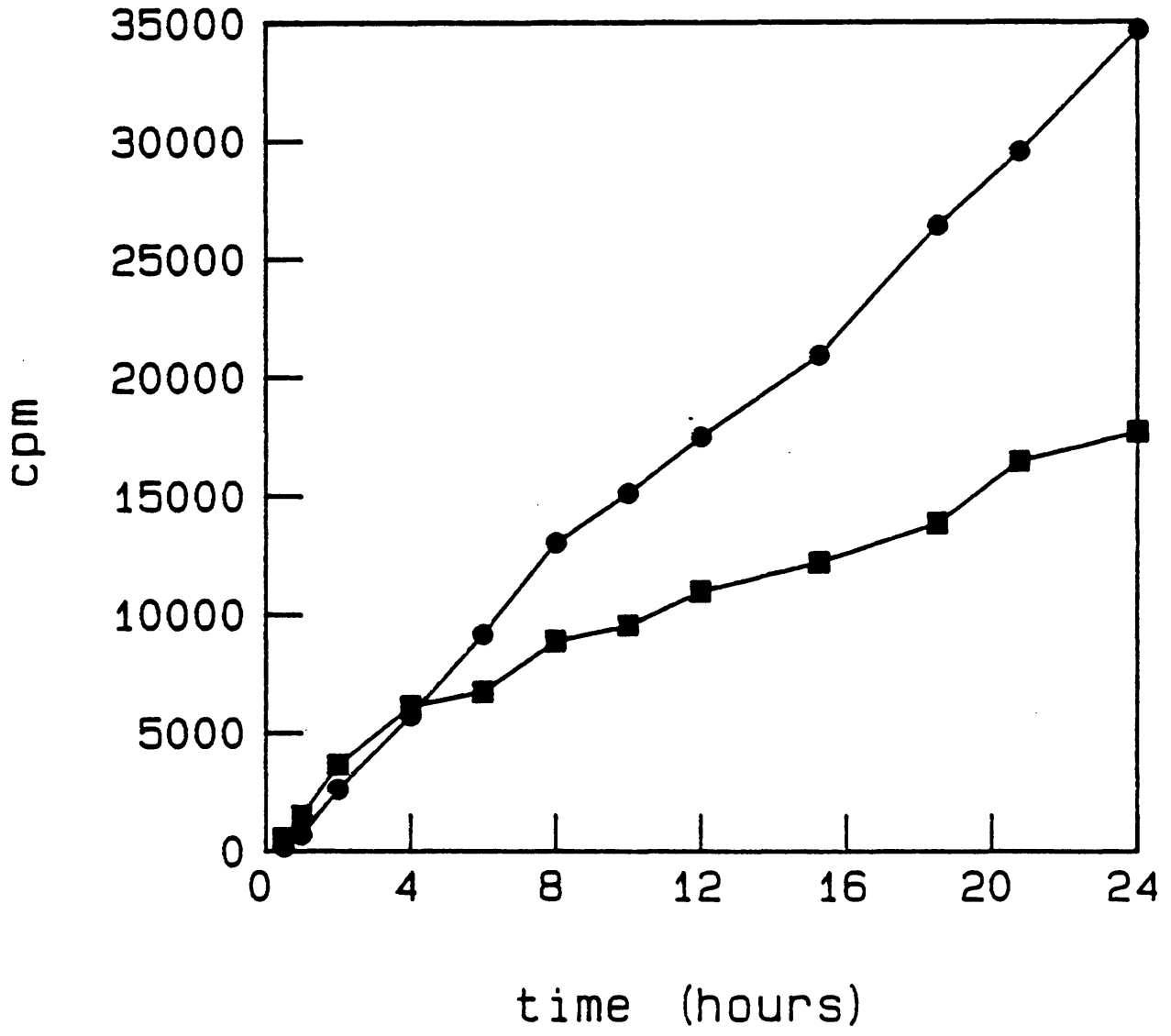

Figure 3.6: Incorporation of sulfate (●) and proline (■) vs. labeling time for the 0 to 24 hour portion of figure 3.5.

incorporation patterns at earlier labeling times. Total sulfate incorporation is relatively linear with an intercept near the origin suggesting that diffusion, uptake, and incorporation of sulfate are rapid. This is consistent with Kimura et al.'s [1981] finding that chondrosacrcoma cells can incorporate ^{35}S-sulfate into newly synthesized PGs during a 1-2 minute labeling period. Accumulation of ^{3}-H labeled macromolecules is linear for the first four hours, then the rate of accumulation drops by approximately 1/3 for the remainder of the labeling periods. One interpretation of this behavior is based on a 2 pool system. One pool, perhaps an intracellular one, reaches a steady state within 4 hours. Steady state is reached when the rate of radiolabel incorporation balances the rate of degradation of labeled molecules so the net number of labeled molecules is constant. The second pool, perhaps an extracellular one, takes much longer to reach steady state so that steady state was not achieved in this experiment and the total incorporation continued to increase linearly.

Alternatively, the different initial incorporation patterns between ^{3}H-proline and ^{35}S-sulfate can be viewed in terms of their ratio. (Figure 3.7) The H/S ratio decays to a constant in 2 to 3 hours. This behavior could be a result of enhanced proline incorporation at early times (as it appeared in the incorporation data of figure 3.6), or it could be a result of delayed sulfate incorporation. Experimental conditions (e.g. temperature) could skew the initial data points with respect to later ones and lead to an incorrect interpretation of the early time behavior. A similar pattern in the ratio between proline and

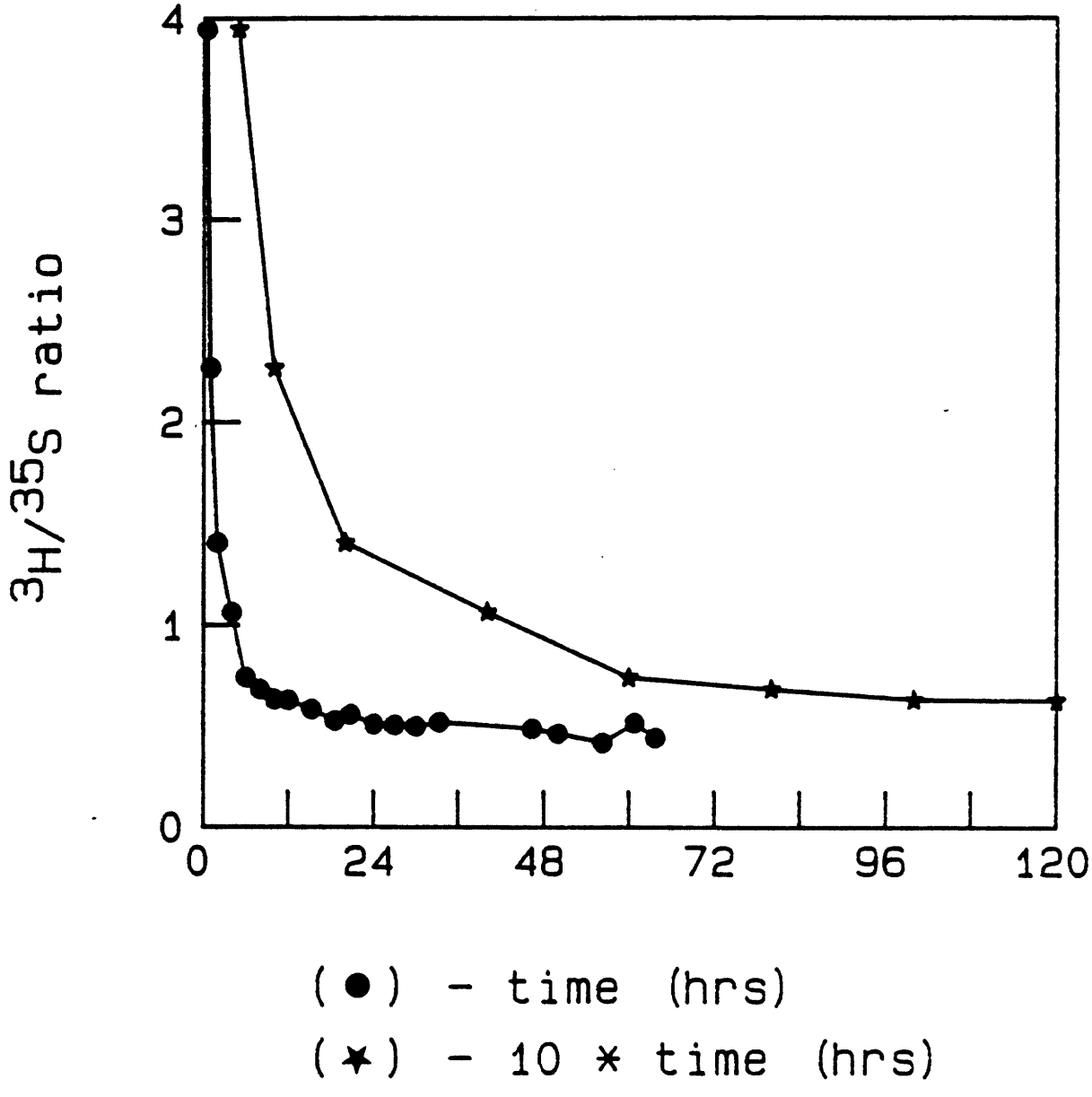

Figure 3.7: Ratio of proline to sulfate incorporation by tissue samples presented in figure 3.5. Data represents the mean and standard deviation of 4 2 mm diameter plugs.

sulfate incorporation was seen in all experiments where the synthesis as a function of labeling time could be determined. The individual patterns of incorporation, however, were not consistent. While the results of some experiments were similar to those of figure 3.5, other results were consistent with a delay in sulfate incorporation and somewhat constant proline incorporation. Diffusion is the most likely cause of a delay in incorporation in organ culture preparations. Diffusion times on the order of 2 minutes are expected for a plug with a 1 mm radius, assuming a diffusivity of 10^{-5} cm^2/s. Thus it seems unlikely that a diffusion process could completely account for the differences in proline and sulfate incorporation during hour long labeling periods. To address the issue of diffusion of radiolabel directly, a slight modification to the protocol was made. The tissue was bathed in labeling medium for one to two hours at 4 °C to allow both labels to equilibrate within the tissue while the metabolic rate considerably slowed. Then incubation was continued at 37 °C for various times. Temperature should affect all metabolic processes to approximately the same extent, so the H/S ratio should be independent of temperature. Figure 3.8 shows H/S ratio patterns for 5 experiments. As indicated, two were preequilibrated in the cold, three were placed directly in the incubator. Nonetheless, the initially high H/S ratio decays to a constant in all cases in 2 to 3 hours. For those equilibrated in the cold, this behavior cannot be explained by differences in sulfate and proline diffusivities. The consistency from experiment to experiment suggests that the H/S ratio is reflecting cell behavior rather than an artifact of the radiolabeling

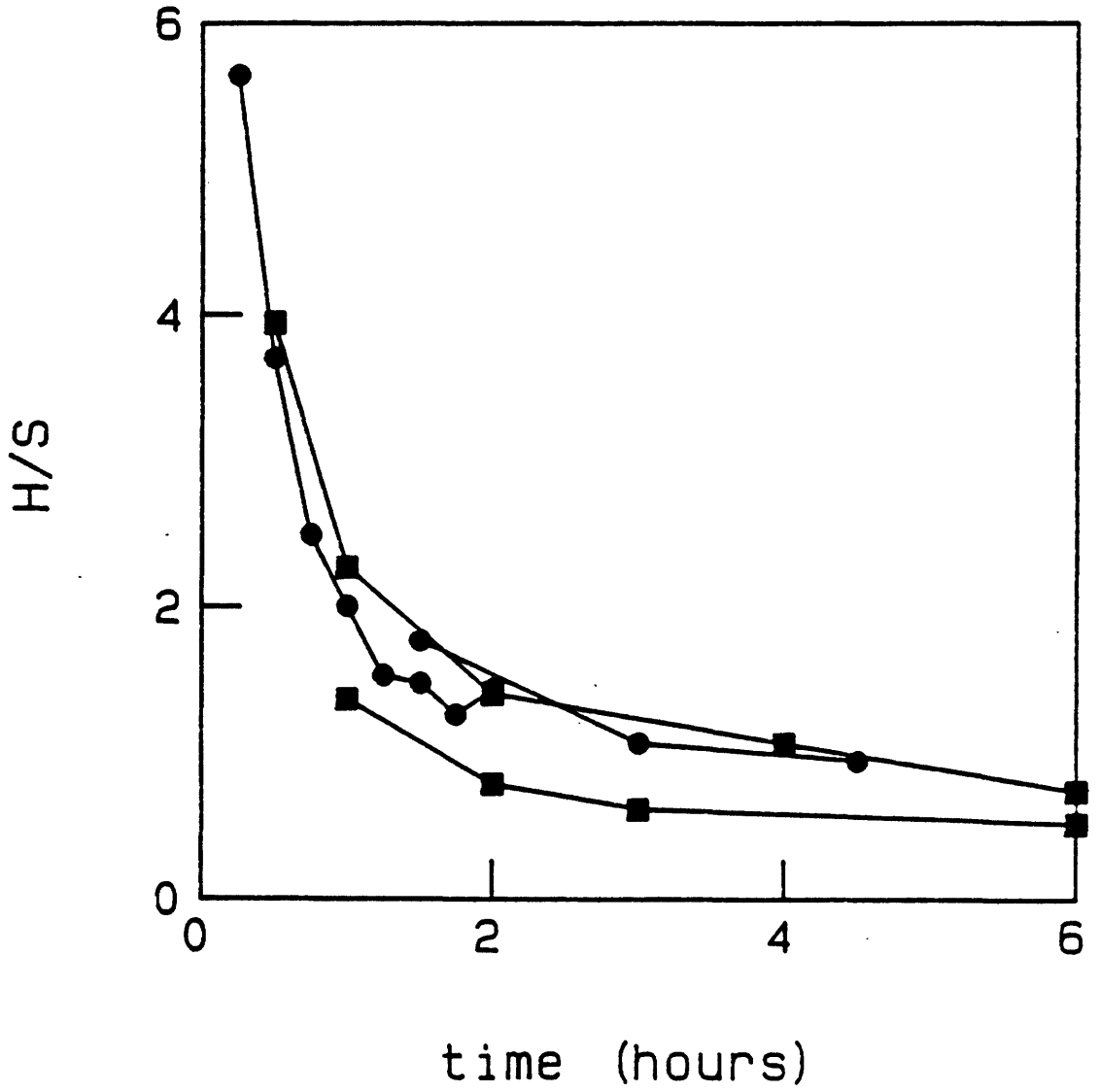

Figure 3.8: Ratio between ^{3}H-proline and ^{35}S-sulfate incorporation as a function of labeling time for 5 independent experiments. Circles (●) indicate that tissue was preincubated in labeling medium for 1 to 2 hours at 4°C before placed in the 37°C incubator. Squares (■) indicate that the tissue was incubated at 37°C immediately after being placed in labeling medium.

and tissue handling techniques.

These results indicate that for proline incorporation, especially, short labeling times may focus on different synthetic pools than longer labeling times. At some point, an effort directed towards understanding where the proline label is being incorporated may be necessary.

3.5.6 Intrajoint variation

The final issues in characterizing biosynthetic behavior concerned variations among plugs taken from a single joint and approaches to data normalization. Figures 3.9, 3.10, and 3.11 show the variation in dry weight, wet weight, and hydration with position on the epiphyseal plate. Level number n represents the nth 800 μm section taken sequentially from metaphyseal to epiphyseal ends of the plate. (The obviously hypertrophic tissue has been discarded prior to numbering). The most clear variation is seen in hydration. Following several days in culture, the lower level samples could be observed grossly to be more swollen than samples taken further from the metaphysis. These samples were more fragile and easier to cut than samples from higher levels. Thus, plugs with dry to wet weight ratios (dry weight/wet weight = 1-hydration) under 15% were excluded from the results.

It is assumed that all cells within a plug behave identically. Thus, ideal normalization would be to cell number. Unfortunately, quantitative isolation of cells from a cartilaginous matrix is impractical for the large number of samples used in each experiment. Alternatively, normalization to tissue volume may be appropriate since

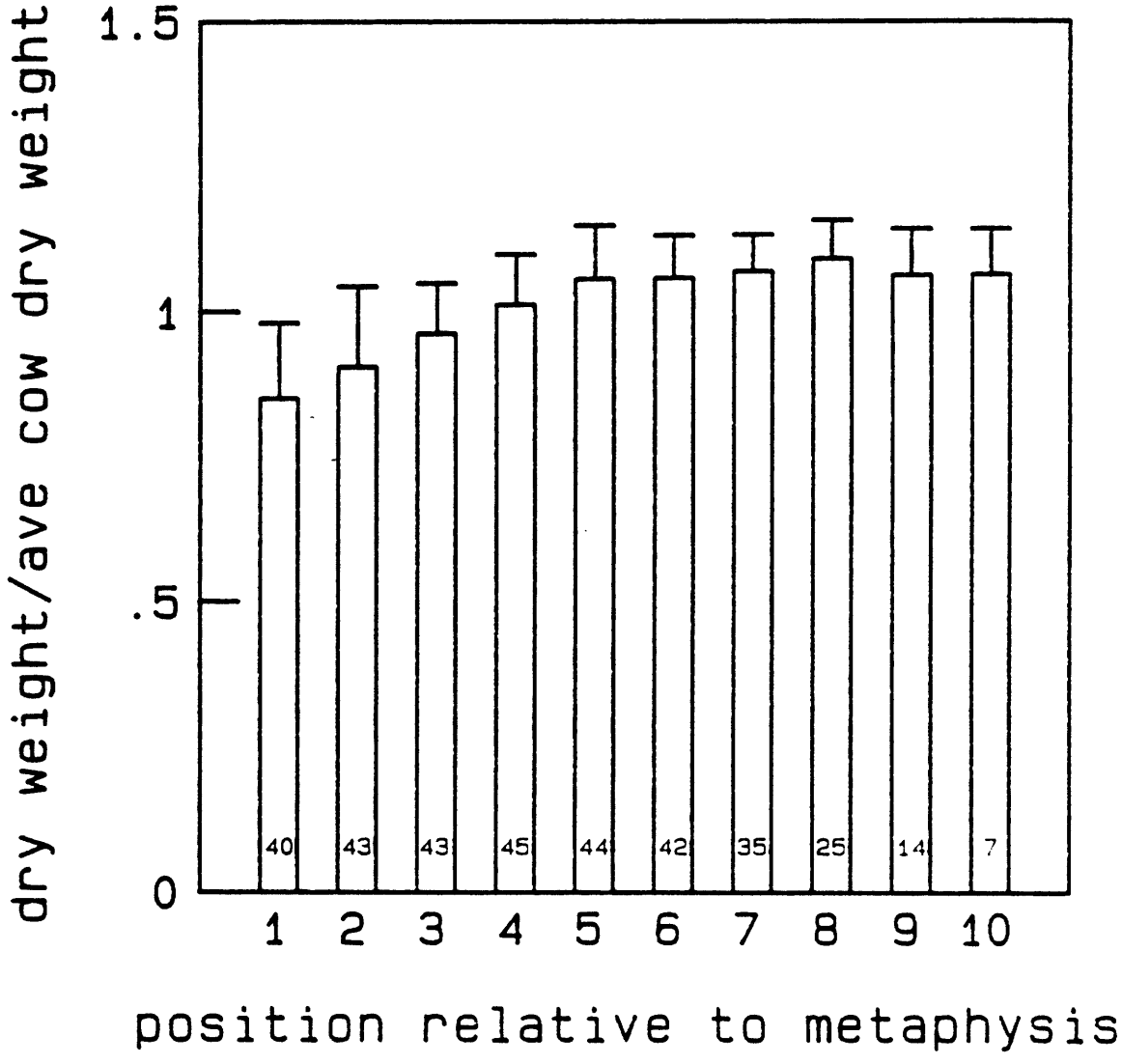

Figure 3.9: Dry Weight as a function of position in the epiphyseal plate for 1/4 in diameter plugs. Level 1 is the metaphyseal-most 800 μm section. Weights are normalized to the mean dry weight for a single joint.

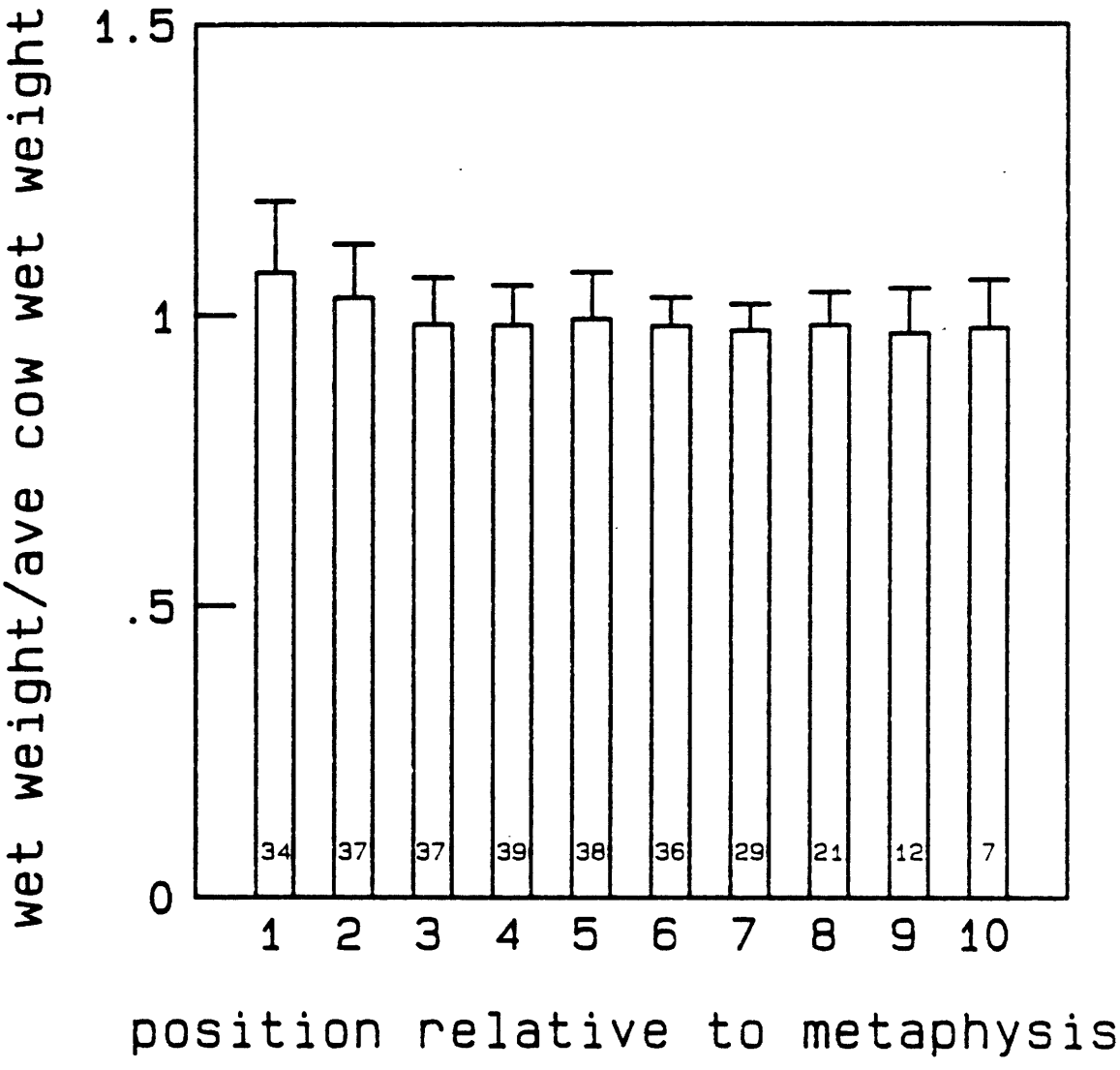

Figure 3.10: Wet Weight as a function of position in the epiphyseal plate for 1/4 in diameter plugs. Level 1 is the metaphyseal-most 800 μm section. Weights are normalized to the mean wet weight for a single joint.

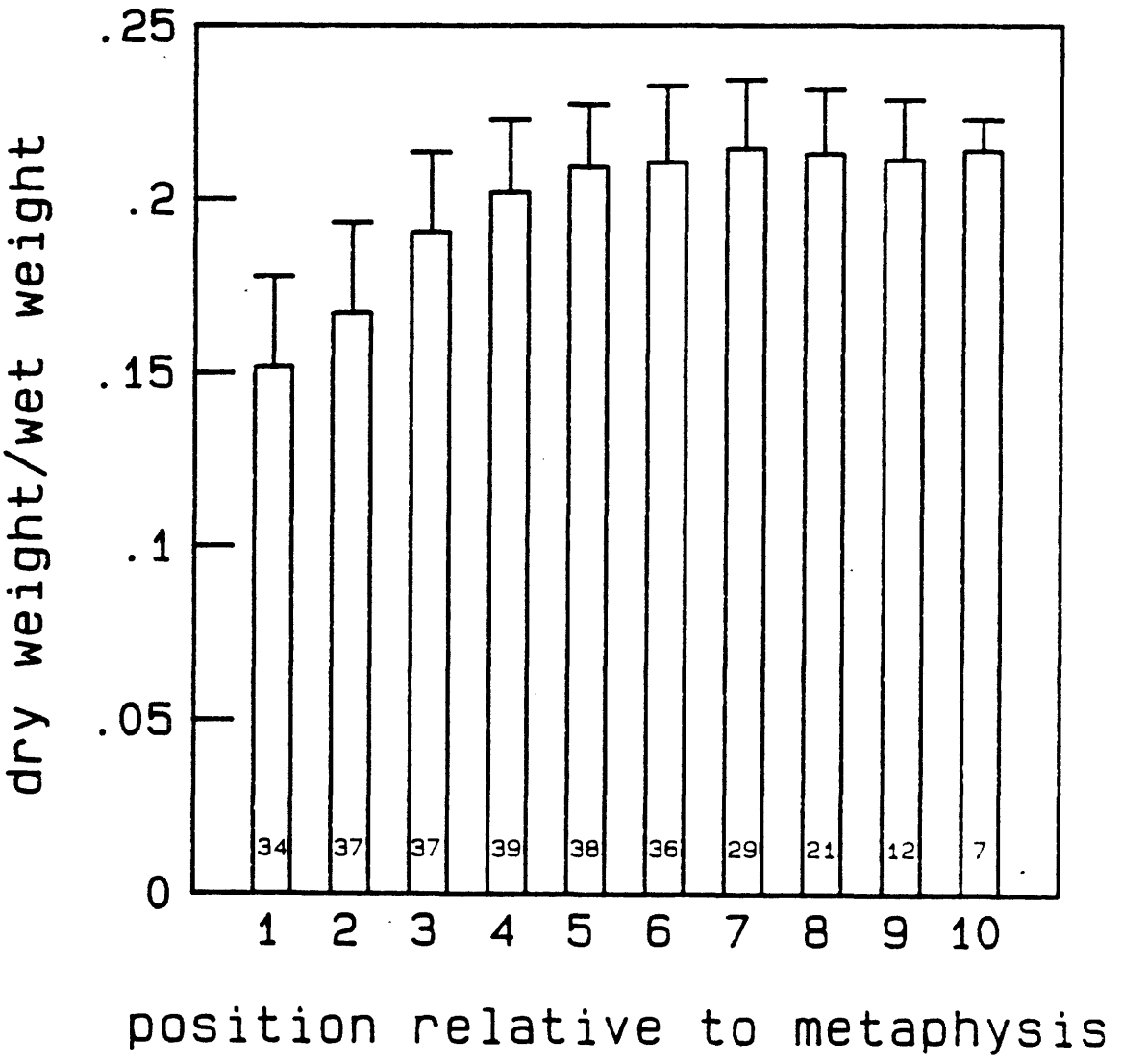

Figure 3.11: dry weight/wet weight = 1 - Hydration is plotted as a function of position in the epiphyseal plate for 1/4 in diameter plugs. Level 1 is the metaphyseal-most 800 μm section.

histologically there appears to be a relatively uniform cell density. Tissue volume can be assessed from cut volume, wet weight, or dry weight. Cut volume is computed from the cut dimensions (e.g. 2 mm diameter, 800 μm thick) assuming a density of 1 gm/cc. Wet weight is measured after removing excess water from tissue samples equilibrated in physiological saline (HBSS). Dry weight is measured following lyophilization, usually for longer than 8 hours.

Figure 3.12 shows the variation in proline and sulfate incorporation during a 12 hour labeling period, normalized to cut volume. Sulfate incorporation is relatively consistent throughout the joint. Proline incorporation is slightly higher at the levels nearest the metaphysis and epiphysis. Normalization to dry or wet weights did not change these trends. In many instances, data was normalized to each of the three factors suggested. The interpretation of the data in these cases was never altered by the type of normalization. Thus, it appears that for epiphyseal plate tissue, cut volume, wet weight, and dry weights are equally appropriate normalizations.

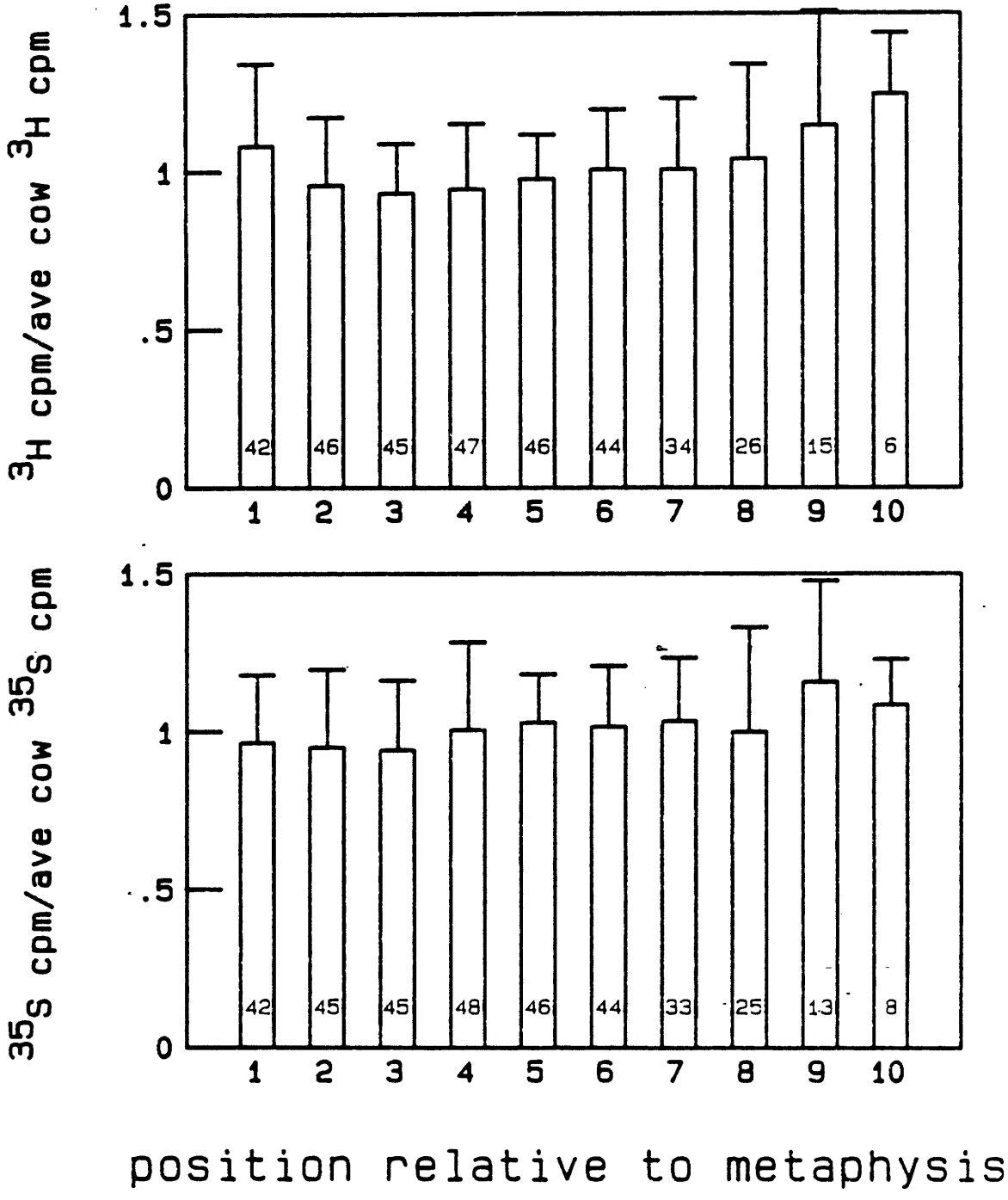

Figure 3.12: Intrajoint variation in proline and sulfate incorporation during a 12 hour labeling period. Data is normalized to the mean incorporation within a single joint in order to minimize variations between animals and radiolabel concentrations.

Chapter IV

RESPONSE TO ELECTRIC FIELDS

4.1 Physiologic Rationale

As discussed in chapter 2, streaming potentials arise when there is relative motion between the matrix and interstitial fluid, as must occur when the tissue is deformed upon loading. The existence of stress generated potentials in connective tissues such as bone and cartilage has led many investigators to suggest that this may be the signal which triggers cells to respond to stress. To test this hypothesis, the effects of current density and fluid flow can be assessed in the absence of deformation and consolidation using the experimental configuration described in section 2.6.3. The experiments described in this chapter examine the biosynthetic response of EPC to sinusoidal current densities in the range of those predicted to occur *in vivo*.

The complex spatial distribution of current density and potential which exist *in vivo* make it difficult to predict the magnitude of local currents and potentials, but *in vitro* experiments can be used to establish upper bounds. The uniaxial confined compression experiments performed under open circuit conditions yield a measurable potential. Because there is no net current flow, this voltage drop is due to the fluid flow through the deforming portion of the matrix. No additional drops occur in non-deforming tissue. *In vivo* the electrical conditions more closely resemble that of a potential shunted by a low resistance

pathway (e.g. interstitial fluid). To estimate the currents, the streaming potential predicted by open circuit measurements can be considered a voltage source. The current density is then predicted based on estimates of the current path and conductivity. Grimshaw [1980] measured the streaming potential in adult bovine articular cartilage in response to step loading under physiologic conditions. For a 5% deformation (approximately 50 μm), an 860 kPa load was required, and a 2 mV streaming potential resulted. A maximum current density of $J=6\ mA/cm^2$ would result if that voltage were to drive current through only 50 μm of tissue.[9] In articular cartilage the area of compression is generally less than the entire articular surface, so return current paths may be relatively short, perhaps on the order of the skin depth, and one might expect maximum currents on the order of $3\ mA/cm^2$. In epiphyseal plate cartilage the loading situation more closely resembles a uniaxial loading condition, so the current paths may be much longer, greatly reducing the prevailing current densities.

In vivo, locomotion and muscle contractions are primary sources of mechanical loading. In a horse, these signals approximate step or triangle loads [Rubin and Lanyon, 1982] with fundamental frequencies ranging from ~0.3 Hz during walking to ~3 Hz during trotting. Most of the energy is confined to frequencies under 40 Hz. Thus, frequencies from zero to 100 Hz are of physiological interest.

One other approach to estimating reasonable electrical parameters

---

[9] based on $J=\sigma E$ where $\sigma=1.5$ mho/m and $E=2$ mV/50 μm.

is to consider those parameters with which other investigators have observed a cellular response. The review in chapter 2 cited several reports in which current densities under 1 mA/cm^2 at frequencies under 60 Hz induced a cellular response.

Based on physiological predictions and experimental results by other groups, the electrical current exposure experiments were designed to span a current density range of 50 $\mu A/cm^2$ to 1 mA/cm^2 at frequencies from 0.1 to 100 Hz. These results should reflect the relative importance of electrical currents with electroosmotically induced fluid flow as a physiological signal.

4.2 Experimental Apparatus

The design of the experimental apparatus required to expose cartilage tissue in organ culture was based on the following criteria:

1. It must be capable of providing the conditions necessary for organ culture. Thus it must be non-toxic and autoclavable and must ensure adequate media coverage.
2. It must ensure that the current densities applied to the sample are uniform and well defined.
3. It must allow for sufficient separation between the electrodes and samples to ensure no electrochemical reaction products will reach a tissue sample in the course of an experiment.
4. It must minimize media usage while maximizing the number of samples.

The following sections describe the electrical stimulation system used for the current exposure studies. The extent to which well defined current densities can be applied has been assessed experimentally. In

addition, the current densities at which ohmic heating becomes significant have been determined.

4.2.1 Description of Experimental System

The chamber, designed and built subject to the above criteria, is diagramed in figure 4.1 and more completely described by Liu [1985]. The chamber is constructed of Teflon, a material which is autoclavable, easy to maintain, and non-toxic. The 1/4 inch diameter cartilage plugs are placed upright within the 1/4 inch channel cut through the diameter of the Teflon sample holders. The sample holders fit snuggly in the chamber so that current is constrained to the channel housing the sample. This well defined geometry allows the applied current densities to be precisely defined.

Current is coupled to the media by means of platinum or stainless steel electrodes. (At the low frequencies of interest, capacitive and inductive coupling techniques are impractical.) The direct contact between electrode and culture media raises the concern that reaction products at the electrode interface may affect cell behavior. The dominant platinum electrode reactions range from the relatively safe electrolysis of water at lower currents to the highly toxic oxidation of metal and organic species at higher currents [Brummer and Turner, 1977]. The i-v characteristics of a platinum media system [McLeod, 1986] suggest that "safe" operation at 0.1 Hz occurs for currents densities under 100 $\mu A/cm^2$ of electrode area. In these chambers, the electrode area was approximately 3 cm^2. For a sample area of 0.3 cm^2, applied

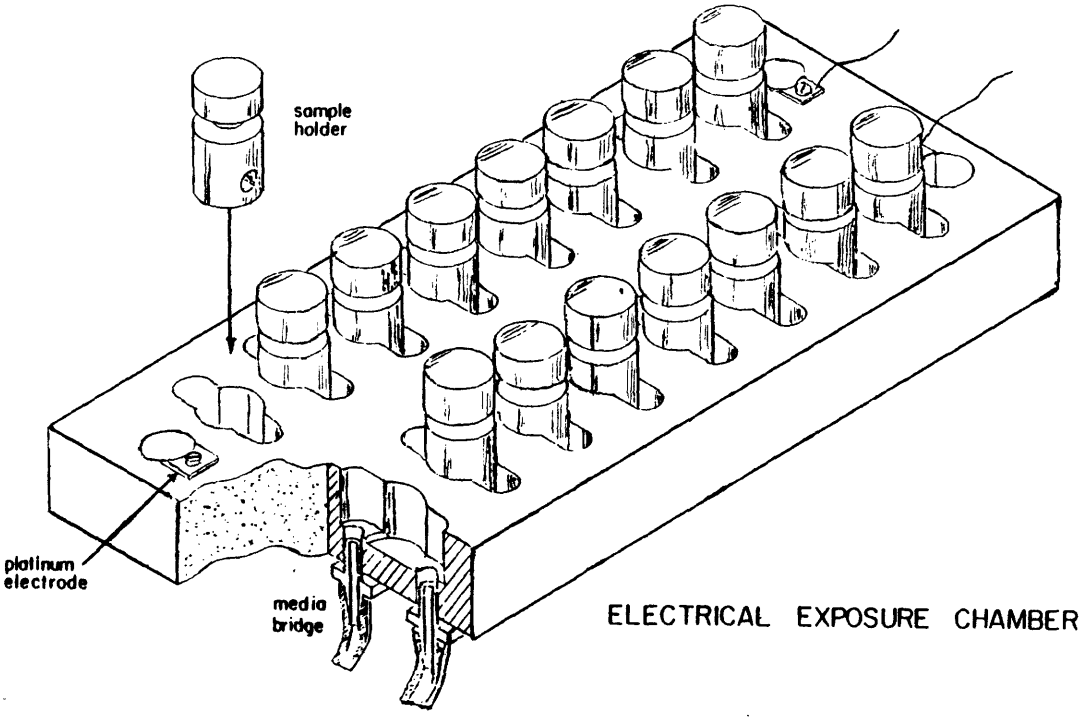

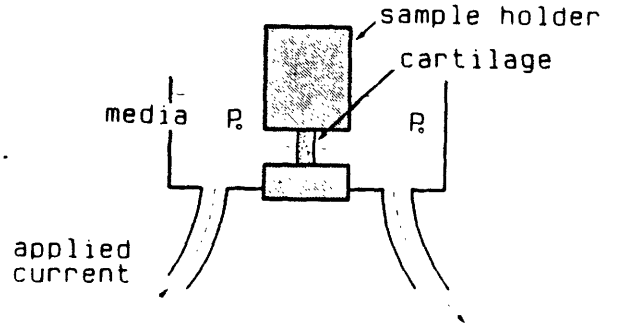

Figure 4.1: Electrical exposure chamber and sample holders. Sample holders have a 1/4 inch diameter channel to hold 1/4 inch diameter cartilage plugs. Holders are placed in individual wells which are connected in series to each other and to the electrodes by Tygon tubing.

current densities of up to 1 mA/cm^2 should result in minimal toxic product formation. The safe limits on current increase with increasing frequency.

In case electrode products were produced, media bridges between electrodes and samples were provided by a media-filled Tygon tubing connection between wells. The length of these bridges were adjustable according to the duration of the experiment. Typically the tubing was 8 cm long, which is approximately 8 times the distance products would be expected to travel during a 12 hour experiment[10].

Two programmable current sources were used to provide the driving signal. Current sources were used to ensure that changes in electrode impedance with time did not affect the stimulus signal. The current source, described more completely by McLeod [1986], was designed to minimize the direct current through the sample.

4.2.2 Leakage Currents

The applied current will flow either through the channel in the sample holder or around the holder itself. Although the holder was designed to fit tightly in the chamber, the magnitude of the leak was determined experimentally by Liu [1985] and Sah [1985]. Sah found that if the holders were placed in an initially dry chamber, at most 5% of the current was shunted. If the media was added before the holders were positioned, the maximum shunt resistance increased to 15%. For the

---

[10] Assuming $D = 10^{-5}$ cm^2/s, the diffusion distance, x, over a time, t, is calculated from $x^2 = 2Dt$.

experiments reported, media was added to the chambers after the sample holders were in place. The applied current density was simply calculated as the applied current divided by the channel area of 0.317 cm^2.

4.2.3 Ohmic Heating

Ohmic heating becomes a concern as the current density increases. Temperature enhances biological processes by a factor of 2-4 for a 10°C rise [Dowben, 1969]. A one degree rise could increase synthesis by as much as 15%. The two regions of the chamber where ohmic dissipation will be greatest are in the channel itself, where the sample would be directly heated and in the small diameter media bridges between sample wells, which could heat the sample by heat conduction. At current densities of 1 mA/cm^2 inside the channel, approximately 25 μWatts will be dissipated. This corresponds to .27 calories over the course of a 12 hour experiment. In a worst case analysis assuming no heat transfer the temperature in the channel would rise about 1/2 °C. (The channel contains ~1/2 ml.) Similarly, in an 8 cm long, 3/16 in. diameter media bridge, 1.5 calories would be expected to heat the 1.5 ml of contained media by a maximum of 1°C during a 12 hour experiment. These calculations suggest that with current densities up to 1 mA/cm^2 within the channel significant temperature rises within the sample are unlikely.

These theoretical predictions have been verified experimentally for current densities up to 5.7 mA/cm^2 (the maximum output capability of the current source). Two of the sample holders were instrumented with

thermistors (Thermometrics, Edison, NJ; P60DB103M) and temperature was monitored using a standard bridge configuration. Following a 3 hour equilibration period, after which the temperature measured by both thermistors was the same and constant, current densities from 1 to 6 mA/cm^2 were imposed. The results, shown in figure 4.2, demonstrate that minimal heating occurs at current densities under 3 mA/cm^2. 5.7 mA/cm^2 resulted in a 0.14°C increase in temperature.

4.3 Electrical Exposure Protocol

The response of epiphyseal plate in organ culture was determined over a current density range of 50 to 1000 $\mu A/cm^2$ at frequencies between 0.1 and 100 Hz. Two to four days following explant, 1/4 inch diameter CEP samples were subjected for 12 hours to a specific electrical stimulus while bathed in labeling media. The 50 $\mu A/cm^2$ data represent glucosamine incorporation. The remaining studies assayed sulfate and proline incorporation. Following exposure, the tissue was treated as described in chapter 3. Data is presented as the ratio of incorporation between exposed and control samples paired according to level relative to the hypertrophic zone.

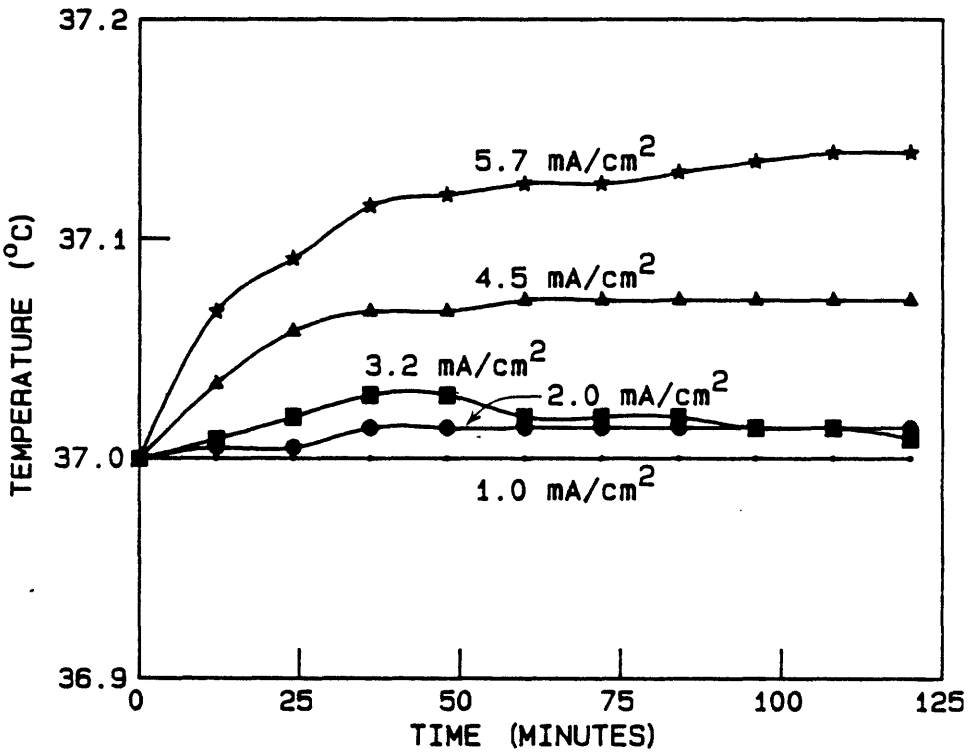

Figure 4.2: Ohmic heating in electrical chambers. (•) 1.0 mA/cm², (●) 2.0 mA/cm², (■) 3.2 mA/cm², (▲) 4.5 mA/cm², (★) 5.7 mA/cm².

4.4 Electrical Exposure Results and Conclusions

Table 4.1 summarizes the number of experimental and control pairs subjected to a given current density and frequency. The specific experimental results are reported in complete detail by Liu [1985] and Wang [1986]. None of the applied electrical currents resulted in a detectable change in ^{35}S-sulfate or ^{3}H-proline incorporation during the 12 hour exposure and label period.[11] The mean experimental to control ratios for a range of current densities at 10 Hz and a range of frequencies at 500 $\mu A/cm^2$ are shown in figure 4.3 The emphasis on frequencies near 10 Hz was motivated by the marked frequency sensitivity of McLeod's [1986] fibroblast preparation.

Current densities in excess of 1 mA/cm^2 have not yet been tested for three reasons. One, the impedance of a chamber using all sample holders exceeds the drive capabilities of the current source. Two, ohmic heating will occur and may directly affect the synthetic behavior at currents in excess of 1 mA/cm^2. Finally, the primary motivation for the study was to assess the likelihood that streaming currents play a major

---

[11] The data was analyzed by both the nonparametric sign test of Dixon and Mood and the parametric t-test. In contrast to the t-test, the nonparametric test does not assume a normally distributed sample population, or that the samples originate from a common population. There were insufficient data to establish that the data were normally distributed. In all but one case, the two approaches agreed that there was no significant difference between experimental and control samples. Sulfate incorporation by a set of 14 pairs, with exposure parameters of 500 $\mu A/cm^2$ and 10 Hz, had a mean ratio of exposed:control of 1.08 ($\pm$ 0.16) which, by the t-test, was significant ($p<0.05$).

	frequency(Hz)			
J($\mu A/cm^2$)	0.1	1.0	10	100
50	8*	24	21	
200			27	
300		19	26	13
500	9	10	14	12
1000			22	

* these samples were tested at 0.2 Hz

Table 4.1: Number of tissue pairs tested at stated current density and frequency.

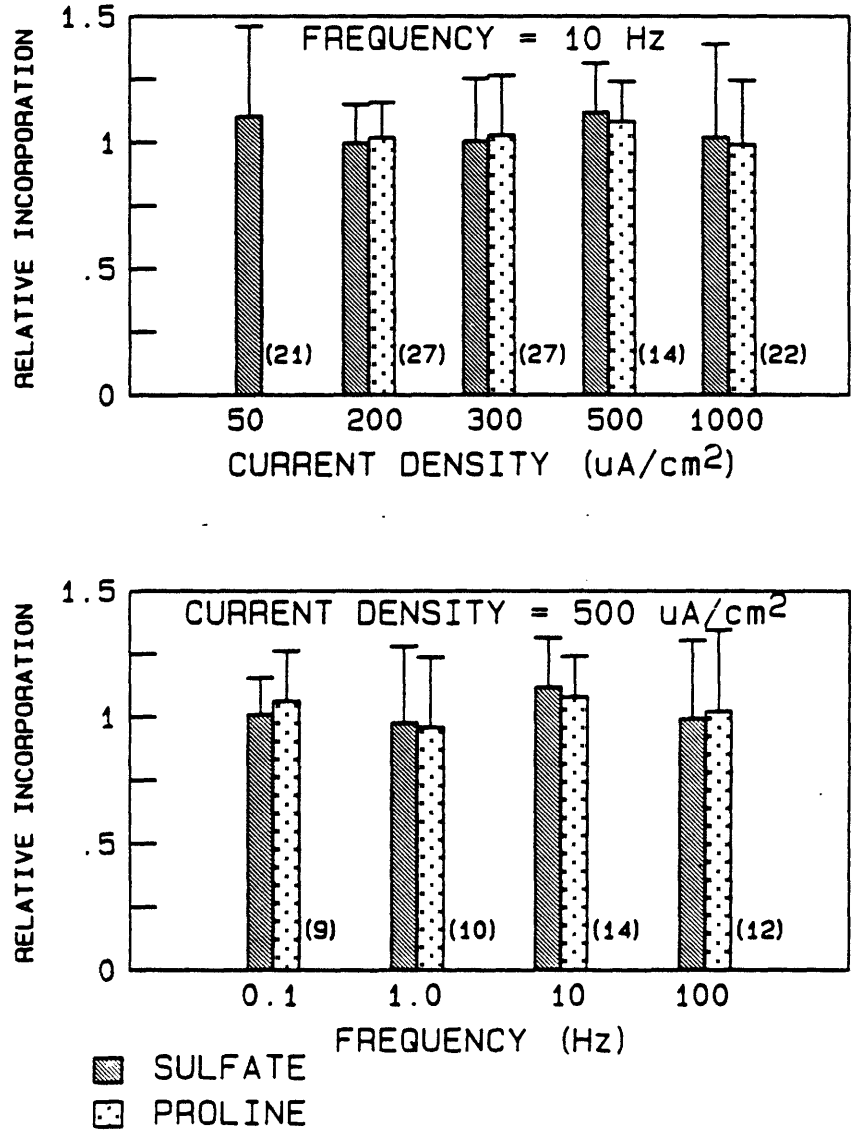

Figure 4.3: Relative incorporation over 12 hours as a function of current density at 10 Hz (upper panel) and frequency at 500 $\mu A/cm^2$ (lower panel).

role in the chondrocyte response to applied loads. It is unlikely that a significant number of chondrocytes are exposed to current densities in excess of 1 mA/cm^2.

In this experimental configuration the applied current will induce fluid flow. Based on typical values for $k_i \approx 10^{-8}$ $m^3/Amp \cdot s$ [Lee et al., 1981], a peak fluid flow of 0.1 μm/s would be expected for a 1 mA/cm^2 current density. At one hertz, the fluid will move less than 0.1 μm thus it is presumed that the fluid flow will have a negligible effect on the bulk transport of nutrients under these experimental conditions.

The motivation for these experiments was to examine the sensitivity of chondrocytes to currents similar in magnitude and frequency to those expected to occur in <u>in vivo</u> loading situations. In this experimental configuration the tissue was subjected to a uniform current density and electroosmotic fluid flow while remaining undeformed. These results suggest either that 1) electrical currents under 1 mA/cm^2 and fluid flows of under 0.1 μm/s do not lead to a change in ECM and thus currents may not be significantly involved in the chondrocyte response to dynamic loading or 2) that the response to dynamic loading involves a small fraction of the biosynthetic activity or 3) that the turn-on time, τ_{c_on}, is long compared to the 12 hour exposure period.

Chapter V

RESPONSE TO STATIC LOADS

5.1 Physiologic Rationale

The next series of experiments was designed to characterize the biosynthetic response to static loading. As discussed in section 2.6.2, in this experimental configuration strain (deformation) and consolidation are distributed uniformly throughout the tissue, and streaming potentials and fluid flow are absent. Three experimental series will be discussed. The first investigates the biosynthetic behavior as a function of load magnitude. The second series probes the kinetics of the response to an increase in load. The final series demonstrates the response following the removal of a static load. The discussion which follows describes the rationale for examining the response to loads up to 3 MPa.

The physiological loads at the growth plate cannot be measured directly without disturbing the normal structure. The plate must support compressive forces imposed by body weight, surrounding musculature, and perhaps periosteum. Rodan et al. [1975] estimated the stress on rat and chick epiphyseal plate to be 5-20 kPa assuming only loads due to body weight. The foreleg from the 50-100 lb calves used in these studies has an area of ~10 cm^2, so the equivalent stress due to 1/4 body weight is 50 - 100 kPa. Actual stresses may be much higher due to the inhomogeneous nature of the epiphysis and metaphysis, the convoluted

plate topology, and the action of the musculature.

A variety of techniques have been employed to determine stresses imposed on articulating cartilage. Hodge and coworkers [1986] have developed an instrumented femoral head prosthesis which measures the spatial distribution of contact stresses during normal ambulation. They have measured peak stresses on the order of 20 MPa.

The compressive load acting on lumbar spinal segments during walking has been investigated by Cappozzo [1984] using photometric data in conjunction with a theoretical model of the trunk. Their results showed that the segments are subjected to cyclic loading with a frequency ranging from 1.2 to 2.5 Hz, and amplitude ranging from 0.2 to 2.5 times body weight. From measurements of supine anesthetized subjects, they determined that the disc was preloaded by approximately 200 N. The load increased to 400 N in nonanesthetized supine subjects. They do not report the segment area, but assuming a cross sectional area of 1500 mm^2 [Sonnerup,1982], ligaments and stablizing musculature impose a static stress on the order of 600 kPa. A walking 70 kg man may impose peak stresses as high as 12 MPa.

Moran et al. [1985] measured contact areas of the phalangeal joints in a frame which simulated the loading and relative positioning for pinch and grasp tasks. Loads at the individual joints were calculated theoretically based on the geometry associated with the task. Contact stresses between 0.8 and 1 MPa were computed during pinch.

These reports of stresses sustained by articular cartilage provide a range of physiologic static loads as high as 1 MPa, and peak dynamic

loads over 20 MPa. Given the similarities between epiphyseal plate and articular cartilage in composition and histological appearance, the plate may be capable of withstanding and responding to loads of similar magnitude. The experiments reported in this chapter were designed to cover a load range of 0 to 3 MPa, with particular emphasis on behavior under 1 MPa.

5.2 Experimental Apparatus

The step loading experimental apparatus was designed according to the following criteria:

1. It must provide the conditions necessary for organ culture. Thus it must be non-toxic and autoclavable and must ensure adequate media supply.
2. It must provide for uniform and well defined application of load to the sample.
3. It must allow testing of a wide range of load amplitudes.
4. It must allow simultaneous testing of a large number of samples.
5. It must minimize media usage.

Two experimental loading chambers were designed to satisfy the above criteria. (figure 5.1) In each apparatus tissue was placed in a media-filled well. A nylon or teflon platen was then placed directly on top of the tissue plug to transmit the applied load. In one apparatus (described more completely by Sah [1986]), 35 wells were machined from a polysulfone block. A platen guide plate mounted several inches over the wells ensured that the platen remained perpendicular to the bottom of

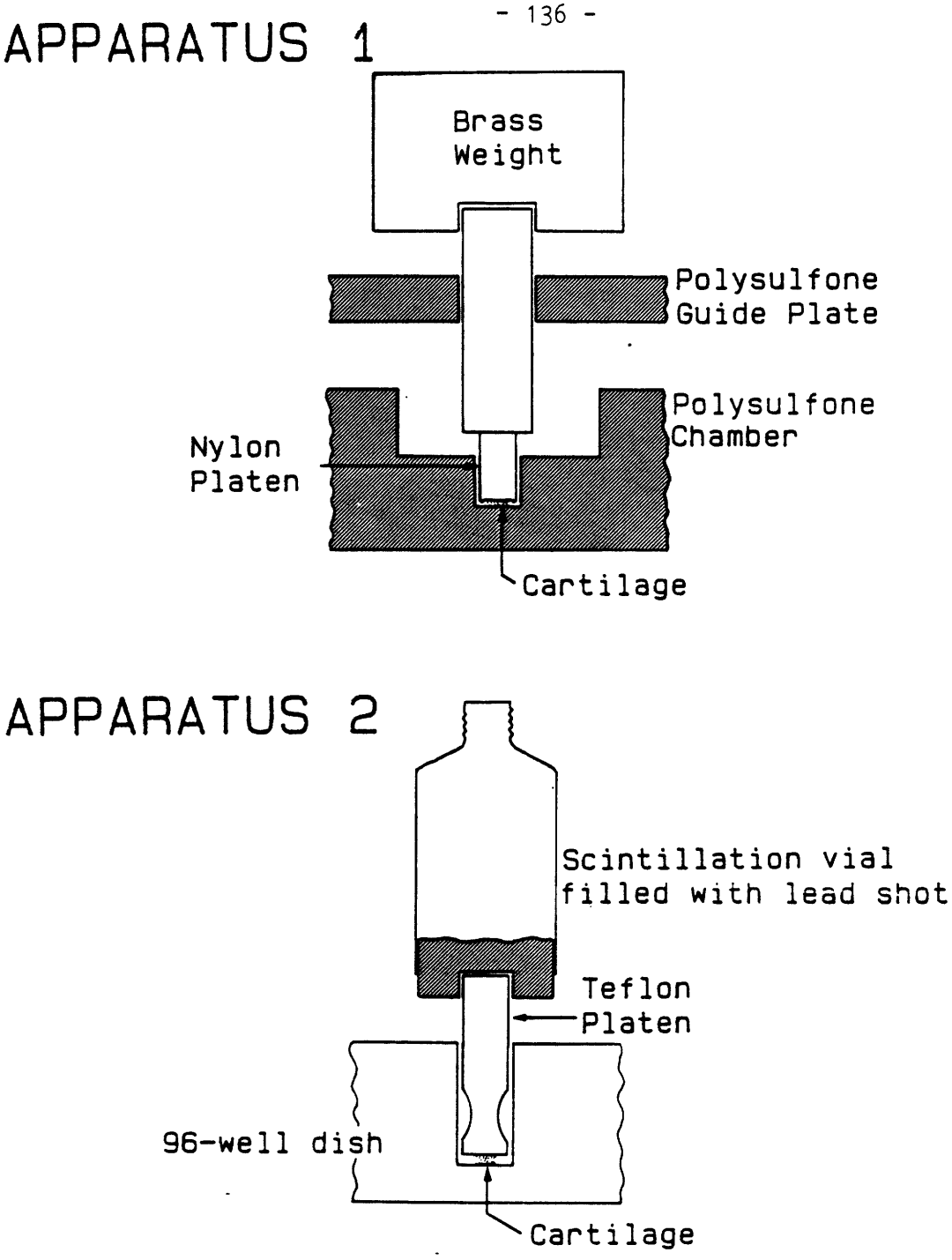

Figure 5.1: Tissue sample is compressed by a cylindrical platen loaded with a brass weight (apparatus 1) or lead weights (apparatus 2). The teflon platen used in apparatus 2 was grooved to allow for an ample media supply. In apparatus 1, the two-well construction provided space for the media bath. The platens are maintained perpendicular to the well bottom either by the chamber walls (apparatus 2) or by a platen guide (apparatus 1). (Apparatus 1 is more completely described elsewhere [Sah, 1986].)

the well. Brass weights placed on top of the platens provided the load. The second apparatus used standard 96-well tissue culture dishes (Falcon, #3072). The 13 mm well was sufficiently deep to keep the Teflon platen perpendicular to the bottom. 20ml glass liquid scintillation vials, modified as shown in figure 5.1, were filled to the desired weight with #9 lead shot. For the purposes of the experiments in this chapter, the two setups are essentially identical. The double-well feature of apparatus 1 is more practical for confined compression studies since sufficient media availability is ensured. For experiments in which more than 35 samples were used, apparatus 2 is necessary.

5.3 Material Behavior Under Step Conditions

Interpretation of the synthetic response to a step load requires characterization of the material response. Two studies, equilibrium load versus deformation and equilibration time versus load were carried out using one of two mechanical spectrometers, each capable of applying a step mechanical displacement (load), while monitoring the resulting load (displacement). To allow extrapolation to later experiments, the data presented in this section represent the behavior of 2 mm diameter, 800 μm cut-thickness epiphyseal cartilage in unconfined compression.

5.3.1 Load versus Deformation

Tissue plugs were harvested and maintained in culture for several days as per the standard protocol. The sample was then equilibrated in HBSS and placed between a glass plate and polysulfone platen. The equilibrium load at each thickness was recorded for step compressions of 25 μm. The criterion for equilibrium was that the load remained constant (to within 2.5 gm) for at least 3 minutes. Three typical load versus compression curves are shown in figure 5.2. Least squares fit of data for loads of less than 30 gms provided an estimate of the free swelling thickness on the order of 1 mm. Note that the tissue has swollen from its initial cut thickness of 800 μm. This observation is consistent with direct measurement and predictions based on wet weight following incubation in tissue culture. The fit also estimates Young's modulus (E) to be 344 kPa, assuming a 2 mm plug diameter. This corresponds to an equilibrium bulk longitudinal modulus[12] of 737 kPa. This value is typical of those reported for hyaline cartilage [Lee et al., 1981].

As can be seen from figure 5.2, the material behavior becomes non-linear for deformations over 40%. This nonlinearity arises from two sources. In unconfined compression, the tissue will expand radially. Poisson's ratio (the ratio of radial to longitudinal strains) for cartilage is reported to be on the order of 0.4 [see discussion in Hoch

---

[12] Bulk longitudinal modulus (H_A) is related to Young's modulus by:

$$H_A = E(1-\nu)/(1-\nu-2\nu^2)$$

where Poisson's ratio, ν, is assumed to be 0.4 [see discussion in Hoch et al., 1983]

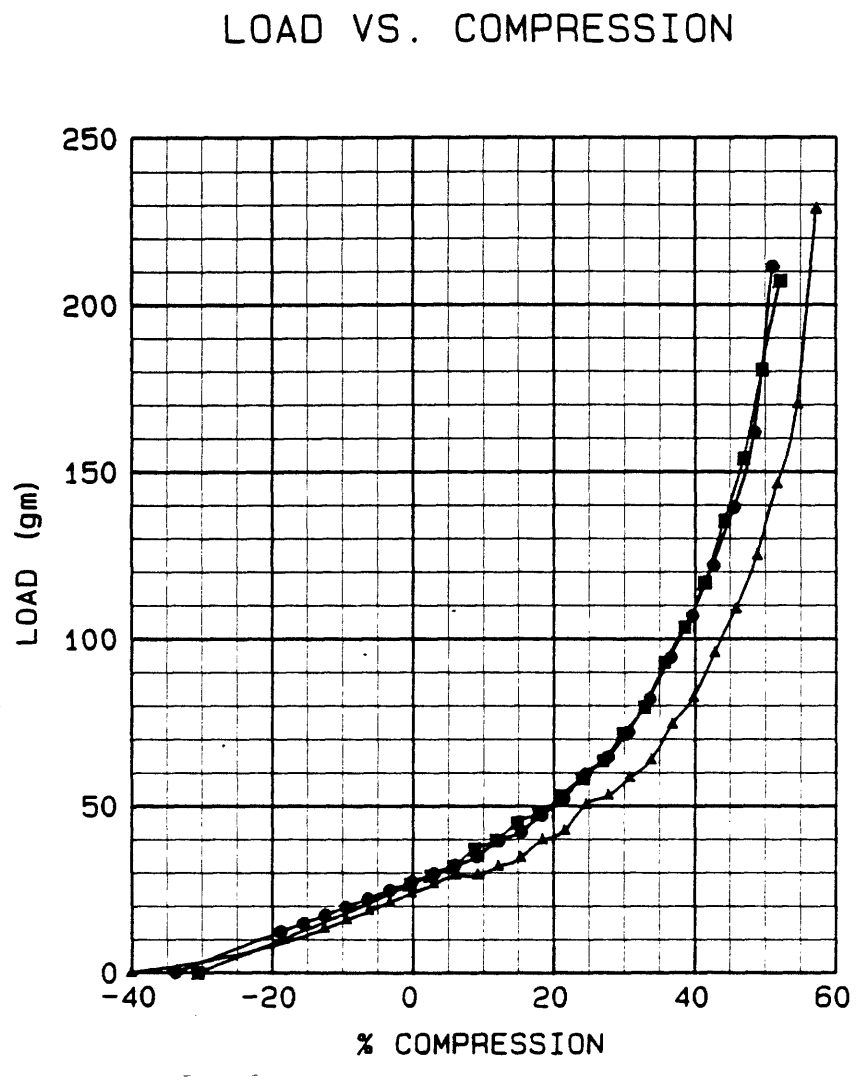

Figure 5.2: The load required to maintain 2 mm diameter cartilage disks at a given compression. Compression is defined relative to the cut thickness of 800 µm. The deformation below 30 gms is extrapolated to zero load using a least squares fit. The free swelling estimate of 20-40% is consistent with the typical swelling of the disks under culture conditions.
Least squares fit of the three runs plotted were:
(■) : load = -108 gm/mm × (thickness - 1.045) r=.999
(▲) : load = -108 gm/mm × (thickness - 1.021) r=.999
(●) : load = -102 gm/mm × (thickness - 1.071) r=.999

et al., 1983]. Under frictionless experimental conditions, a longitudinal compression of 40%, for example, will increase the loading area by ~35%, thereby decreasing the stress imposed by the given load. Thus, in unconfined compression even a perfectly linear elastic tissue will require progressively more load to achieve a given change in displacement for large enough displacements.

A perhaps more significant source of nonlinearity arises from the two-phase nature of the tissue. As the compressed volume approaches the solid volume (~20%), it is expected that the material properties begin to resemble that of the solid, rather than that of the porous network. Furthermore, if cell volume is maintained during compression, cells will account for up to 10% of the unstressed volume [Stockwell and Meachim, 1972]. Thus, the maximum possible deformation by physiologically realistic loads is on the order of 70%.

The data presented in the following sections demonstrate a synthetic response to an applied load. They are interpreted in terms of the resulting deformation, as estimated by the data of figure 5.2. In addition, if the applied stress is estimated assuming the free swelling plug diameter, comparisons can be made to experiments on different plug sizes and to reported in vivo stresses and deformations. The deformations and stresses predicted in this way should represent an upper bound on those which result from the same load in vivo because of the unconfined configuration.

5.3.2 Mechanical Equilibrium

The designation of these experiments as "static" is based on the assumption that all mechanical processes occur on a time scale very short compared to the testing time. The time required to be within 8 gm of the final equilibrium load (approximately 5 1/e time constants) was measured in the stress relaxation studies described above. The time increased with increasing compression implying that the permeability decreases faster than the modulus increases[13]. The equilibration time was under 5 minutes for deformations under 40%. The time increased to approximately 8 minutes at 50% compression and by 60% compression it was over 15 minutes. The tracing in figure 5.3(a) shows typical stress relaxation behavior for tissue compressed to approximately 40%. Tissue behavior under an applied load rather than applied deformation requires longer to reach equilibrium. To quantify this, creep deformation experiments were performed for loads of 70 and 140 gm. Figure 5.3(b) is a typical tracing. Deformation was within 10% of the equilibrium value after 30 minutes. Reswelling following unloading was significantly more rapid and was essentially complete within 15 minutes.

5.4 Synthetic behavior as a function of step load magnitude

Several studies were performed to determine the synthetic behavior

---

[13] The time constant is proportional to $x^2/H_A k$, where x is the characteristic distance, H_A the modulus, and k the permeability.

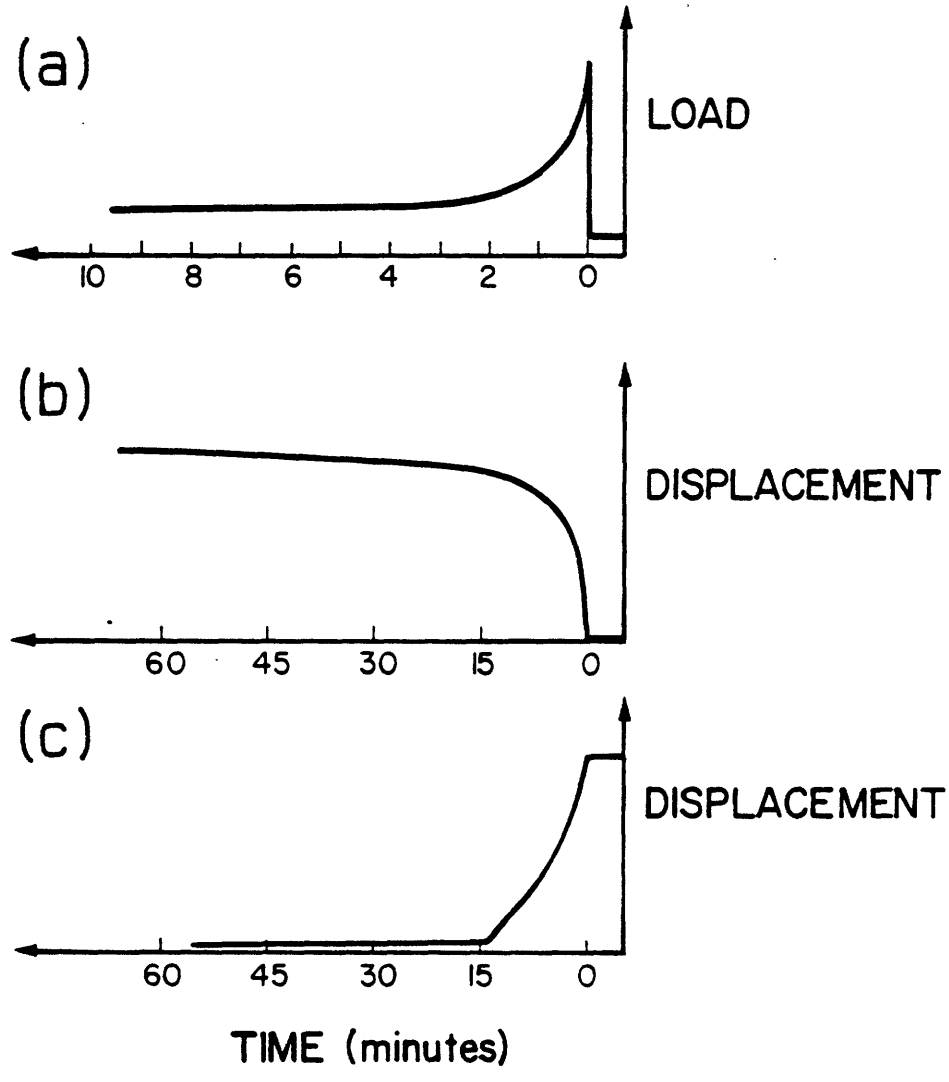

Figure 5.3: (a) Stress relaxation: Chart recorder tracing of the load experienced by a 2 mm diameter cartilage plug, initially loaded by 45 gms (~40% compression), following a 25 μm step deformation. The final equilibrium load is reached in approximately 5 minutes.
(b) Creep deformation - step load: Chart recorder tracing of the deformation experienced by a 2 mm diameter cartilage plug resulting from a step 140 gm load. (c) Creep deformation - step load removal: Chart recorder tracing of the reswelling experienced by a 2 mm diameter cartilage plug following load removal. Tissue was initially at equilibrium under a 140 gm compressive load.

of cartilage as a function of applied load. Following the protocol in figure 5.4, loads up to 3 MPa were applied for 12 hours while the tissue was bathed in labeling medium. Figure 5.5 shows incorporation of ^{35}S-sulfate and ^{3}H-proline by 1.8 mm diameter plugs subjected to loads from 0 to 735 grams. (estimated stresses from 0 to 2.7 MPa). Both proline and sulfate incorporation exhibited a dose dependent depression.

Three subsequent series of experiments focused on stresses under 1 MPa. As shown in figure 5.6 the dose dependent depression in both GAG and protein synthesis (as estimated by ^{35}S-sulfate and ^{3}H-proline incorporation, respectively) by 2 mm diameter cartilage plugs was confirmed. Figure 5.7 shows the pooled data from figures 5.5 and 5.6 in terms of estimated stress and indicates a consistent degree of depression for a given load.

Alternatively, incorporation can be viewed (Figure 5.8) as a function of tissue compression where compression is estimated from figure 5.2. Here, synthesis decreases abruptly for compressions under ~35%.

The apparent, although not statistically significant, enhancement in synthesis for the 25 gram load is interesting. Under a 25 gram load the tissue is compressed to approximately the original cut thickness. The appearance of the synthesis versus deformation curves is consistent with a threshold phenomenon associated with the response to account for the behavior at lower load levels. At very high loads (>1 MPa), the depression in synthetic rate plateaus, suggesting that there is a maximum effect.

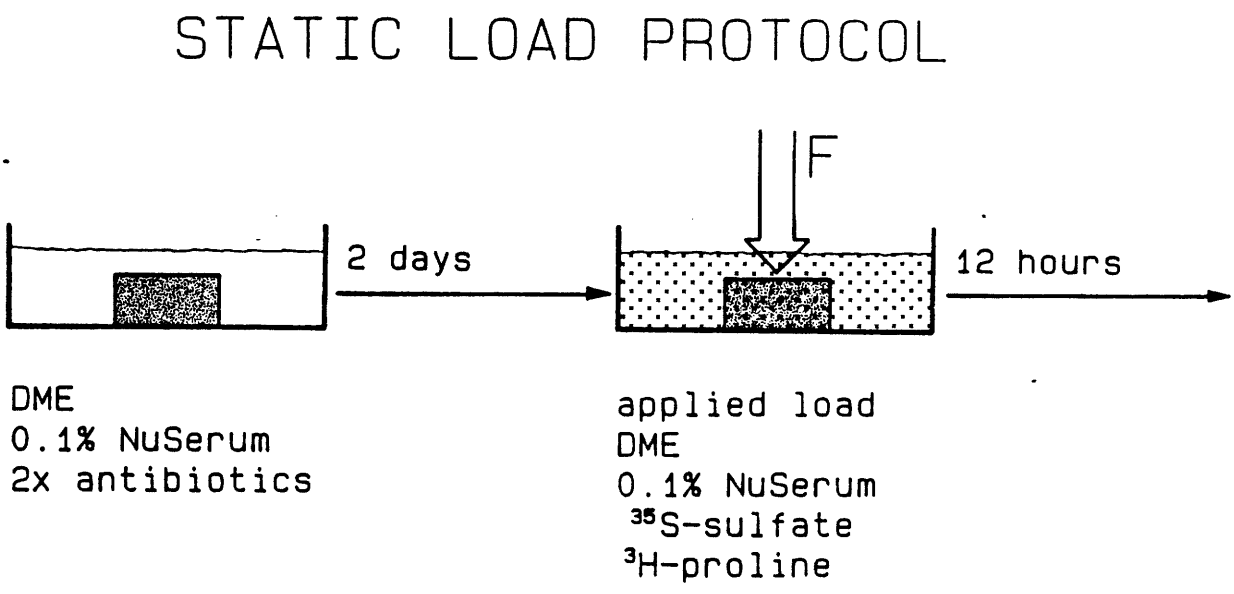

Figure 5.4: Protocol for the synthesis versus load experiments. After 2 days in culture, tissue was transferred to the experimental chamber containing labeling medium (DMEM supplemented with 0.1% NuSerum, 20 µCi/ml ^{35}S-sulfate, 10 µCi/ml ^{3}H-proline, and 0.5 mM proline). Tissue was incubated and loaded for 12 hours, then washed and analyzed as described in chapter 3.

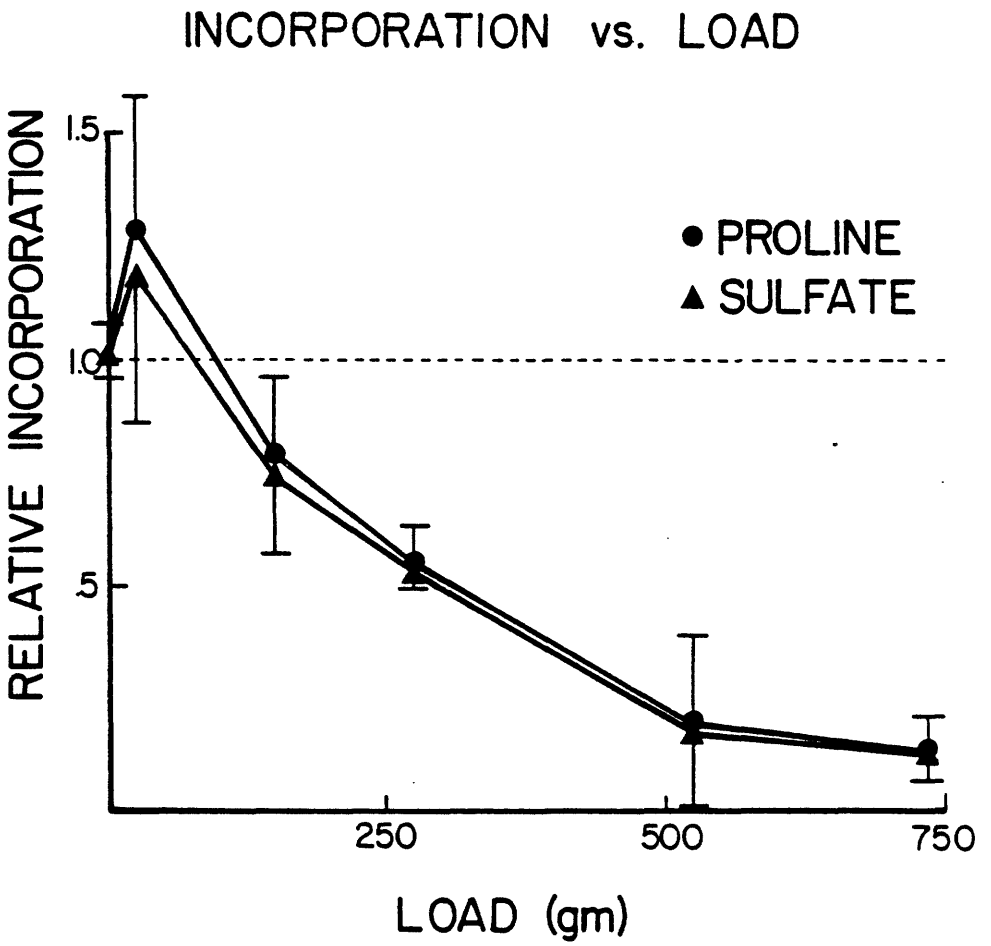

Figure 5.5: ^{35}S-sulfate and ^{3}H-proline incorporation normalized to the mean of the no-load controls is plotted versus applied load. Estimated stresses range from 0 to 2.7 MPa. Tissue plugs were 1.8 mm in diameter. Incorporation was assessed over 12 hours. Each point represents the mean and standard deviation of 4 to 5 specimens.

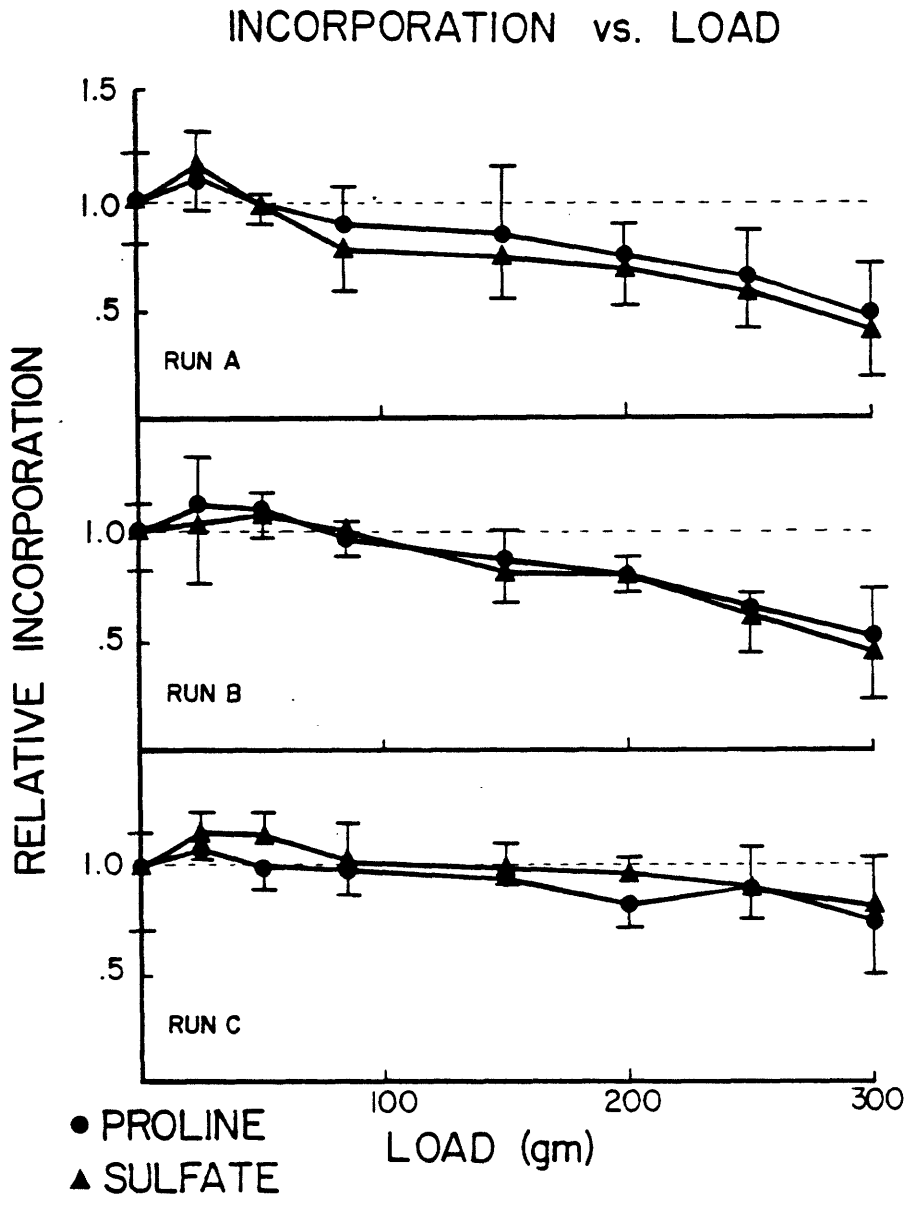

Figure 5.6: ^{35}S-sulfate and ^{3}H-proline incorporation normalized to the mean of the no-load controls is plotted versus applied load. Estimated stresses range from 0 to 936 kPa. Each of three independent runs are plotted separately. Tissue plugs were 2 mm in diameter. Incorporation was assessed over 12 hours. Each point represents the mean and standard deviation of 4 to 5 specimens.

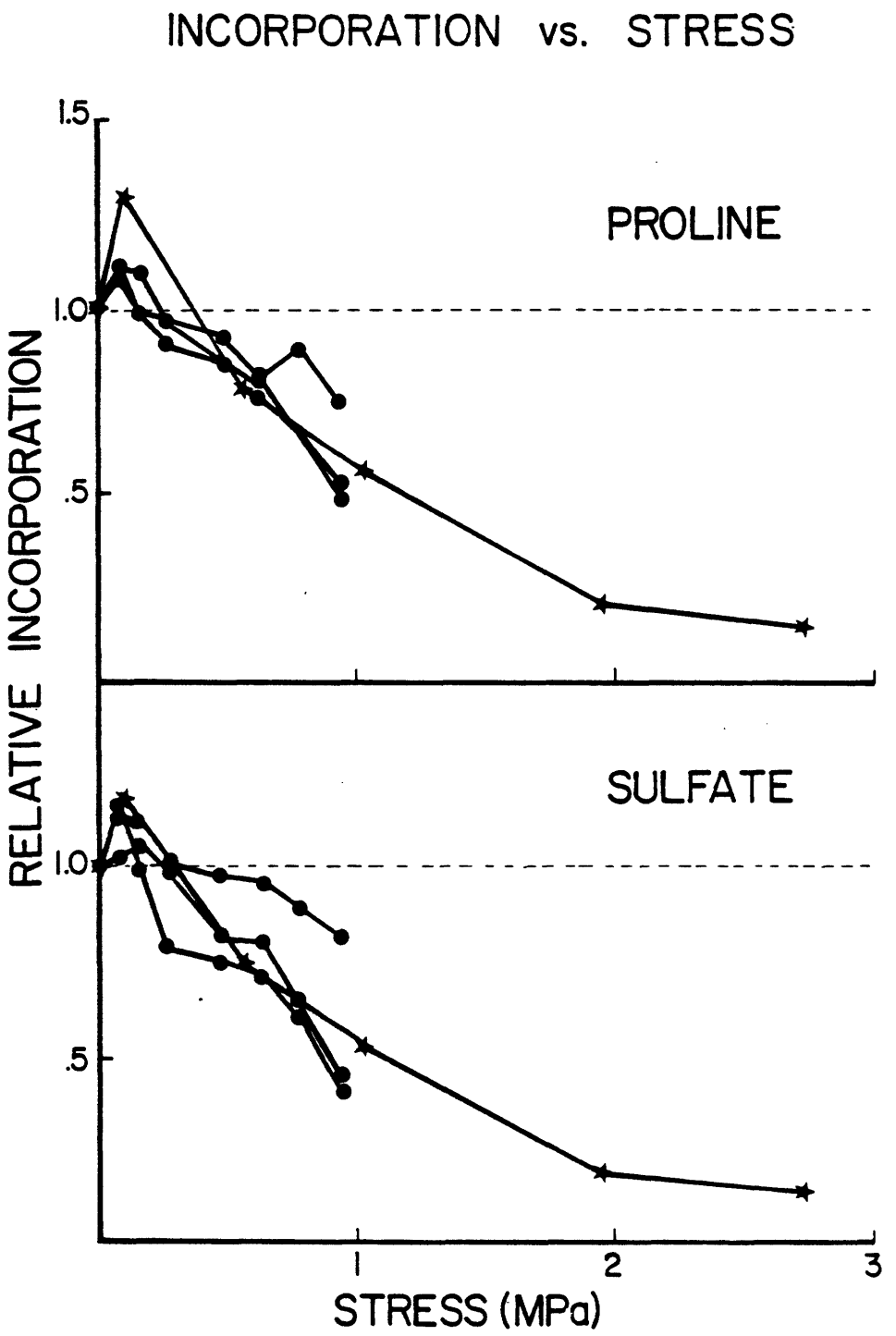

Figure 5.7: Data from figures 5.5 and 5.6 are replotted here as a function of estimated stress. Data from individual experiments are connected by a line.

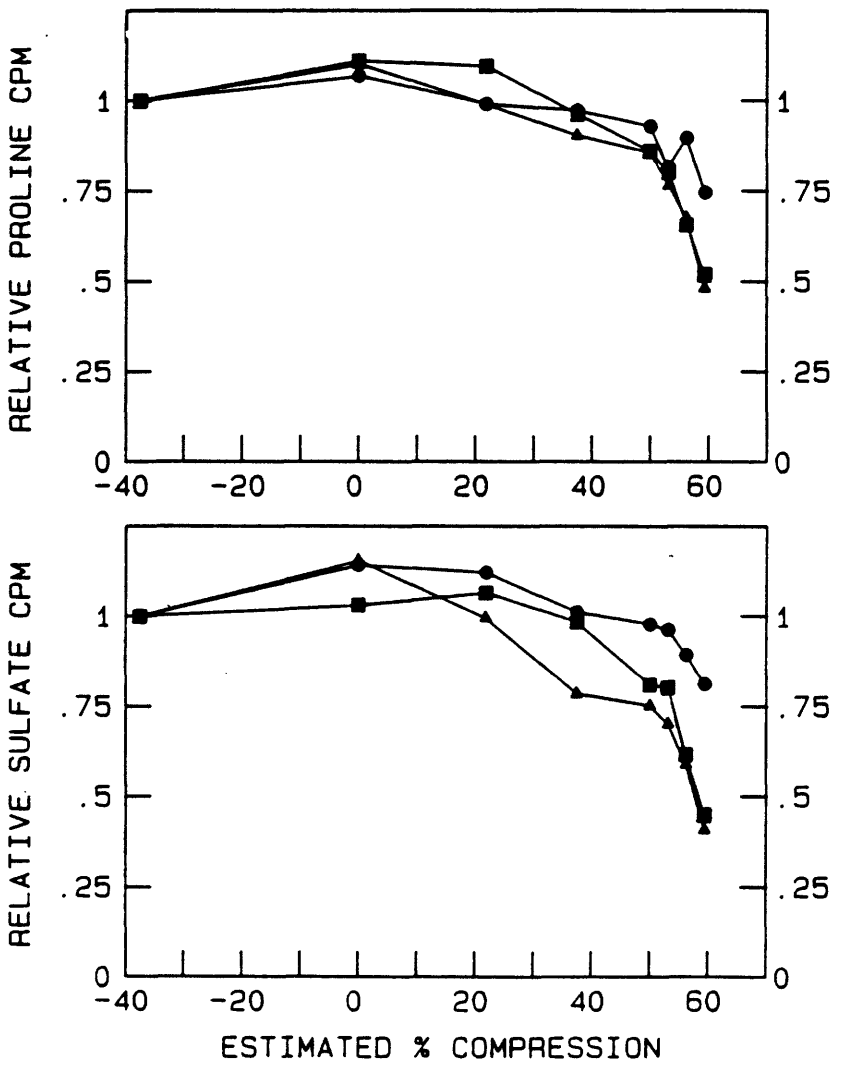

Figure 5.8: Data from figure 5.6 is replotted versus compression as estimated from figure 5.2.

The magnitude of depression was very similar for proline and sulfate incorporation. This indicates either a generalized synthetic depression, or an artifact of radiolabel diffusion. The results of section 5.6 will demonstrate that this depression cannot be accounted for simply by decreased diffusion of radiolabel.

In summary, a dose dependent depression in both protein and GAG synthesis has been observed for stresses up to 2.7 MPa. The dose dependence is more abrupt when viewed as a function of tissue deformation.

5.5 Synthetic behavior as a function of time during load

In order to determine the kinetics of the depression in synthesis, samples were subjected to 0, 70, or 140 grams for various time periods during labeling.

The experiments of figure 5.9 span loading times up to 26 hours. There is a monotonic increase in proline and sulfate incorporation at all load levels. Synthesis relative to unloaded values is 45% less for 140 grams (~0.5 MPa) and 30% less for 70 grams (~0.25 MPa). The results of figure 5.10 span shorter loading times of up to 12 hours. Again, sulfate and proline incorporation increases monotonically at all load levels. Proline incorporation by loaded samples was consistently depressed. Sulfate incorporation by loaded samples was near control levels at early loading times and became progressively depressed. To estimate the characteristic time constant for onset of depression, the

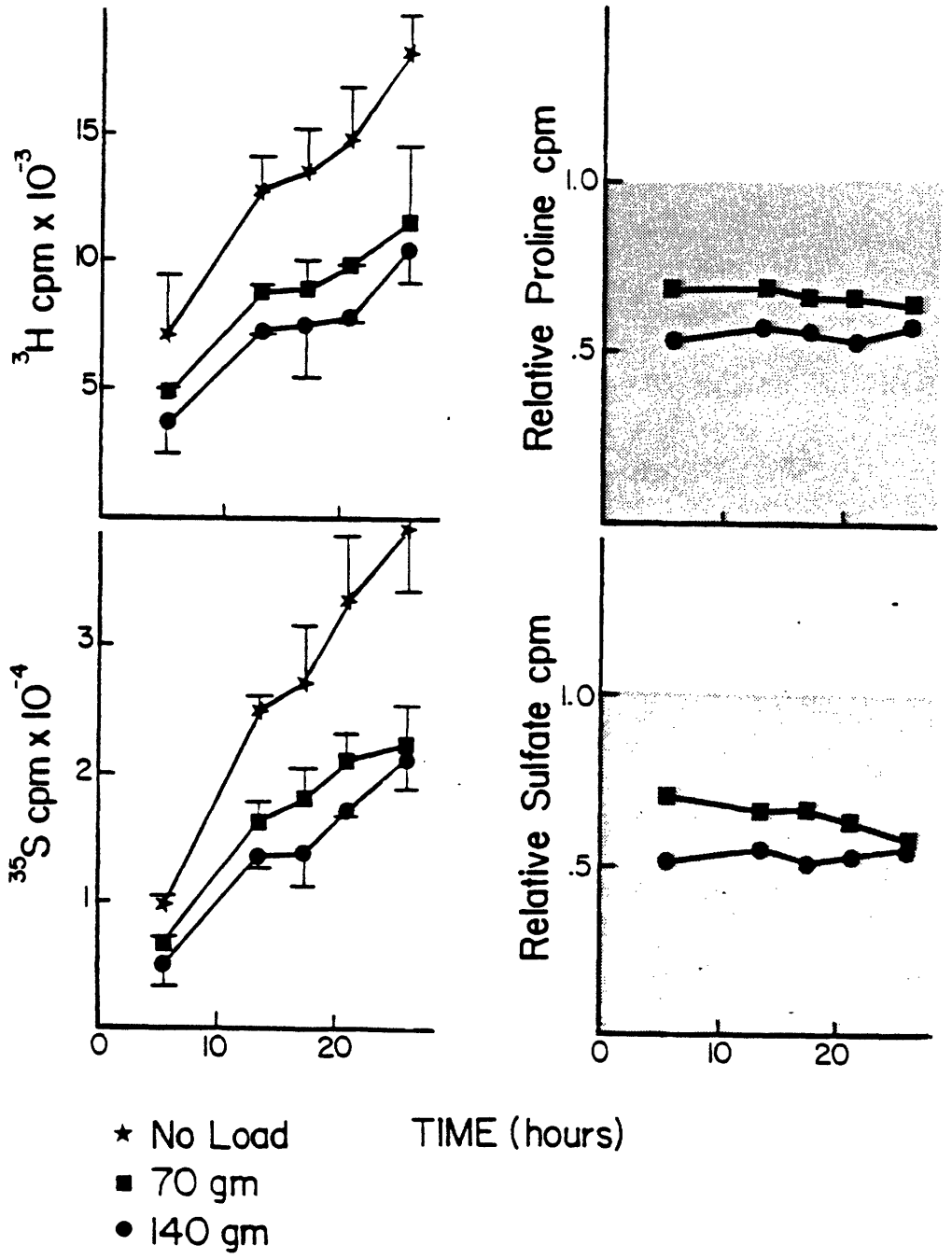

Figure 5.9: Incorporation of proline and sulfate as a function of load and labeling time. The lefthand panels present the mean and standard deviation of radiolabel counts for 3 to 4 samples. The righthand panels depict the incorporation relative to unloaded controls. no load (★), 70gm (■) 140gm (●).

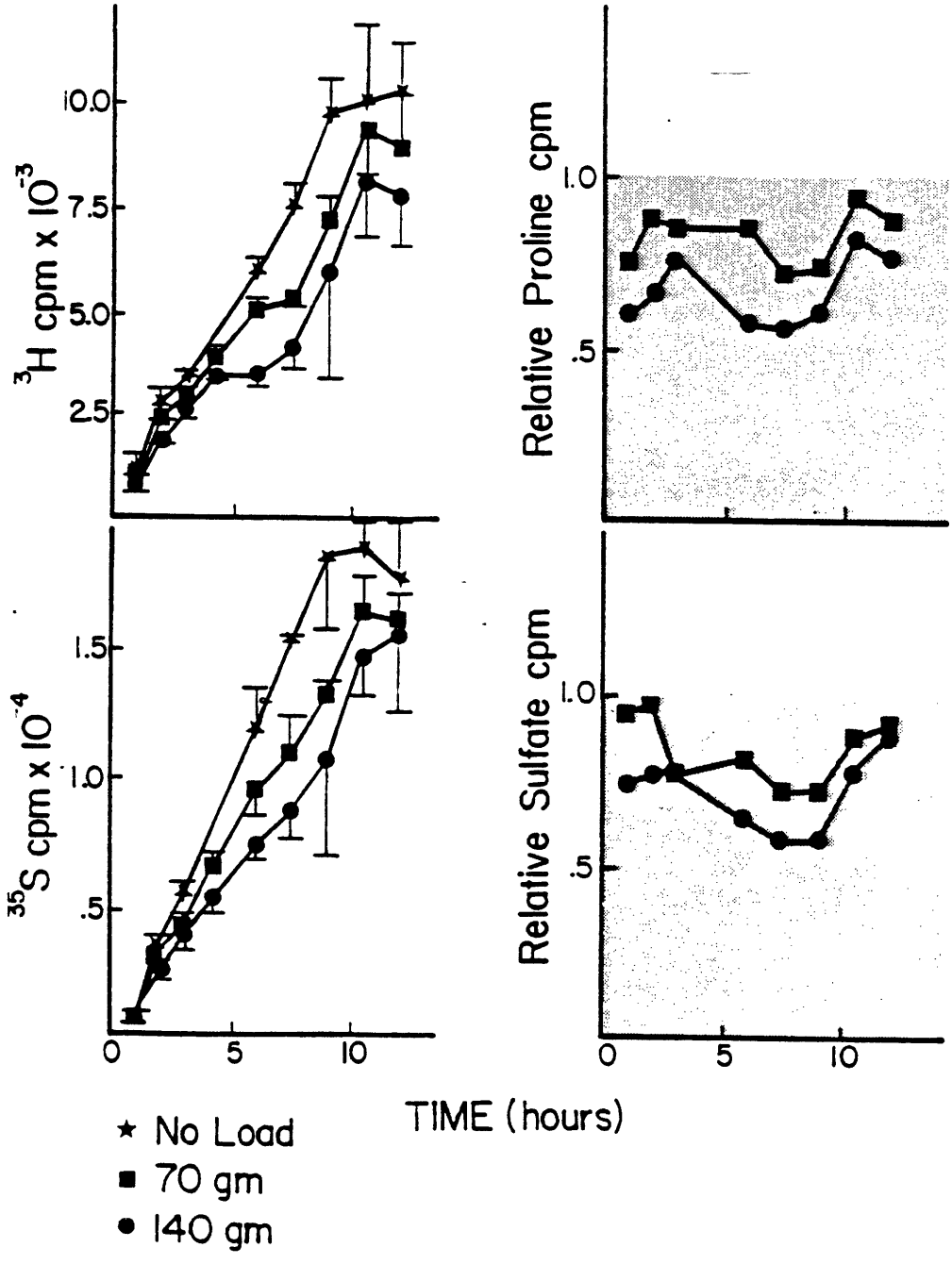

Figure 5.10: Incorporation of proline and sulfate as a function of load and labeling time. The lefthand panels present the mean and standard deviation of radiolabel counts for 3 to 4 samples. The righthand panels depict the incorporation relative to unloaded controls. no load (★), 70gm (■), 140gm (●).

results of the 140 gram groups from the experiments of figure 5.9 and 5.10 are presented in figure 5.11 with exponential curves which bound the data. Proline incorporation reaches a steady 55% depression with a time constant between 0.5 and 3 hours. Sulfate incorporation takes somewhat longer, 2 to 6 hours, to reach a steady 50% depression. The plateau seen in incorporation by unloaded samples in the latest two data points of figure 5.10 was atypical behavior so these data points were omitted from the data summary.

A modified protocol was used to examine more closely the synthetic behavior at shorter times. Unloaded tissue was bathed in labeling media at 4°C for 1.5 to 2 hours to ensure that the radiolabel had equilibrated within the sample. The tissue was then loaded and placed in the 37°C incubator. Control studies confirmed that there was no detectable synthesis during the 2 hour incubation at 4°C. Protein synthesis was significantly depressed after only 15 minutes of loading and remained similarly depressed throughout the 2 hours studied (figure 5.12(upper panel)). Sulfate incorporation (figure 5.12(lower panel)), however, remained at control levels throughout the 2 hour time tested.

These data, taken together with those of figures 5.9 and 5.10, suggest that depression in proline incorporation is immediate, while depression in sulfate incorporation requires 2 to 6 hours.

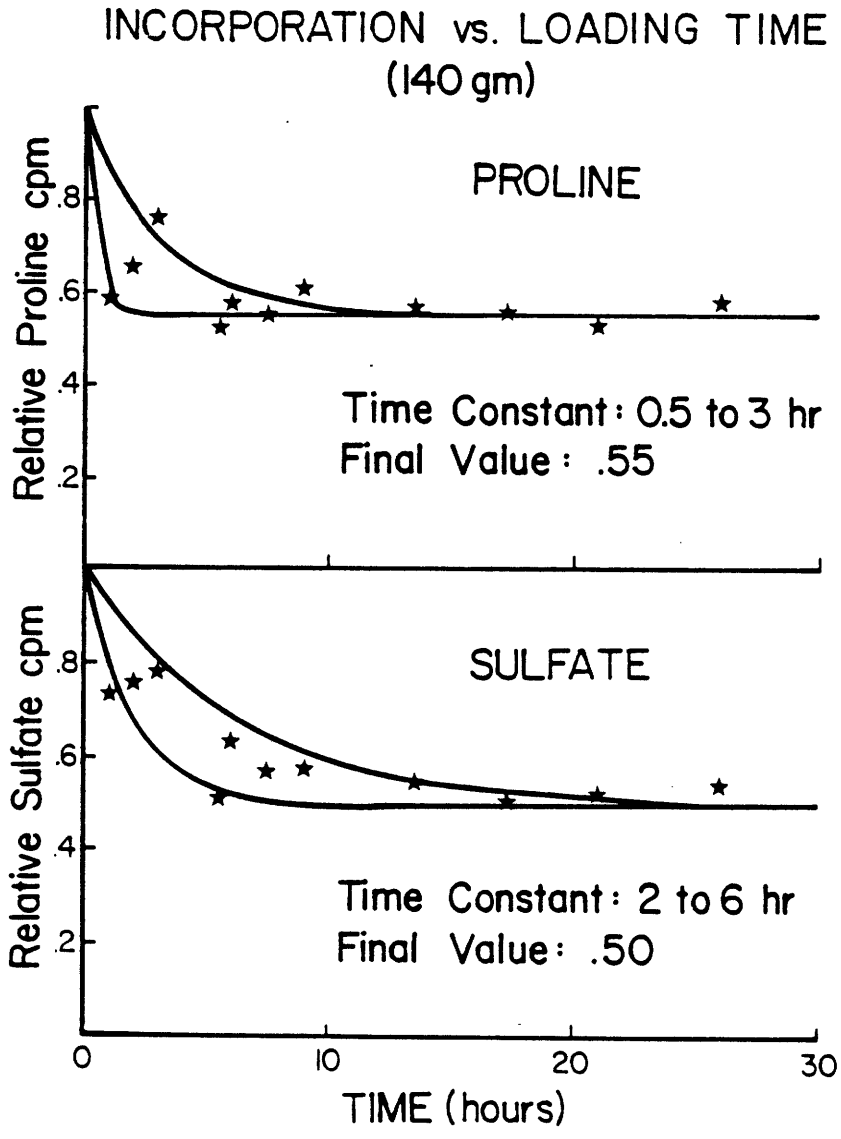

Figure 5.11: Relative incorporation of proline and sulfate versus time under a 140 gm load. The data points summarize the results of 5.9 (all data) and 5.10 (all but the latest two time points). The curves represent single exponential decays to final depression of 55% (proline) and 50% (sulfate). Time constants of 0.5 to 2 hours bound the proline incorporation kinetics. Sulfate kinetics are bounded by a time constant from 2 to 6 hours.

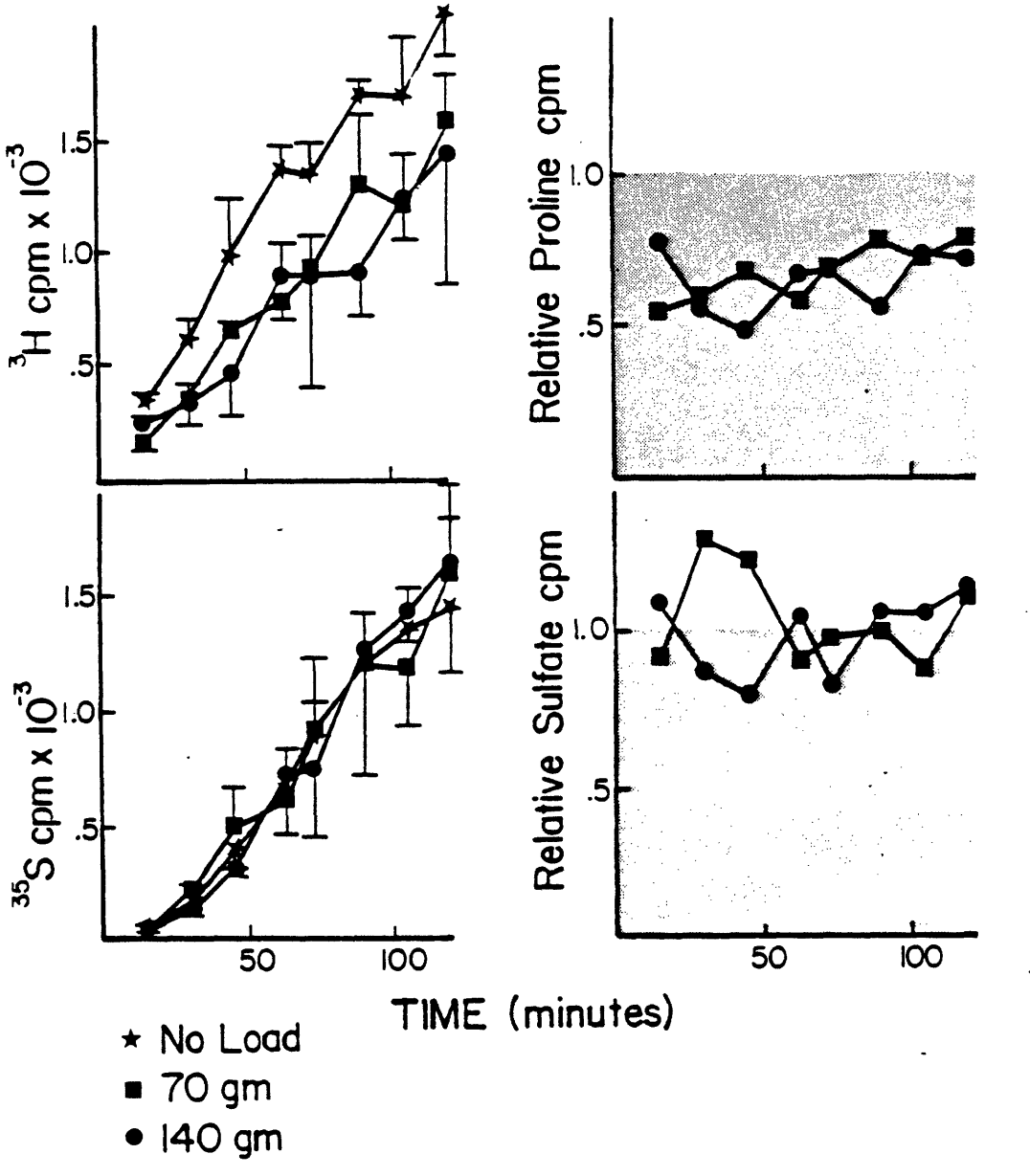

Figure 5.12: Incorporation of proline and sulfate as a function of load and labeling time. The lefthand panels present the mean and standard deviation of radiolabel counts for 3 to 4 samples. The righthand panels depict the incorporation relative to unloaded controls. no load (★), 70gm (■), 140gm (●). Samples were preincubated, without load, for 2 hours at 4°C prior to loading and labeling at 37°C.

5.6 Synthetic behavior following a step release of load

The final series of "static load" experiments examined the response to a step reduction in load. From a systems point of view, these experiments are a test of linearity. A linear response would show unloading kinetics identical to step load kinetics. Proline incorporation would therefore be expected to return immediately to control levels, and the sulfate should reach control levels after 2-6 hours.

Alternately, if compression sufficient to depress synthesis is viewed as a physiologic insult, these unloading experiments represent the recovery behavior. This series of experiments will henceforth be referred to as load-recovery experiments.

The protocol for the load-recovery experiments is diagramed in figure 5.13. The tissue was loaded with 0, 70, or 140 grams while bathed in unlabeled media. After 12 hours, the load was removed and, at various time points later, the media was replaced by labeling media and the plugs incubated 2 more hours.

Several observations can be made from the typical load-recovery results shown in figure 5.14. First, those samples subjected to a 140 gram preload retain a depressed sulfate incorporation rate throughout the three hour period. With time, incorporation by those preloaded with 70 grams approaches control levels. Since the tissue reswells to its free swollen volume within 15 minutes, the diffusion of radiolabel will be the same for control and preloaded samples. The

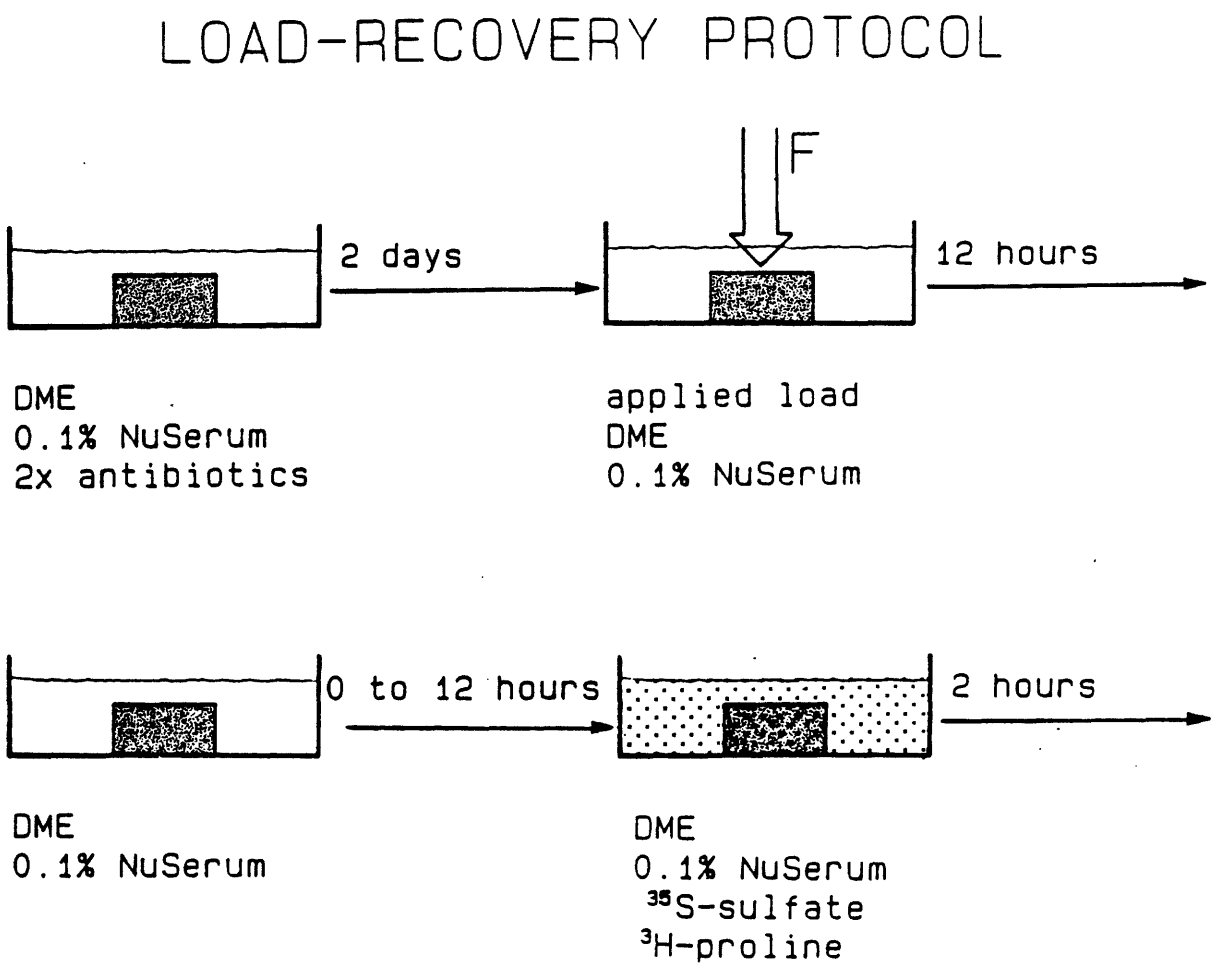

Figure 5.13: Protocol for load-recovery experiments. After 2 days in culture, tissue was transferred to the experimental chamber containing standard medium (DMEM supplemented with 0.1% NuSerum). After 12 hours the load was removed and the samples allowed to recover for a specified amount of times. At the end of the recovery time, the tissue was placed in labeling medium (DMEM supplemented with 0.1% NuSerum, 20 µCi/ml ^{35}S-sulfate, 10 µCi/ml ^{3}H-proline, and 0.5 mM proline) and incubated for 2 hours. Following the labeling period, the tissue was washed and analyzed as described in chapter 3.

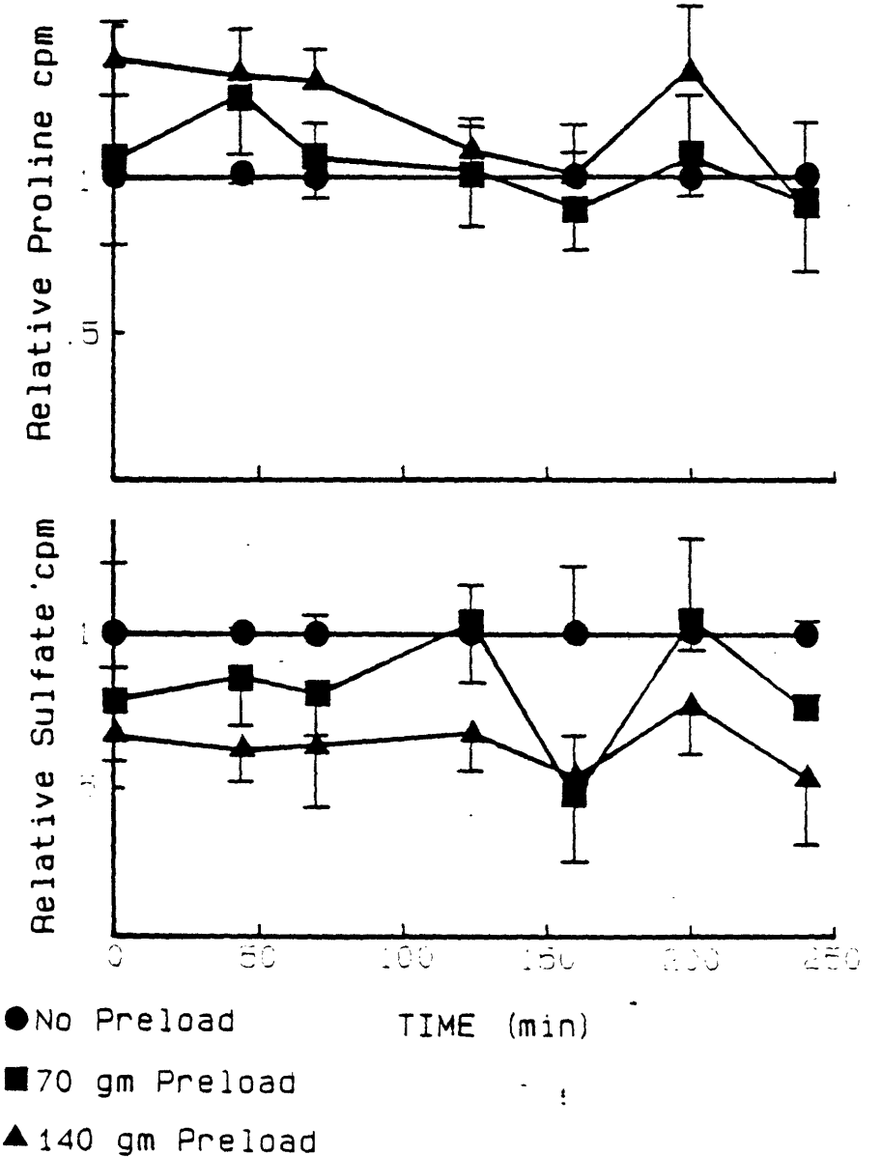

Figure 5.14: Following a 12 hour preload, incorporation of proline and sulfate was assessed during a 2 hour labeling period beginning at the time specified by the x-axis. Preloads were 0(●), 70(■), or 140(▲) grams. Data presented as the mean and standard deviation relative to the no-preload controls of 3 to 4 specimens. Incorporation was also assessed during the 12 hour loading period:

Proline:	140gm/0gm	.81 ± .36	Sulfate:	140gm/0gm	.91 ± .31
	70gm/0gm	.73 ± .11		70gm/0gm	.87 ± .07
	0gm/0gm	1.0 ± .33		0gm/0gm	1.0 ± .17

continued depression in sulfate incorporation indicates that the dose dependent depression described in section 5.4 is, in fact, a prolonged cellular response, rather than a manifestation of decreased radiolabel diffusivity.

In contrast, proline incorporation substantially exceeded control levels for 1 to 2 hours following the load removal. This rebound behavior was seen in each of 3 experimental series.

The data from figure 5.14 is represented in figure 5.15 as the ratio between ^{3}H-proline and ^{35}S-sulfate incorporation (H/S ratio). Variation across samples is less using this representation, presumably because each plug is, in a sense, normalized to itself. The control samples (those not subjected to a preload) demonstrate a constant H/S ratio as expected, since control samples are assumed to be identical[14]. The H/S ratios for samples loaded with 140 gm are greater than those for controls throughout the 3 hour period, while those for samples loaded with 70 gm reach control levels by 2 hours.

H/S ratios from three independent runs using the protocol in figure 5.13 are summarized in figure 5.16. The increased ratio seen for samples subjected to a 140 gm preload is, in all cases, the result of both enhanced proline incorporation and depressed sulfate incorporation. In all experiments the samples preloaded with 70 grams returned to control levels within 2 hours.

---

[14] H/S ratios were approximately constant for samples in which incorporation was assessed during loading (as, for example, in section 5.4).

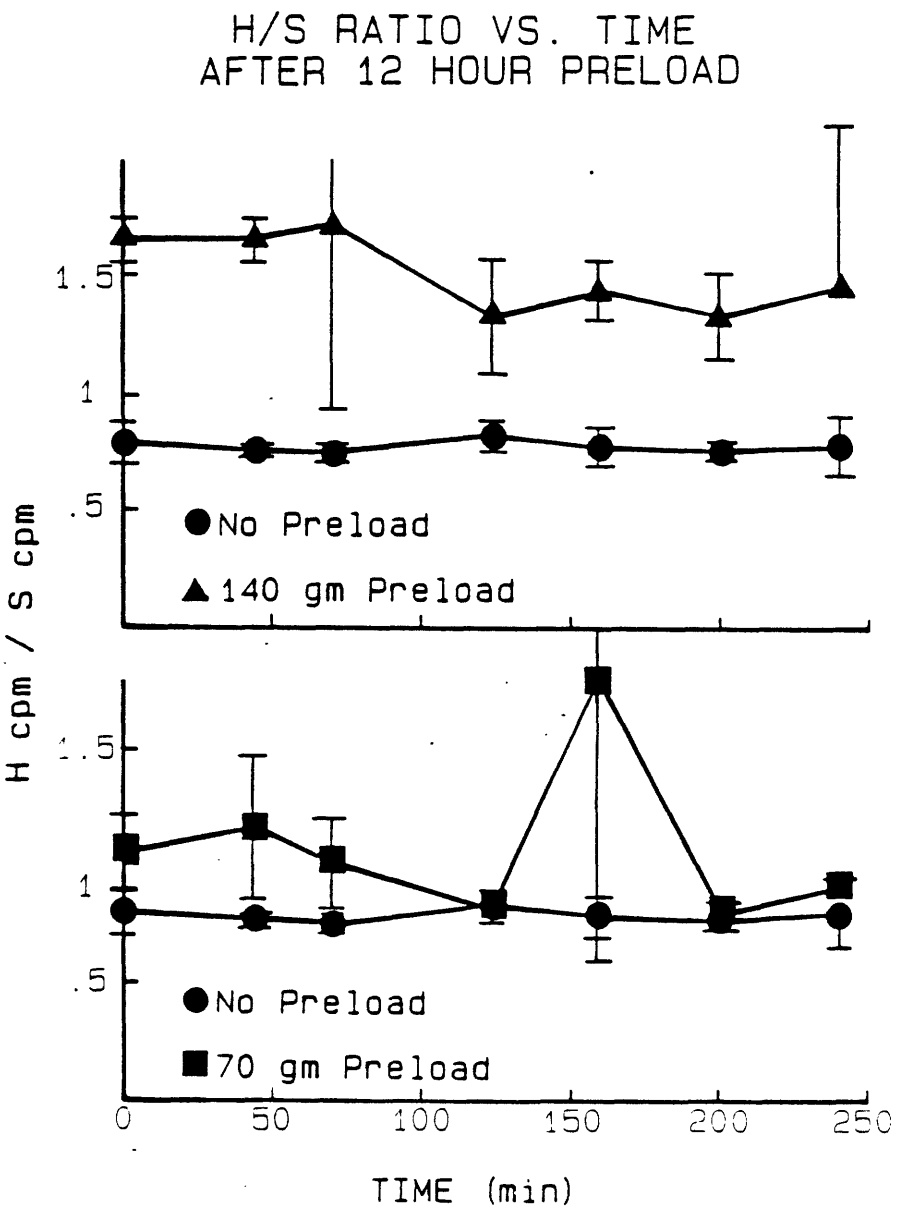

Figure 5.15: Mean ^{3}H-proline to ^{35}S-sulfate ratio (H/S ratio) and corresponding standard deviation for same experiment shown in figure 5.14.

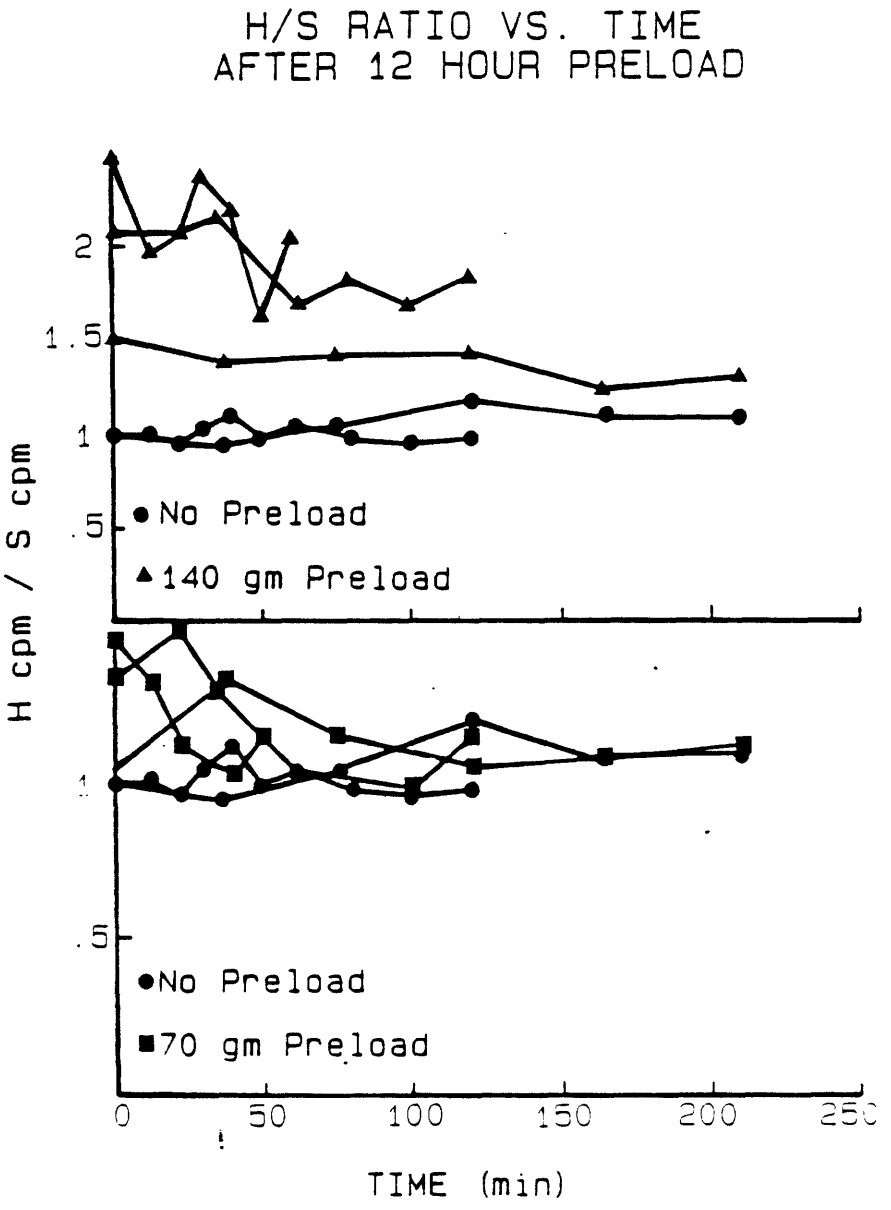

Figure 5.16: 12 hour preload-recovery. Following a 12 hour preload, incorporation of proline and sulfate was assessed during a 2 hour labeling period beginning at the time specified by the x-axis. Plot shows ratio of ^{3}H-proline to ^{35}S-sulfate incorporation for 3 independent experiments. Ratios are normalized to the ratio of the 0 gm preload control ratio at time zero. Upper panel compares results of 0(●) to 70(■) gram preload. Lower panel compares results of 0(●) to 140(▲) gram preload.

To test if the rebound behavior could be accounted for by the reswelling behavior alone, a similar load-recovery series was performed using only 1/2 hour of preload. No depression in sulfate incorporation, no enhancement in proline incorporation and no difference in H/S ratio (figure 5.17) was seen at any time point following load removal.

When the preload time was increased to 2 hours, there was a statistically significant increase in the H/S ratio immediately following unloading (due primarily to enhanced proline incorporation). The H/S ratio returned to control levels by 3 hours for preloads of both 140 and 70 grams. (See figure 5.18.)

To further examine the dependence of the recovery response on preload time, a series of experiments was performed using a 36 hour preload beginning soon after explant. The corresponding H/S ratios are shown in figure 5.19. Immediately following a preload of 140 grams, samples exhibited an H/S ratio four times the control levels. This was due to both enhanced proline and depressed sulfate incorporation. The fall off to twice control levels was dominated by continued depression in sulfate incorporation. Samples preloaded by 70 grams reached control level H/S ratios by 1.5 hours.

In summary, samples subjected to step unloading exhibit a behavior that is not merely the reverse of the step loading response. This is clearest for 140 gram preloads where proline synthesis is enhanced and sulfate synthesis remains depressed, leading to an H/S ratio greater than controls. This behavior is not evident after a 1/2 hour preload, but once present, it appears to remain for longer periods as the preload

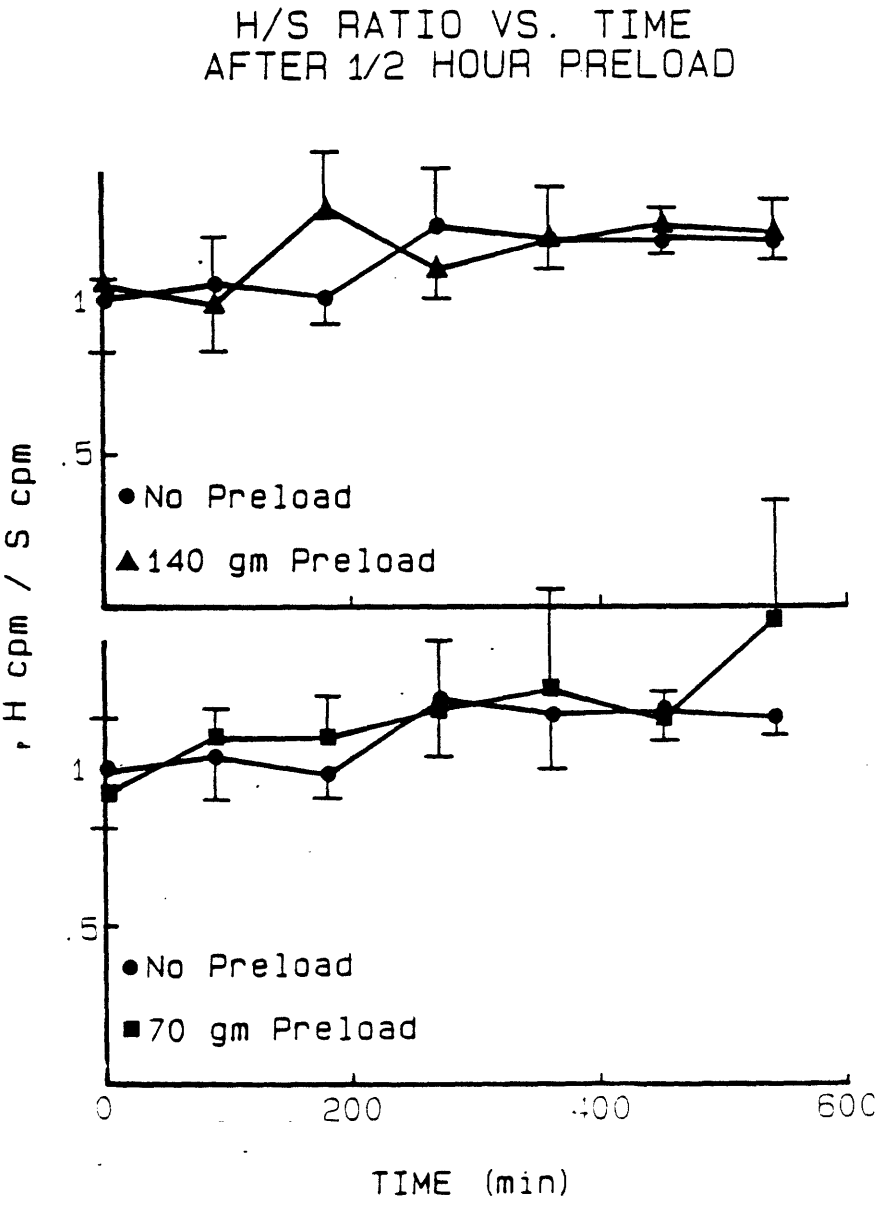

Figure 5.17: 1/2 hour preload-recovery. Following a 1/2 hour preload, incorporation of proline and sulfate was assessed during a 2 hour labeling period beginning at the time specified by the x-axis. Plot shows ratio of ^{3}H-proline to ^{35}S-sulfate incorporation. Upper panel compares results of 0(●) to 70(■) gram preload. Lower panel compares results of 0(●) to 140(▲) gram preload. Data presented as the mean and standard deviation relative to the no-preload controls of 3 to 4 specimens.

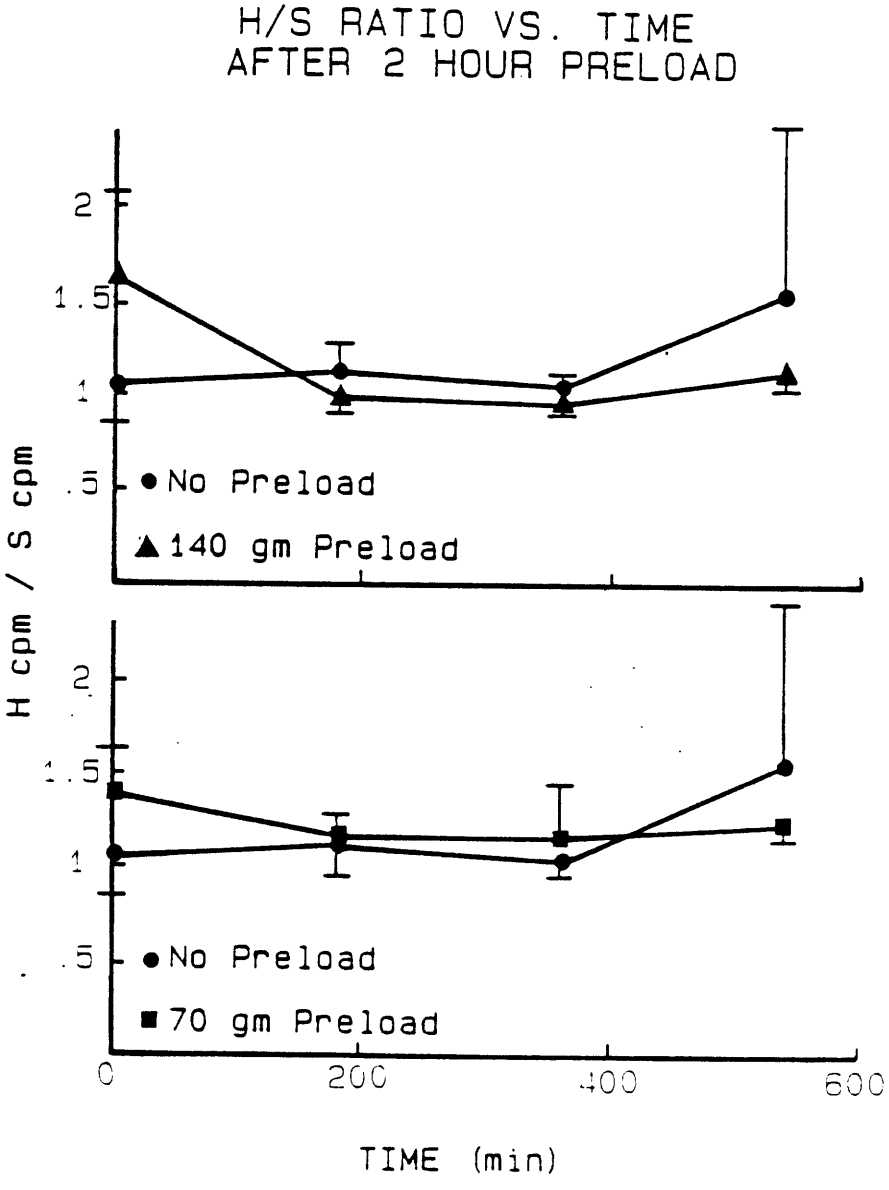

Figure 5.18: 2 hour preload-recovery. Following a 2 hour preload, incorporation of proline and sulfate was assessed during a 2 hour labeling period beginning at the time specified by the x-axis. Upper panel compares results of 0(●) to 70(■) gram preload. Lower panel compares results of 0(●) to 140(▲) gram preload. Data presented as the mean and standard deviation relative to the no-preload controls of 3 to 4 specimens.

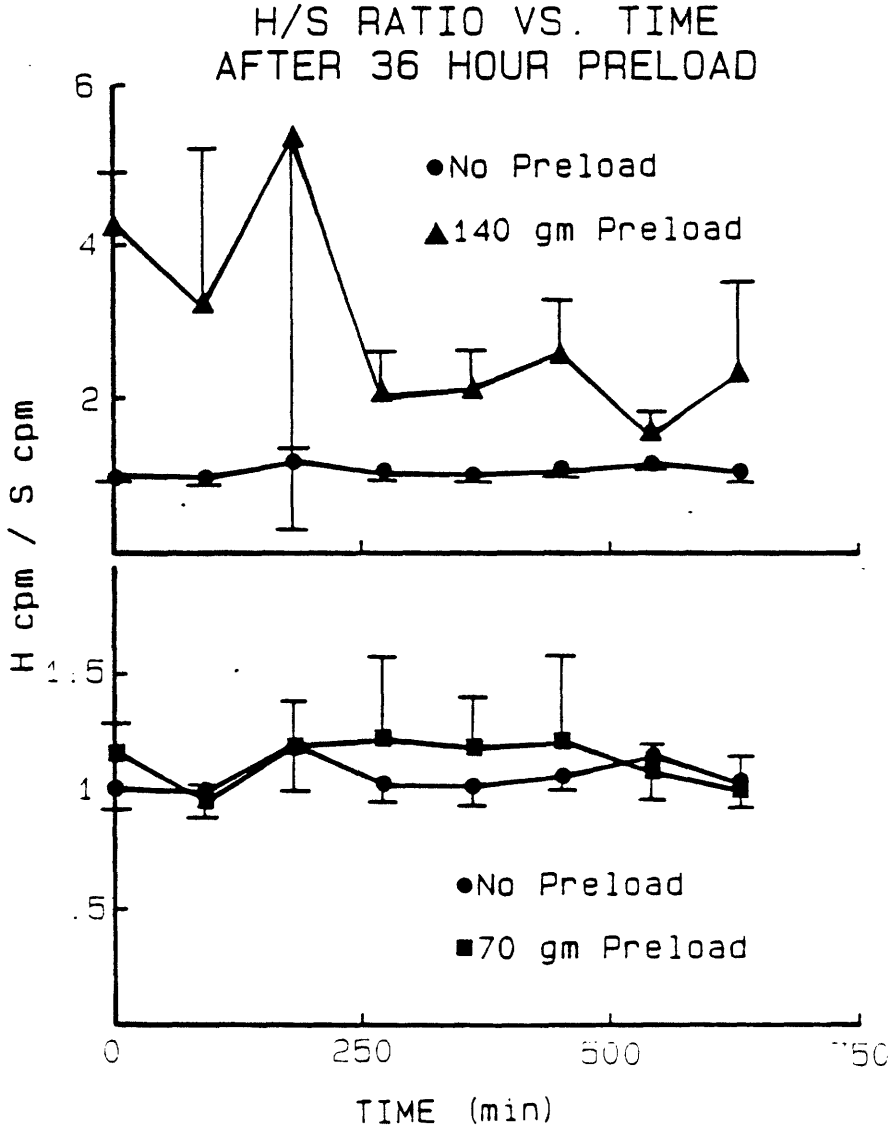

Figure 5.19: 36 hour preload-recovery. Following a 36 hour preload, incorporation of proline and sulfate was assessed during a 2 hour labeling period beginning at the time specified by the x-axis. Upper panel compares results of 0(●) to 70(■) gram preload. Lower panel compares results of 0(●) to 140(▲) gram preload. Data presented as the mean and standard deviation relative to the no-preload controls of 3 to 4 specimens.

time is increased.

A single experiment to examine the spectrum of proteins synthesized during the rebound period was performed using the protocol of figure 5.13, except that a ^{35}S-methionine radiolabel was used in methionine free medium. SDS gel electrophoresis and autoradiography (kindly performed by Zeke Gluzband and Laura MacGinitie in our laboratory) of the intracellular proteins showed no apparent difference in the distribution of proteins synthesized by samples preloaded for 12 hours with 0, 70, or 140 grams (figure 5.20).

5.7 Summary of response to step changes in loads

This chapter describes several characteristics of the cellular response to step loads regimens. Glycosaminoglycan (GAG) and protein synthesis rates, as assayed by sulfate and proline incorporation, are depressed in a dose dependent manner. This depression cannot be accounted for solely by decreased diffusion of radiolabel. The incorporation of sulfate and proline as a function of estimated compression demonstrates an abrupt, threshold-like behavior. In the 12 hour studies proline and sulfate incorporation showed identical trends.

An estimate of the turn on time, τ_{c_on}, was obtained by examining progressively shorter loading times. Proline incorporation was shown to depress within 15 minutes while sulfate incorporation remained at control levels for at least 2 hours.

The response of cartilaginous epiphyseal plate to step unloading

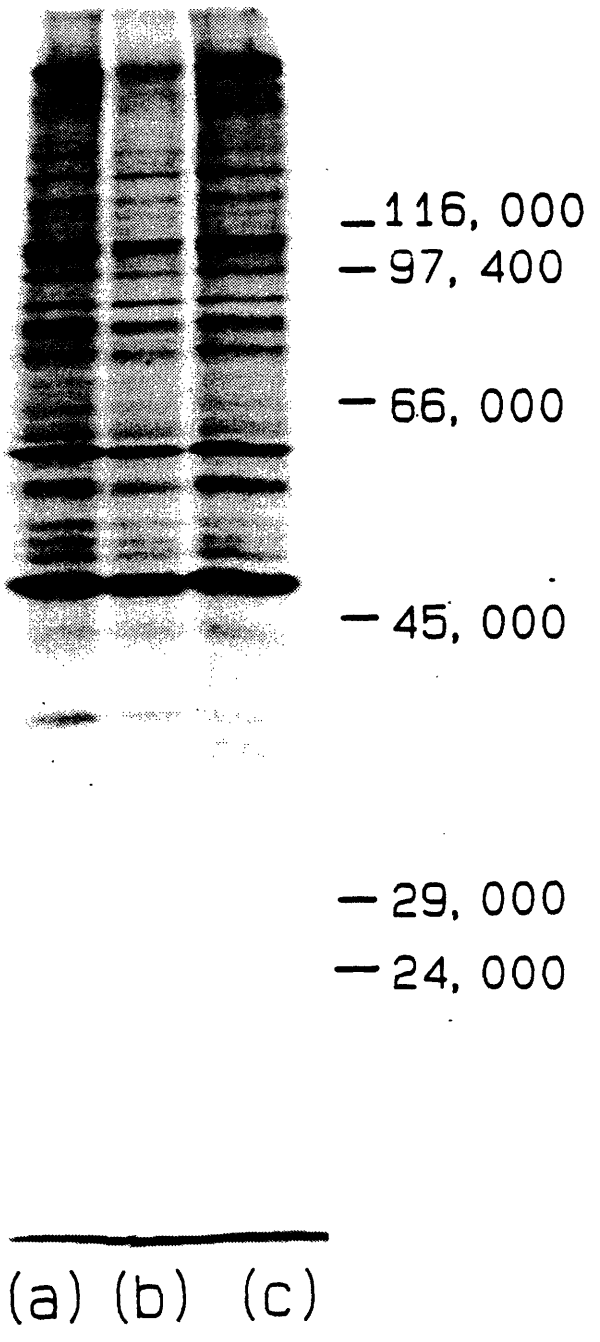

Figure 5.20: SDS electrophoresis of proteins synthesized during 3 hour time period immediately following a 12 hour preload. (a) 140 gm preload, (b) 70 gm preload, (c) control.

is not a simple return of synthesis to control levels. Following a 12 hour 70 gm preload, the sulfate incorporation remained depressed for ~2 hours following load removal. In contrast, depression existed for over 4 hours with a 140 gm preload. Proline incorporation exceeded control levels for at least 3-5 hours after load removal. If the preloading time was shortened to 1/2 hour, proline and sulfate incorporation did not deviate from control levels. This result suggests that fluid flow and strain rate alone do not account for the rebound behavior of proline incorporation.

As discussed in section 2.6.2, in this experimental configuration strain and the associated physicochemical changes are distributed uniformly throughout the tissue. The results of this section indicate that one or both of these output signals modulate cell synthetic behavior. In section 2.3.7 it was shown that the increased charge density resulting from consolidation will cause ions to redistribute, changing the concentration of salts, pH, etc. Section 2.4.5 was devoted to discussing potential cellular behavior in response to the consolidation-induced changes in the interstitial milieu. The next chapter describes experiments investigating the sensitivity of this EPC preparation to changes in the composition of the bathing medium.

Chapter VI

RESPONSE TO PHYSICOCHEMICAL CHANGES

Consolidation of a tissue such as cartilage which has a net fixed charge leads to changes in the interstitial mobile ion concentrations consistent with Donnan equilibrium. Inn Chapter 2, changes in interstitial concentration were suggested to be possible input signals to the cellular unit. The experiments described in this chapter were designed to test the sensitivity of chondrocytes to specific changes in their physicochemical environment in the absence of mechanical deformation. The concentration of every charged species is altered by tissue consolidation. The species examined here (potassium, hydrogen, and sulfate) have been shown in other systems to be important to cell behavior and can be experimentally manipulated in a relatively straightforward manner.

6.1 Static Compression Apparatus

The material properties of cartilage are a strong function of the physicochemical environment [Eisenberg, 1983; Maroudas, 1979; Myers et al. 1984]. The deformation occurring under a given load depends on mobile ion and fixed charge concentrations. Therefore, to isolate chondrocyte response to physicochemical changes, experiments are best performed under conditions of constant deformation. The constant deformation configuration used is diagramed in figure 6.1. The cartilage

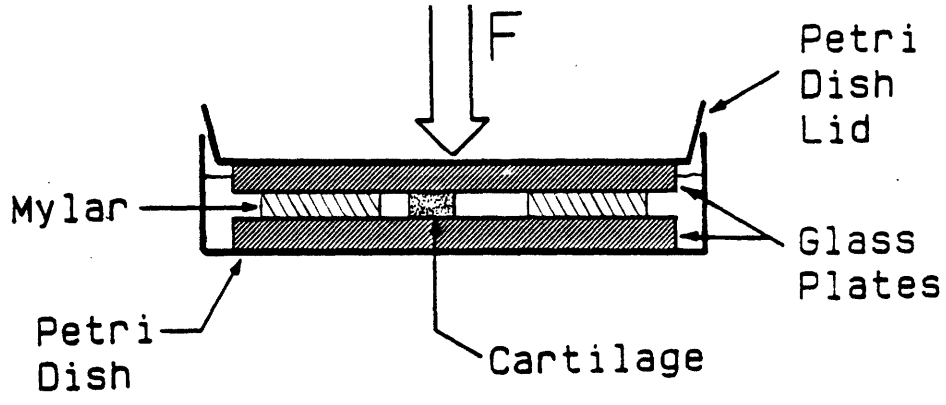

Figure 6.1: Constant deformation Apparatus. Two glass plates are placed in a 100 cm^2 petri dish and separated by mylar strips of known thickness. Cartilage specimens are placed near the mylar sheets between the glass. The dish is filled with media and the glass is covered with an inverted petri dish lid. A weight is placed in the lid so that the glass plates are separated by a known amount (the mylar thickness) resulting in a constant cartilage compression.

tissue and strips of mylar were placed between two glass plates. The mylar was of constant and known thickness. A weight was used to compress the tissue so that the plate separation is equivalent to the mylar thickness.

A control series was performed to ensure that the reduction in synthetic rate seen with increasing load (Chapter 5) was reproduced using this unconfined, constant compression setup. Two groups of four plugs were incubated for 12 hours under each of the following conditions: free swelling, glass plate only, 25% compression (relative to 800 μm cut thickness), and 50% compression. Comparison of incorporation by free swelling plugs to those bounded by glass (Figure 6.2) shows that the presence of the glass does not itself depress synthetic rate. 25% and 50% compression lead to a ~25% and ~35% reduction, respectively, in synthetic rate. The similarity between the proline and sulfate incorporation and the dose dependent depression are consistent with the results seen under applied load conditions (chapter 5).

6.2 Effect of Increasing [SO_4]

Below a critical sulfate concentration, the degree of sulfation of newly synthesized GAGs depends on the bathing sulfate concentration [Ito et al., 1982; Maroudas and Evans, 1974]. Because sulfate is a co-ion, its concentration in the interstitium is less than in the bath. As the tissue is compressed, the interstitial concentration will decrease.

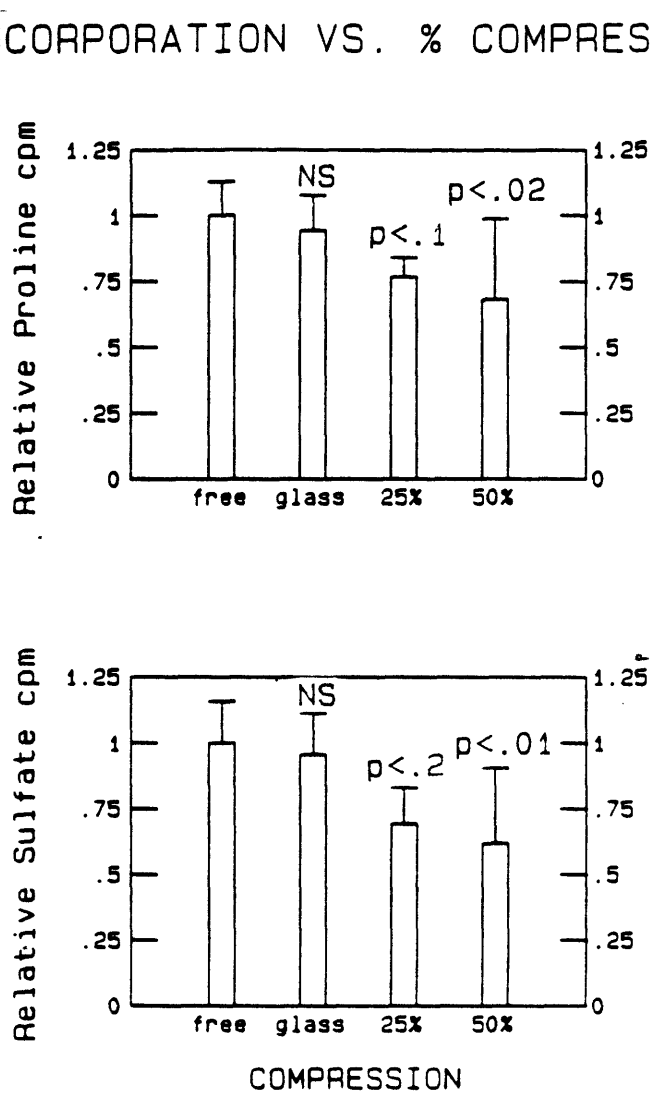

Figure 6.2: Incorporation of ^{3}H-proline (upper panel) and ^{35}S-sulfate (lower panel) as a function of compression relative to free swelling controls. free=free swelling, glass= 0% compression with glass plate on top of tissue, 25% = 600 µm compressed thickness, 50% = 400 µm compressed thickness. Bars show relative mean and standard deviation for 8 plugs. Statistical significance was determined using the two-tailed t-test comparing glass, 25%, and 50% compression groups to free group.

Calculations based on reported critical sulfate requirements and typical free swelling charge densities of cartilage (Chapter 2) indicate that compressions greater than 35% in DMEM will result in an interstitial [SO_4] below the critical level. The experiments described in this section test the effect of increasing bath [SO_4] on the synthetic behavior under compression.

Tissue was incubated for 12 hours at either 0%, 25%, or 50% compression in labeling medium having a sulfate concentration of 0.8, 1.2, or 1.6 mM. The sulfate concentration was adjusted by addition of sodium sulfate. Sulfate incorporation data were corrected for the specific radioactivity. Compression was achieved as described in the previous section. The table below summarizes the interstitial sulfate concentrations expected as a function of bath concentration and compression computed from Donnan theory. (See Chapter 2 for details of calculation.)

Interstitial [SO_4] (mM)

	Bath [SO_4]mM	Compression 0%	25%	50%
(normal medium)	0.8	.315	.216	.094
	1.2	.470	.324	.141
	1.6	.630	.432	.188

Based on a critical interstitial concentration of 197 μm,[15] the conditions at 50% compression [SO_4] are expected to induce interstitial

[15]Calculated in Chapter 2 assuming 20% solid volume, 0.15 M fixed charge density and a critical bath sulfate concentration of 500 μm [Maroudas and Evans, 1974].

concentration below the critical interstitial level.

Proline and sulfate incorporation under these conditions are shown in figure 6.3. At all sulfate concentrations incorporation was seen to decrease with increasing compression. Sulfate and proline incorporation were independent of sulfate concentration at all levels of compression. These data suggest that the decrease in sulfate incorporation seen with increasing load (compression) cannot be accounted for by decreased GAG sulfation due to critically low [SO_4].

6.3 Effect of Increasing [K^+]

As the tissue consolidates, the interstitial counterion concentration rises. The next experiments to be described tested the effect of raising the potassium concentration on the biosynthetic behavior of EPC. Potassium was selected because (1) it may have an effect on transmembrane potential or intracellular processes, and (2) its concentration is sufficiently low to ensure that the osmolarity of the medium or electrochemical interactions between fixed charge groups will not be significantly affected by alterations in [K^+].

9 groups of 5 specimens were incubated for 12 hours in labeling medium with a potassium concentration ranging from 5.4 mM to 10.4 mM. This corresponds to the range of interstitial concentrations expected to occur for compressions ranging from 0 to 60%.

The results shown in Figure 6.4 demonstrate no dependence of sulfate and proline incorporation on potassium concentrations up to two

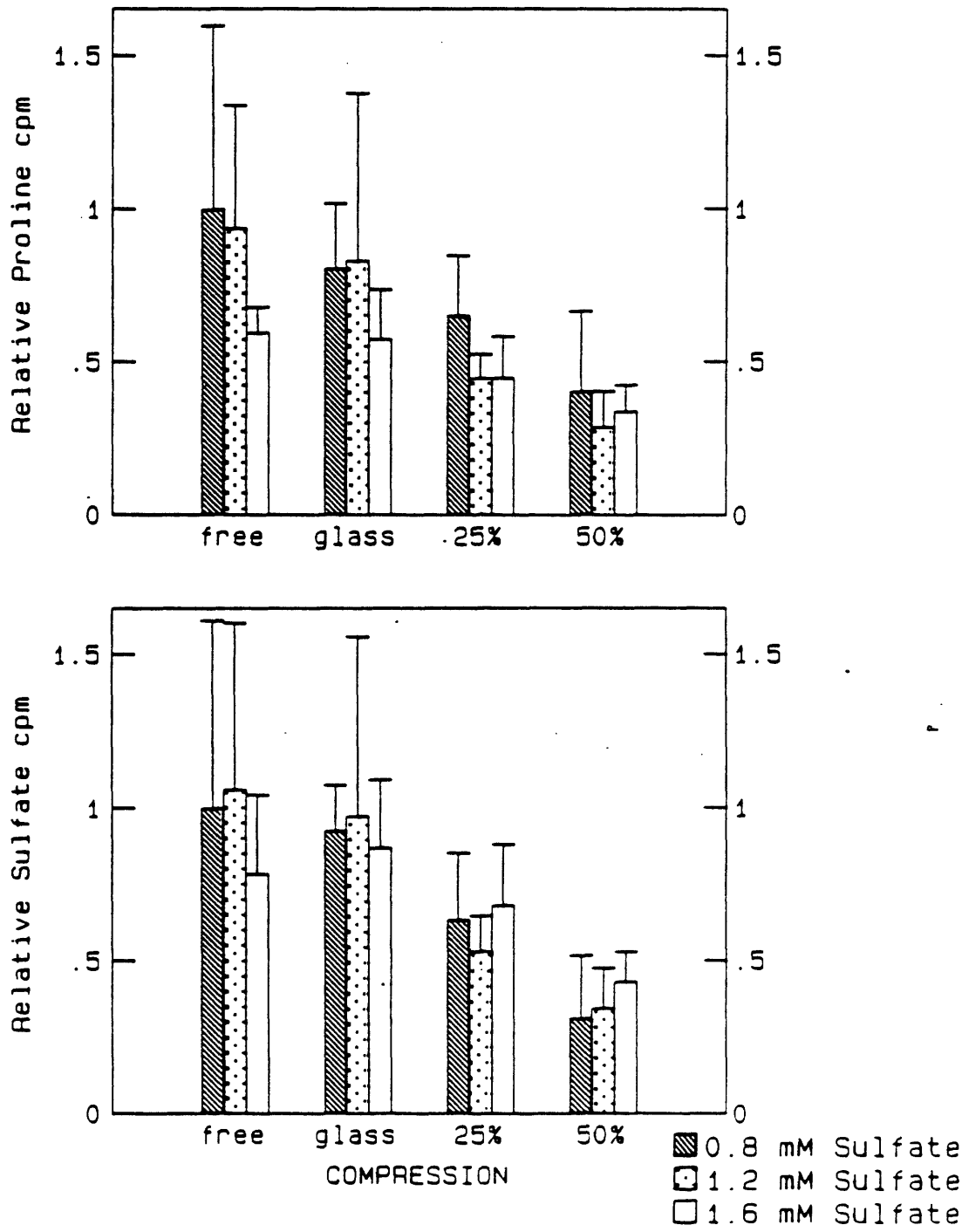

Figure 6.3: Proline (upper panel) and sulfate (lower panel) incorporation as a function of sulfate concentration and compression. Sulfate concentration: hashed bars - 0.8 mM; dotted bars - 1.2 mM; white bars - 1.6 mM. free=free swelling, glass= 0% compression with glass plate on top of tissue, 25% = 600 µm compressed thickness, 50% = 400 µm compressed thickness. Mean and standard deviation of 8 specimens are presented relative to mean of free swelling controls incubated with 0.8 mM SO_4.

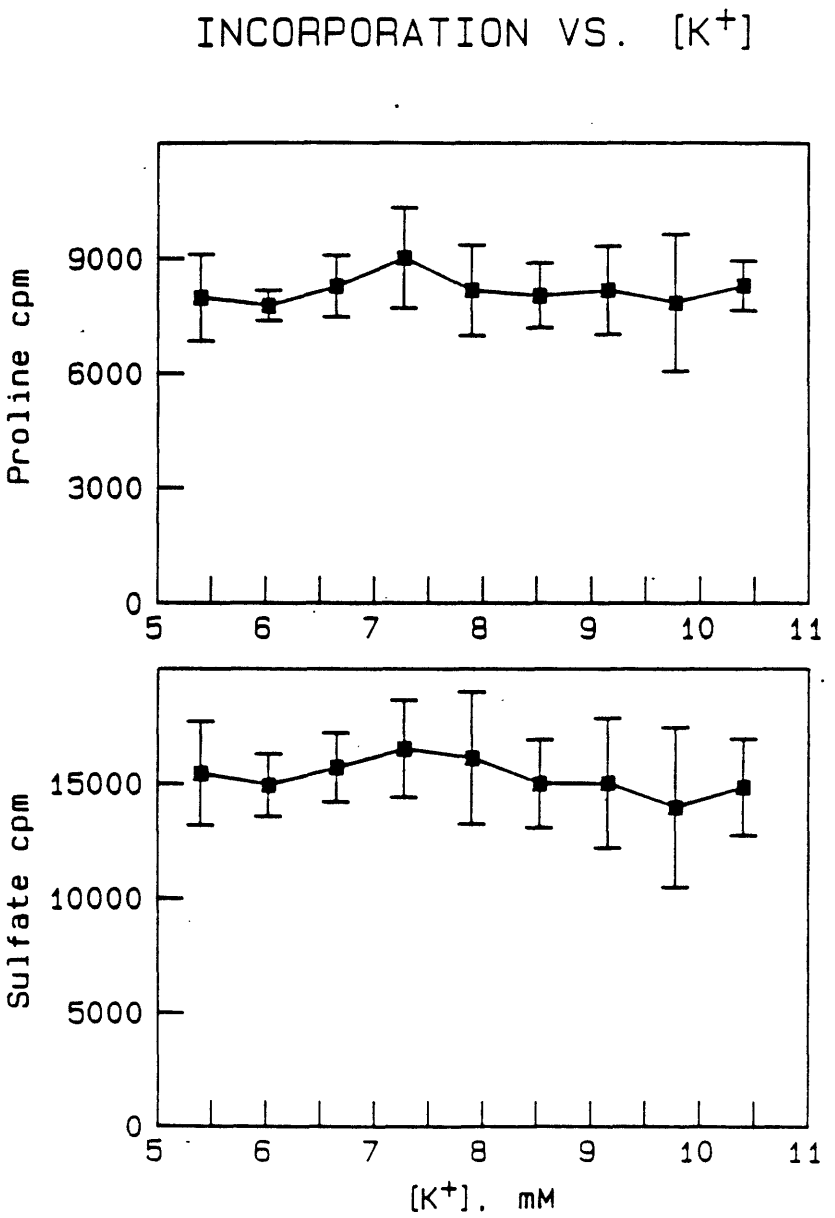

Figure 6.4: Incorporation of proline (upper panel) and sulfate (lower panel) versus potassium concentration. Data represents mean and standard deviation of 5 plugs.

times normal. An identical experiment run in parallel using tissue from a different animal, also showed no significant effect of $[K^+]$, although the scatter in the data exceeded 50%, perhaps from some unknown contamination. These results suggest that it is unlikely that the interstitial changes in $[K^+]$ which occur with compression contribute to the compression response.

6.4 Effect of Changing pH

The experiments described in this section examined the response of EPC to changes in the concentration of the counterion, H^+. Media pH was adjusted by modifying the bicarbonate content of DMEM prepared from powder (Gibco, Grand Island, New York). Control studies ensured that the media pH remained stable throughout a 12 hour period. In one series of tests, 9 groups of 7 specimens were incubated (free swelling) for 12 hours in media having a pH ranging from 5.5 to 7.9.

In figure 6.5, the pH dependence of both proline and sulfate incorporation is clearly seen. These results are consistent with Schwartz et al. [1976] who reported a 3 fold depression in sulfate incorporation as the pH dropped from 8 to 7. 50% consolidation of a tissue (0.15 M fixed charge density) equilibrated in media with a pH of 7.2 will result in an interstitial pH of 6.74. 0% consolidation in a bath of pH 6.94 will have a similar interstitial pH.

In a second series, 10 groups of 8 specimens were incubated for 12 hours in media having a pH ranging from 5.5 to 7.2 while subjected to

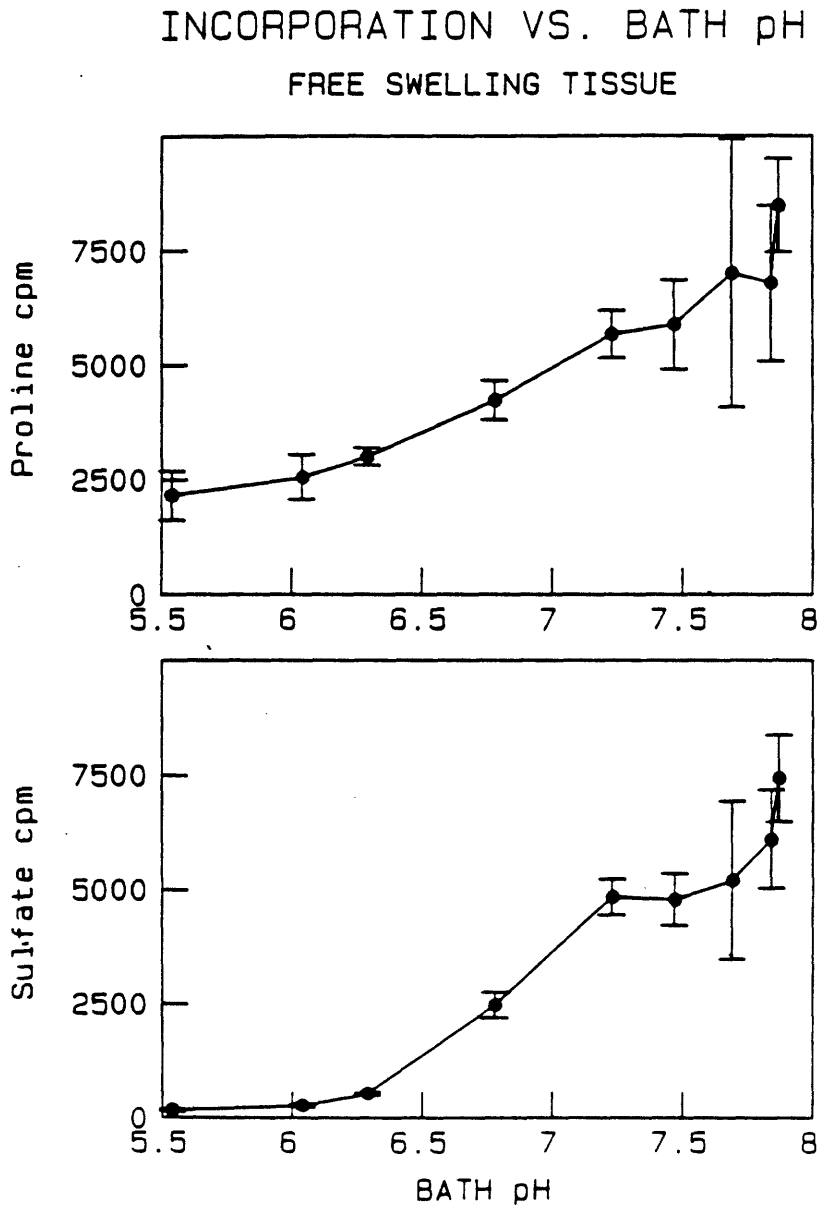

Figure 6.5: Incorporation of proline (upper panel) and sulfate (lower panel) by EPC as a function of bath pH. Mean and standard deviation of 7 specimens are shown.

50% compression. This series tests if the pH sensitivity is retained under compression and is necessary to determine the extent to which the pH dependent behavior could be responsible for the compression dependent behavior. Again, a strong pH dependence was seen between pH 6 and 7 (figure 6.6).

The data from these experiments were corrected for relative media concentration and replotted in terms of the estimated interstitial pH in figure 6.7. The interstitial pH was calculated according to Donnan theory assuming a 0.15 M fixed charge density for the free swelling plugs of figure 6.5 and a 0.4 M fixed charge density for the compressed plugs of figure 6.6. pH appears to account entirely for the compression-dependent sulfate incorporation behavior over the entire pH region tested. For interstitial pH in the range 6.6 to 7.0 (which corresponds to 0 to 60% compression), proline incorporation also appears independent of compression per se. For interstitial pH is below 6.5, compressed samples show ~50% less synthesis than uncompressed specimens.

Although this discussion has focussed on the pH dependence, the pH change was achieved by addition of bicarbonate. Thus, the response could be a direct result of bicarbonate concentration.

The site of action or mechanism relevant to this pH response is not clear. Many reactions are pH dependent. Changes in pH may also modify the conformation of proteins, for example, those at the cell surface, which may indirectly lead to a modulation of synthetic behavior. Waddell and Bates [1969], in their review of intracellular pH literature, conclude that an extracellular pH change effected by

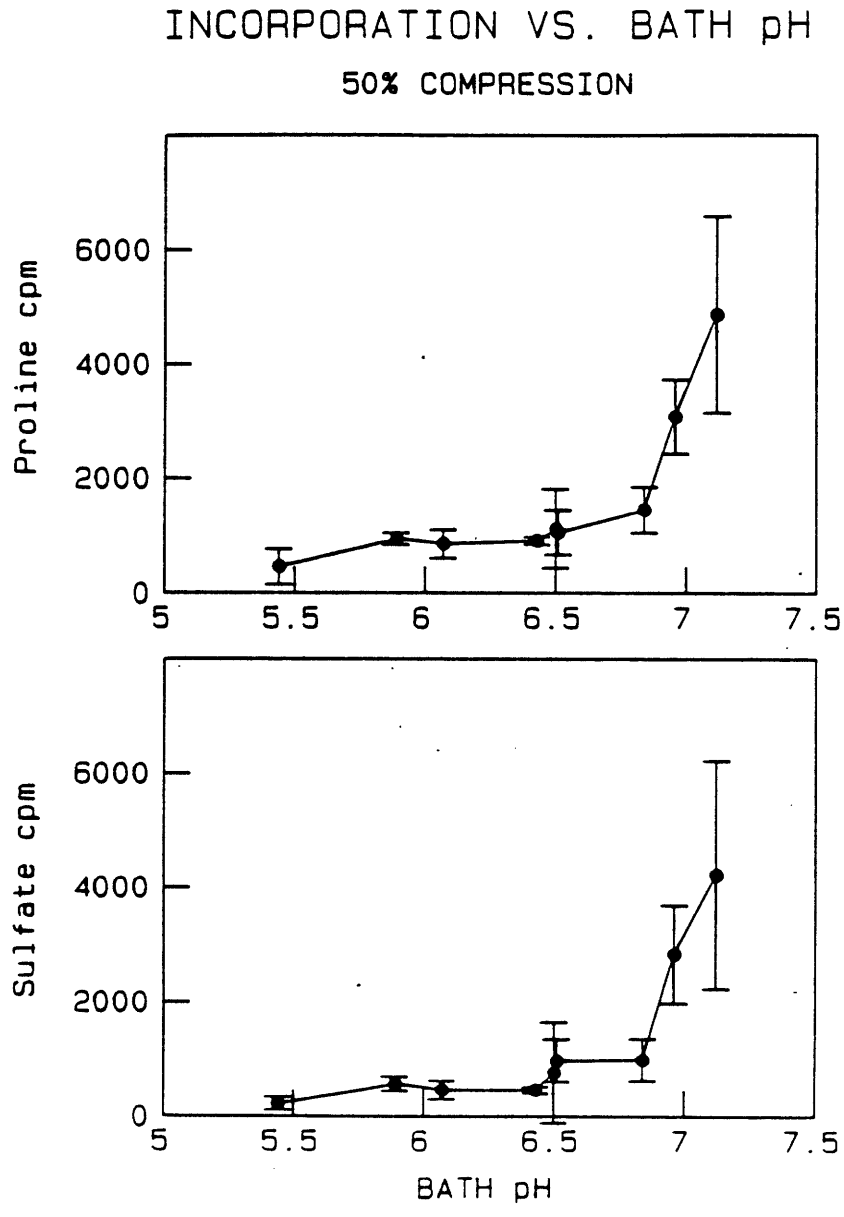

Figure 6.6: Incorporation of proline (upper panel) and sulfate (lower panel) as a function of bath pH for EPC maintained at 50% compression. Mean and standard deviation of 8 specimens are shown.

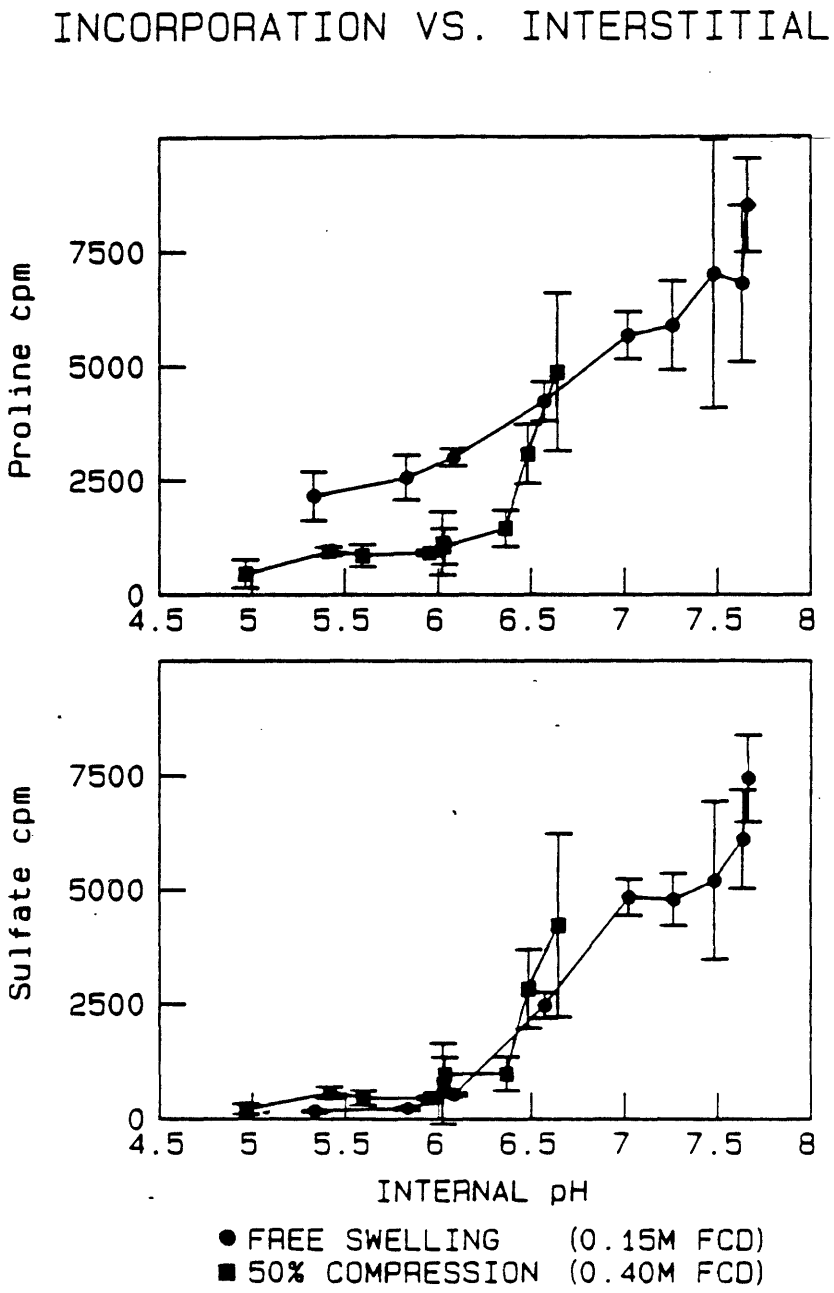

Figure 6.7: Proline (upper panel) and sulfate (lower panel) incorporation from figures 6.5 and 6.6 in terms of interstitial pH. The interstitial pH was calculated according to Donnan theory assuming a fixed charge density of 0.15 M for free swelling tissue (●) and 0.4 M for tissue compressed by 50% (■).

modifying the bicarbonate (or any highly ionized acid or base) concentration leads to a negligible (generally < 0.1 pH unit for a .5 pH unit external shift) change in intracellular pH. If intracellular pH is not affected, then the mechanism must be initiated extracellularly or at the membrane surface.

6.5 Summary

The synthetic responses to alteration of several mobile ion concentrations were described. Incorporation appears to be independent of sulfate and potassium concentration over a range predicted from consolidation. Incorporation of both proline and sulfate exhibited a pH dependence which may substantially account for the response to mechanical consolidation.

Chapter VII

DISCUSSION AND CONCLUSIONS

The objectives of this thesis have been to provide a conceptual model and experimental approach for studying the response of a connective tissue to mechanical loading. In Chapter 2, the connective tissue system was represented by three elementary response units: mechanical, cellular, and output conversion. An applied mechanical load produces several events within the tissue including deformation, fluid flow, streaming current, changes in hydrostatic pressure, and physicochemical changes associated with consolidation. These events were considered to be outputs of the mechanical unit and, in turn, inputs to the cellular unit. In general all of the events occur with their magnitude a function of time and space. Experimental configurations which decouple these events and which provide a spatially uniform signal were suggested as a means of probing the cellular response under mechanical loads.

The fundamental premise of this work has been that the cell modifies its behavior to alter the ECM and thereby accommodate to changes in mechanical loading. Therefore, cellular behavior was studied using sulfate and proline incorporation as markers for synthesis of matrix components. This approach was based on the assumption that the time required to complete the matrix adaptation is relatively long (days or more).

In this chapter the experimental results are discussed in the

context of the conceptual model and in terms of the implications for physiologic behavior under changes in loading. The chapter closes with suggestions regarding the direction of future research.

7.1 Discussion of 12 hour exposure results

7.1.1 Summary of results

When subjected to 12 hours of specific, uniformly distributed signals, chondrocytes in tissue culture altered their incorporation of sulfate and proline in the following ways (see also table 7.1):

(1) Applied signal: electric field

Input signals: electric field; fluid flow

Proline and sulfate incorporation was unaffected by applied current densities of 1 mA/cm^2 or less at frequencies from 0.1 to 100 Hz.

(2) Applied signal: static compressive load

Input signals: deformation; concentration changes

Proline and sulfate incorporation decreased monotonically with static loads up to 3MPa or compressions up to ~50%.

(3) Applied signal: concentration change

Input signal: physicochemical change

Proline and sulfate incorporation increased with decreasing $[H^+]$ (increasing pH.) Incorporation was unaffected by changes in $[K^+]$ and $[SO_4^=]$.

Input signal to cell under physiologic loading conditions	Experimentally Applied Signal		
	(1) Current	(2) Load	(3) Concentration
Deformation		++	
Hydrostatic Pressure			
Streaming Current	++		
Fluid Flow	**		
Physicochemical change		**	++
Biosynthetic probe			
Sulfate Incorporation	no change	++	++ (pH)
Proline Incorporation	no change	++	++ (pH)

++ indicates signal is applied

** indicates signal is present under the specified experimental conditions

Table 7.1: Table shows input signals to the cell induced by the three experimentally applied signals (1-3) together with the resulting proline and sulfate incorporation behavior assayed during a 12 hour exposure. (1) Applied electric currents with electroosmotically induced fluid flow; (2) static compressive loads with associated changes in mobile and fixed ion concentration; and (3) changes in interstitial mobile ion concentration.

7.1.2 Input signals: electric current and fluid flow

The absence of a response to applied electric fields is somewhat surprising given that several investigators have demonstrated a response to fields of much lower intensity. However, most investigators who have reported a biosynthetic sensitivity to electric fields have used either a monolayer or fabricated tissue preparation. In either case, the extracellular environment of the cell is quite different from that in organ culture preparations and *in vivo*. Since chondrocytes are believed to be very sensitive to the extracellular composition, the results reported may accurately reflect that in the native state chondrocytes are insensitive to fields.

Alternatively, if chondrocytes in organ culture are sensitive to fields, the lack of response indicates that a 12 hour accumulation of newly synthesized products containing proline and sulfate is not an appropriate probe. In this case, the data might be explained in several ways. For example, the fields could act to modify a cellular process which has no effect on synthesis or which is not reflected by total proline or sulfate incorporation. Sulfate is incorporated into GAGs and quickly (~10 minutes) exported from the cell. Proline is incorporated into most proteins and therefore is a nonspecific marker of products destined for both intracellular and extracellular sites.

If electric fields act to modify the synthetic rate of a specific protein this modification may not be detectable over the large background of proline incorporation. Recent work in this laboratory [MacGinitie et al, 1986; McLeod, 1986] and results of other

investigators [e.g. Goodman, 1983] suggest that an intracellular synthetic product may be affected by applied fields. Proline incorporation by chondrocytes in organ culture was shown to have 2 phases (Chapter 3), implying that 2 synthetic pools may exist. One pool reaches steady state in approximately 2 hours and is most likely intracellular. If fields were to modify incorporation into this pool, shorter labeling times or isolation of intracellular products would be necessary to observe the modification.

Finally, if fields actually do modify the extracellular matrix then this study implies that the adaptation time required must be long compared to 12 hours. Electric fields and fluid flow are present during dynamic deformation. It can be concluded that if electric fields and (or) the associated fluid flow provide(s) a modulating signal to cells in tissue undergoing dynamic loading, then the modulation either is slow or involves a very small fraction of the total biosynthetic products.

7.1.3 Input signals: deformation and physicochemical changes

The decreased synthetic rate seen with applied loads over 100 kPa is consistent with the Heuter-Volkmann hypothesis that increased compression leads to decreased growth. At loads on the order of 100 kPa, incorporation by loaded specimens tended to exceed incorporation by unloaded controls (although this tendency was not statistically significant). This is analagous to the chondral modeling theory described by Frost [1979] in which increasing load leads to increasing cartilage growth rates until a breakpoint is reached where further

increases in load lead to decreasing growth rates.

If the response to applied loads is viewed in terms of the predicted deformation, it appears that there is a threshold deformation above which incorporation decreases rapidly with compression. This interpretation is highly dependent on an accurate estimation of compressed thickness because load-deformation behavior is very nonlinear.

Applying the synthesis versus load data to growth physiology, these results suggest that growth rate will decrease with increasing stress. If total longitudinal growth is to be maintained in the event of an increase in load, then a mechanism such as appositional growth must act to decrease the applied stress. The kinetics of adaptation by appositional growth compared to that of longitudinal growth will determine the net effect on bone elongation.

7.1.4 Input signals: physicochemical changes

It was not feasible to exhaustively examine chondrocyte sensitivity to the concentration of each charged species. The three mobile ions examined in these studies were selected for their general relevance to cellular processes and the ease with which they could be modified. Incorporation was independent of potassium and sulfate concentration, but sensitive to pH under both free swelling and compression conditions. Intratissue pH correlated with incorporation, so pH changes induced by consolidation may account for part of the response to mechanical loading.

7.2 Discussion of kinetic results

7.2.1 Summary of results

The kinetics of the response to step changes in load were examined for a step increase and step decrease. Comparison to unloaded controls showed:

(1) Proline ; Load

Relative incorporation decreased rapidly (< 30 minutes) to a steady level which was maintained up to 30 hours.

(2) Sulfate ; Load

Relative incorporation decreased more slowly (2-6 hours) reaching a steady level which was maintained up to 30 hours.

(3) Proline ; Unload

For preload times of 2, 12, and 36 hours, relative incorporation increased for approximately 4 hours after unloading. A 30 minute preload did not perceptibly affect incorporation.

(4) Sulfate ; Unload

For preload times of 12 and 36 hours, relative incorporation decreased for at least 4 and 12 hours, respectively. 1/2 and 2 hour preloads did not affect incorporation.

7.2.2 Discussion

Modulation of proline incorporation by both loading and unloading was more rapid than modulation of sulfate incorporation. The response to unloading was not the inverse of the response to loading. Sulfate incorporation remained consistently depressed for over 4 hours, thereby taking longer to "recover" after unloading than it took to decrease incorporation after loading. Proline incorporation does not simply return to control levels, but overshoots control levels for ~4 hours. This nonlinear response suggests that the response to dynamic loads may not simply reflect the time average value of the load. For example, a signal train comprised of a 2 hour load, 4 hour unload sequence should have no effect on sulfate incorporation and will perhaps enhance proline incorporation. In contrast, a continuous load of 1/3 the amplitude (equivalent to the time averaged dynamic load) would be expected to depress both proline and sulfate incorporation. At higher frequencies (e.g. 1 Hz), it seems unlikely that incorporation of either species will follow the loading rate and so will now likely reflect the static (time average) load. The sulfate kinetics support this directly; the proline kinetics are not sufficiently defined to be certain. Aside from the kinetics of incorporation, the kinetics of mechanical deformation are such that few cells will experience deformation at higher frequencies.

7.3 Suggestions For Future Work

Several studies which would strengthen the implications of these results are categorized here according to the experimental configurations described in chapter 2.

(1) Applied compressive load

A precise knowledge of the tissue deformation would aid in the characterization of the cell response to deformation and physicochemical changes. Under static loading conditions, the applied load is not a direct signal to the cell but acts to deform the tissue as dictated by the tissue material properties. Therefore, the incorporation versus constant deformation studies could further substantiate the incorporation versus load experiments. Ideally, both load and deformation information should be available for each specimen as this provides more information regarding the state of the tissue under study and presumably reflects its in vivo mechanical conditions.

Local tissue deformation under compressive loads is dependent upon the boundary conditions. For example, radial strains are absent in confined compression, and the collagen fibers are probably unstrained. In unconfined compression radial strain may be limited by the collagen network. Local differences of this type may provide different signals to the cell, and so require examination of the effect of changing boundary conditions in the static load configuration. Confined compression also allows more accurate quantification of the volume change which occurs under compression.

(2) Applied electric fields

As suggested in the discussion above, chondrocyte sensitivity to fields may be dependent on the specific extracellular environment. Physiological fields are associated with time varying deformations, and the cellular response may be secondary to the response to static deformations. The act of explanting the tissue provides a mechanical "unloading" signal which may dominate the tissue's biosynthetic behavior in culture. Experiments which examine the chondrocyte sensitivity to fields under different loading conditions may provide different results than applied loads alone. The loading could be applied mechanically or could be induced by the applied field.

Other more obvious directions include: looking at specific classes of proteins; using higher current densities; and examining much shorter and/or much longer exposure periods. Finding a response to electric fields may provide clues regarding the appropriate dynamic mechanical parameters capable of eliciting a response. Alternatively, a consistent response to dynamic mechanical loading would provide guidelines for choosing relevant electrical test parameters.

(3) Physicochemical changes

To further examine the role of pH in the cellular response, experiments analagous to the kinetic experiments would be very useful. In particular, the sulfate incorporation kinetics under load may reflect the diffusion of hydrogen ion. If the kinetics of the response to a step increase in pH mimics the unloading behavior, it would be a strong indication that pH plays a major role in the response mechanism.

An important physicochemical modification would be to alter the composition of the extracellular matrix. It is believed that the cell acts to appropriately maintain the ECM. Therefore, response to compression should differ if the ECM differs. Enzymatic treatments provide a means of modifying the ECM. Those specific for the GAG constituents such as chondroitinase or hyaluronidase may lead to different behavior than treatment with a more general protease such as trypsin or pronase. Comparison of the response to load following these various physicochemical modifications should provide more insight regarding the mechanism of ECM control.

(4) Applied hydrostatic pressure

The response of this EPC preparation to hydrostatic pressures has not been examined. In vivo loading conditions include both static and dynamic components which may influence cell behavior in different ways. Under dynamic loading conditions, each of the suggested signals will be present. The kinetics of the response to loading has provided some clues as to what the response to dynamic loads may be. However, if there is a significant response to hydrostatic pressure, that response may dominate the cellular response to dynamic loading. This may be particularly true for higher frequency components where all cells will experience the change in hydrostatic pressure compared to the few which experience deformation.

Appendix A

MEDIA AND BIOCHEMICAL FORMULATIONS

Explant Medium:

Dulbecco's Modified Eagle Medium (Gibco, Grand Island NY)
0.1% NuSerum (Collaborative Research, Waltham, MA)
1000 U/ml Penicillin (Gibco, Grand Island NY)
1000 µg/ml Streptomycin (Gibco, Grand Island NY)

Maintenance Medium:

Dulbecco's Modified Eagle Medium
0.1% NuSerum

Labeling Medium :

Dulbecco's Modified Eagle Medium
0.1% NuSerum
^{35}S-sulfate (NEX041, New England Nuclear, Boston MA)
^{3}H-proline (NET573, New England Nuclear, Boston MA)
0.5 mM proline (Sigma, St. Louis MO)

Radiolabel concentrations:
1/4 inch diameter disks - 5 µCi/ml ^{3}H-proline
10 µCi/ml ^{35}S-sulfate
2 mm diameter disks - 10 µCi/ml ^{3}H-proline
20 µCi/ml ^{35}S-sulfate

Papain solution:

125 µg/ml papain (Sigma, St. Louis MO)
5 mM EDTA
5 mM Cysteine hydrochloride
0.1 M Phosphate buffer, pH 5.7

20 µl/mg tissue dry weight
incubate at 60 °C for 24 to 48 hours
[Handley and Lowther, 1977]

REFERENCES

Alberts B, Bray D, Lewis J, Raff M, Roberts K, Watson JD, Eds.: The Molecular Biology of the Cell, Garland, NY, 1983.

Arkin AM, Katz JF: The Effects of Pressure on Epiphyseal Growth. J. Bone Joint Surg. 38-A:1056-1076 1956.

Armstrong CG, Lai WM, Mow VC: An analysis of the unconfined compression of articular cartilage. J. Biomech. Eng. 106:165-173 1984.

Brighton CT, Sugioka Y, Hunt RM: Quantitative Zonal Analysis of Cytoplasmic Structures of Growth-Plate Chondrocytes in Vivo and in Vitro. J. Bone Joint Surg. 64-A:1336 1982.

Broom ND, Myers DB: A Study of the Structural Response of Wet Hyaline Cartilage to Various Loading Situations. Connective Tiss. Res. 7:227-237 1980.

Brummer SB, Turner MJ: Electrochemical considerations for safe electrical stimulation of the nervous system with platinum electrodes. IEEE Trans. Biomed. Enf. 24:59-63 1977.

Cappelletti R, Del Rosso M, Chiarugi VP: Anal. Bioch. 99:311 1979.

Cappozzo A: Compressive Loads in the Lumbar Vertebral Column During Normal Level Walking. J. Orthop. Res. 1:292-301 1984.

Casley-Smith JR: The fine structure of tissues and tissue channels, in Tissue Fluid Pressure and Composition , AR Hargens ed., Williams and Wilkins, Baltimore:99-112 1978.

Comper WD, Laurent TC: Physioligical function of connective tissue polysaccharides. Physiol. Reviews 58:255 1978.

Copray JCVM, Jansen HWB, Duterloo HS: Effects of Compressive Forces on Proliferation and Matrix Synthesis in Mandibular Condylar Cartilage of the Rat in-Vitro. Archs oral Biol. 30:299-304 1985.

Copray JCVM, Jansen HWB, Duterloo HS: An In-Vitro System for Studying the Effect of Variable Compressive Forces on the Mandibular Condylar Cartilage of the Rat. Archs oral Biol. 30:305-311 1985.

Corey DP, Dubinsky JM, Schwartz EA: The calcium current in inner segments of rods from the salamander (Ambystoma tigrinum) retina. J. Physiol. 354:557-575 1984.

DeWitt MT, Handley CJ, Oakes BW, Lowther DA: In Vitro Response of Chondrocytes to Mechanical Loading. The Effect of Short Term Mechanical Tension. Connective Tissue Res. 12:97-109 1984.

Degroot SR, Mazur P: Nonequilibrium Thremodynamics, North Holland, Amstrdam, 1969.

Diem K. and Lentner C., Eds.: Scientific Tables, Ciba-Geigly Ltd, Switzerland, 1970

Dowben RW: General Physiology, Harper & Row, NY :242 1969.

Eisenberg SR, Nonequilibrium Electromechanical Interactions in Cartilage: Swelling and Electrokinetics, Ph.D. thesis, Department of Electrical Engineering and Computer Science, Massachusetts Institute of Technology, Cambridge, 1983.

Frank EH, Grodzinsky AJ: Cartilage electromechanics II: A continuum model of cartilage electrokinetics and correlation with experiments. submitted to J. Biomech. : 1986.

Frank EH, Grodzinsky AJ: Cartilage electromechanics I: Electrokinetic transduction and the effects of electrolyte pH and ionic strength. submitted to J. Biomech. : 1986.

Freeman MAR and Kempson GE: Load Carriage, in Adult Articular Cartilage, MAR Freeman, Ed., Grune & Stratton, Inc., New York, 228-246, 1972.

Frost HM: A Chondral Modeling Theory. Calcif. Tissue Int. 28:181-200 1979.

Gillard GC, Merrilees MJ, Bell-Booth PG, Reilly HC, Flint MH: The Proteoglycan Content and the Axial Periodicity of Collagen in Tendon. Biochem. J. 163:145-151 1977.

Gillard GC, Reilly HC, Bell-Booth PG, Flint MH: The Influence of Mechanical Forces on the Glycosaminoglycan Content of the Rabbit Flexor Digitorum Profundus Tendon. Connective Tiss. Res. 7:37-46 1979.

Goodman R, Bassett CAL, Henderson AS: Pulsing electromagnetic fields induce cellular transcription. Science 220:1283-1285 1983.

Granger HJ: Physicochemical properties of the extracellular matrix. in Tissue Fluid Pressure and Composition, AR Hargens, ed., Williams & Wilkins :43-62 1978.

Grimshaw PE, Compression, Stress Relaxation and Streaming Potential Relaxation of Cartilage, S.M. thesis, Department of Electrical Engineering and Computer Science, Massachusetts Institute of Technology, Cambridge, 1980.

Grodzinsky AJ: Electromechanical and Physicochemical Properties of Connective Tissue. CRC Critical Reviews in Biomedical Engineering 9:133-199 1983.

Gross J: An essay on biological degradation of collagen. in Cell Biology of Extracellular Matrix ED Hay, ed. Plenum Press:217-258 1981.

Hall-Craggs ECB, Lawrence CA: The effect of epiphysial stapling on growth in length of the rabbit's tibia and femur. J. Bone Joint Surg. 51:359-365 1969.

Handley CJ, Lowther DA: Extracellular matrix metabolism by chondrocytes III. Modulation of proteoglycan synthesis by extracellular levels of proteoglycan in cartilage cells in culture. Biochim. Biophys. Acta

500:132-139 1977.

Hardingham TE, Fitton-Jackson S, Muir H: Replacement of Proteoglycans in Embryonic Chick Cartilage in Organ Culture after Treatment with Testicular Hyaluronidase. Biochem. J. 129:101-112 1972.

Hascall VC, Handley CJ, McQuillan DJ, Hascall GK, Robinson HC, Lowther DA: The Effect of Serum on Biosynthesis of Proteoglycans by Bovine Articular Cartilage in Culture. Arch. Biochem. Biophys. 224:206-223 1983.

Hay ED, Ed.: Cell Biology of Extracellular Matrix, Plenum Press, New York, 1981a.

Hay ED: Collagen and embryonic development, in Extracellular Matrix ED Hay, ed.. Plenum Press, NY :379-410 1981b.

Heinegard D, Paulsson M: Structure and Metabolism of Proteoglycans. in Extracellular Matrix Biochemistry, KA Piez and AH Reddi, Ed.,Elsiver,NY :277-328 1984.

Heuter C: Anatomische studien an den extremitatengelenken neugeborener und erwachsener. Virchows Arch. 25:572-599 1862.

Hille B: Ionic Channels of Excitable Membranes, Sinauer Associates, Sunderland, MA, 10-14, 1984.

Hoch DH, Grodzinsky AJ, Koob TJ, Albert ML, Eyre DR: Early Changes in Material Properties of Rabbit Articular Cartilage After Meniscectomy. J. Orthop. Res. 1:4-12 1983.

Hodge WA, Fijan RS, Carlson KL, Burgess RG, Harris WH, Mann RW: Contact pressures in the human hip joint measured in vivo. Proc. Natl. Acad. Sci. USA 83:2879-2883 1986.

Holton T, Hudspeth AJ: A micromechanical contribution to cochlear tuning and tonotopic organization. Science 222:508-510 1983.

Hook M, Kjellen L, Johansson S, Robinson J: Cell-surface glycosaminoglycans. Ann. Rev. Biochem. 33:847-869 1984.

Huang D: Effect of extracellular chondroitin sulfate on cultured chondrocytes. J. Cell Biol. 62:881-886 1974.

Huang D: Extracellular Matrix-Cell Interactions and Chondrogenesis. Clin. Orthop. Rel. Res. 123:169-176 1977.

Ito K, Kimata K, Sobue M, Suzuki S: Altered Proteoblycan Synthesis by Epiphyseal Cartilages in Culture at Low SO_4^{2-} Concentration. J. Biol. Chem. 257:917-923 1982.

Jones IL, Klamfeldt A, Sandstrom T: The Effect of Continuous Mechanical Pressure Upon the Turnover of Articular Cartilage Proteoglycans In Vitro. Clin. Orthop. Rel. Res. 165:283 1982.

Kalmijn Ad. J: Electric and magnetic field detection in elasmobranch fishes. Science 218:916-918 1982.

Kempson GE, Muir H, Swanson SAV, Freeman MAR: Correlations between stiffness and the chemical constituents of cartilage on the human femoral head. Biochim. Biophys. Acta 215:70-77 1970.

Ketchum LD: Hypertrophic scars and keloids, in Plastic Surgery, WC Grabb and JW Smith, eds.. Little, Brown and Co., Boston :552-558 1979.

Kimura JH, Schipplein OD, Keuttner KE, Andriacchi TP: Effects of hydrostatic loading on extracellular matrix formation. Trans. ORS, Las Vegas, Nevada 10:365 1985.

Kimura JH, Thonar EJ-MA, Hascall VC, Reiner LA, Poole AR: Identification of core protein, and intermediate in proteoglycan biosynthesis in cultured chondrocytes from the Swarm rat chondrosarcoma. J. Biol. Chem. 256:7890-7897 1981.

Koob TJ, Gutierrez MJ, Vogel KG: Site-related variations in proteoglycan composition of the bovine flexor tendon. Trans. ORS, New Orleans, Louisiana 11:212 1986.

Kregenow FM: The response of duck erythrocytes to hypertonic media. Further evidence for a volume controlling mechanism. J. Gen. Physiol. 58:396-412 1971.

Lai WM, Mow VC: Drag-induced compression of articular cartilage during a prmeation experiment. Biorheology 17:111-123 1980.

Lane JM, Brighton CT: In Vitro Rabbit Articular Cartilage Organ Model I. Morphology and Glycosaminoglycan Metabolism. Arthritis Rheum. 17:235 1974.

Lee RC, Cartilage Electromechanics: The Relationship of Physicochemical to Mechanical Properties, Ph.D. thesis, Department of Electrical Engineering and Computer Science, Massachusetts Institute of Technology, Cambridge, 1979.

Lee RC, Frank EH, Grodzinsky AJ, Roylance DK: Oscillatory compressional behavior of articular cartilage and its associated electromechanical properties. J. Biomech. Eng. 103:280-292 1981.

Lee RC, Rich JB, Kelley KM, Weiman DS, Mathews MB: A Comparison of In Vitro Cellular Responses to Mechanical and Electrical Stimulation. American Surgeon 48:567-574 1982.

Leung DYM, Glagov S, Mathews MB: A New in Vitro System for Studying Cell Response to Mechanical Stimulation. Different Effects of Cyclic Stretching and Agitation of Smooth Muscle Cell biosynthesis. Exp. Cell Res. 109:285-298 1977.

Lippiello L, Kaye C, Neumate T, Mankin HJ: In Vitro Metabolic Response of Articular Cartilage Segments to Low Levels of Hydrostatic Pressure. Connective Tiss. Res. 13:99-107 1985.

Liu PY, The Effect of Electrical Stimulation at Different Frequencies on Glycosaminoglycan Biosynthesis in Cartilage, S.B. thesis, Department of Electrical Engineering and Computer Science, Massachusetts Institute of Technology, Cambridge, 1985.

MacDonald AG: The effects of pressure on the molecular structure and physiological functions of cell membranes. Phil. Trans. R. Soc. Lond. B 304:47-68 1984.

MacGinitie LA, preliminary results; PhD. thesis, Department of Electrical Engineering and Computer Science, Massachusetts Institute of Technology, Cambridge, 1986.

Mackie JS, Meares P: The diffusion of electrolytes in a cation-exchange resin membrane. I. Theoretical. Proc. Royal Soc. A 232:498 1955.

Macknight ADC, Leaf A: Regulation of Cellular Volume, in Membrane Physiology, Andreoli TE, Hoffman JF, Fanestil DD, eds. :Plenum,p315-334 1980.

Mansour JM, Mow VC: The permeability of articular cartilage under compressive strain and at high pressures. J. Bone Jt. Surg. 58-A:509-516 1976.

Maroudas A: Distribution and diffusion of solutes in articular cartilage. Biophys. J. 10:365-379 1970.

Maroudas A: Physico-chemical Properties of Articular Cartilage, in Adult Articular Cartilage, MAR Freeman, Ed., Grune & Stratton, Inc., New York, 131-170, 1972.

Maroudas A: Physico-chemical Properties of Articular Cartilage, in Adult Articular Cartilage, 2nd ed., MAR Freeman, Ed., Pitman Medical, London, 279, 1979.

Maroudas A, Evans H: A study of ionic equilibria in cartilage. Connective Tissue Res. 1:69-77 1972.

Maroudas A, Evans H: Sulphate Diffusion and Incorporation into Human Articular Cartilage. Biochem. Biophys. Acta 338:265-279 1974.

McLeod KJ, Modulation of Biosynthesis by Physiologically Relevant Electric Fields, Ph.D. thesis, Department of Electrical Engineering and Computer Science, Massachusetts Institute of Technology, Cambridge, 1986.

McKenzie LS, Horsburgh BA, Ghosh P, Taylor TK: Organ Culture of Human Articular Cartilage: Studies on Sulphated Glycosaminoglycan Synthesis. In Vitro 13:423-428 1977.

Miller EJ: Chemistry of the collagens and their distribution. in Extracellular Matrix Biochemistry, KA Piez and AH Reddi, Ed.,Elsiver,NY :41-82 1984.

Moran JM, Hemann JH, Greenwald AS: Finger Joint Contact Areas and Pressures. J. Orthop. Res. 3:49-55 1985.

Morey-Holton ER, Arnaud SB: Spaceflight and calcium metabolism. Physiologist 28:S9-S12 1985.

Mow VC, Kuei SC, Lai WM, Armstrong CG: Biphasic creep and stress relaxation of articular cartilage in compression: theory and experiments. J. Biomech. Eng. 102:73-84 1980.

Mow VC, Lai WM: Mechanics of animal joints. Ann. Rev. Fluid Mech. 11:247-288 1979.

Mow VC, Lai WM: Mechanics of Animal Joints. Annual Review of Fluid Mechanics, Vol. II :247-288 1979.

Myers ER, Lai WM, Mow VC: A continuum theory and an experiment for the ion-induced swelling behavior of articular cartilage. J. Biomech. Eng. 106:151-158 1984.

Norton LA, Rodan GA, Bourret LA: Epiphyseal Cartilage cAMP Changes Produced by Electrical and Mechanical Perturbations. Clin. Orthop. Rel. Res. 124:59 1977.

Ogston AG, Preston BN, Wells JD: On the transport of compact particles through solutions of chain-polymers. Proc. R. Soc. Lond. A. 333:297-316 1973.

Okuda Y, Gorski JP, Amadio PC: Biochemical and histochemical analysis of anatomical regions of canine flexor tendon. Trans. ORS, New Orleans, L Louisiana 11:213 1986.

Palmoski MJ, Brandt KD: Effects of Static and Cyclic Compressive Loading on Articular Cartilage Plugs in Vitro. Arthritis Rheumatism 27:675-681 1984.

Peruchon E, Bonnel F, Baldet P, Rabischong P: Evaluation and control of growth activity of epiphyseal plate. Med. & Biol. Eng. & Comput. 18:396-400 1980.

Phillips SL, The Determination of Charge Density in Articular Cartilage via Chemical Titration, S.M. thesis, Department of Electrical Engineering and Computer Science, Massachusetts Institute of Technology, Cambridge, 1984.

Poole CA, Flint MH, Beaumont BW: Morphological and functional interrelationships of articular cartilage matrices. J. Anat. 138:113-138 1984.

Porter RW: The Effect of Tension Across A Growing Epiphysis. J. Bone Joint Surg. 60-B:252 1978.

Porter KR, Byers HR, Ellisman MH: The Cytoskeleton. Neurosciences Fourth Study Program 703 1979.

Rodan GA, Mensi T, Harvey A: A Quantitative Method for the Application of Compressive Forces to Bone in Tissue Culture. Calcif. Tiss. Res. 18:125-131 1975.

Rodan GA, Bourret LA, Norton LA: DNA Synthesis in Cartilage Cells Is Stimulated by Oscillating Electric Fields. Science 199:690-692 1978.

Rubin CT, Lanyon LE: Regulation of Bone Formation by Applied Dynamic Loads. J. Bone Joint Surg. 66-A:397-402 1984.

Rubin CT, Lanyon LE: Limb Mechanics as a Function of Speed and Gait: A Study of Functional Strains in the Radius and Tibia of Horse and Dog. J. exp. Biol. 101:187-211 1982.

Rubin CT, Lanyon LE: Regulation of bone mass by mechanical strain magnitude. Calcif. Tissue Int. 37:411-417 1985.

Rubin CT: Skeletal Strain and the Functional Significance of Bone Architecture. Calcif Tissue Int 36:S11-S18 1984.

Sah RA, Personal communication, summer 1985.

Sah RA, Ph.D. Thesis, Division of Health Sciences and Technology, Massachusetts Institute of Technology, Cambridge, in preparation, 1986.

Sandy JD, Brown HLG, Lowther DA: Control of Proteoglycan Synthesis. Studies on the Activation of Synthesis Observed During Culture of Articular Cartilage. Biochem. J. 188:119-130 1980.

Schneiderman R, Keret D, Maroudas A: Rate of glycosaminoglycan synthesis as a function of matrix hydration in adult human articular cartilage. Trans. ORS, New Orleans, LA 11:210 1986.

Schwartz ER, Kirkpatrick PR, Thompson RC: The effect of environmental pH on glycosaminoglycan metabolism by normal human chondrocytes. J. Lab. Clin. Med. 87:198-205 1976.

Shepherd GM: Neurobiology, Oxford University Press, New York, 235-239,1983.

Smith RA, Dodson BA, Miller KW: The interactions between pressure and anaesthetics. Phil. Trans. R. Soc. Lond. B 304:69-84 1984.

Smith EL, Smith PE, Ensign CJ, Shea MM: Bone involution decrease in exercising middle-aged women. Calcif. Tissue Int. 36:S129-S138 1984.

Sobue M, Takeuchi J, Ito K, Kimata K, Suzuki S: . J. Biol. Chem. 253:6190-6196 1978.

Sokoloff L: Elasticity of articular cartilage: effects of ions and viscous solutions. Science 141:1055 1963.

Sonnerup L: Stress and strain in the intervertebral disk in relation to spinal disorders. in Osteoarthromechanics DN Ghista, ed., McGraw-Hill, New York :315-352 1982.

Stambaugh JE, Brighton CT: Diffusion in the Various Zones of the Normal and the Rachitic Growth Plate. J. Bone Jt. Surg. 62-A:740-748 1980.

Stockwell RA and Meachim G: The Chondrocytes, in Adult Articular Cartilage, MAR Freeman, Ed., Grune & Stratton, Inc., New York, 51-99, 1972.

Tilney LG: Actin, motility, and membranes. in Membrane Transduction Mechanisms RA Cone and JE Dowling, eds., Raven Press, New York :163-188 1979.

Tulloh NM, Romberg B: An effect of gravity on bone development in lambs. Nature 200:438-439 1963.

van Kampen GPJ, Veldhuijzen JP, Kuijer R, van de Stadt RJ, Schipper CA: Cartilage Response to Mechanical Force in High-Density Chondrocyte Cultures. Arthritis Rheumatism 28:419-423 1985.

Vander AJ, Sherman JH, Luciano DS: Human Physiology - The Mechanisms of Body Function, McGraw-Hill, New York, 539-540, 1975.

Venn MF: Chemical composition of human femoral head cartilage: influence of topographical position and fibrillation. Ann. Rheum. Dis. 38:57-62 1979.

Volkmann R: Chirurgische erfahrungen uber knochenverbiegungen und knochenwachsthum. Arch. f. Pathol. Anat. 24:512-540 1862.

Waddell WJ, Bates RG: Intracellular pH. Physiological Reviews 49:285-329 1969.

Wang CW, The Effect of Low Frequency Currents on Glycosaminoglycan and Protein Synthesis in Epiphyseal Cartilage Matrices, S.B. thesis, Department of Electrical Engineering and Computer Science, Massachusetts Institute of Technology, Cambridge, 1986.

Wilsman NJ, Farnum CE, Reed-Aksamit DK: Incidence and morphology of equine and murine chondrocytic cilia. Anatomical Record 197:355-361 1980.

Wilsman NJ, Farnum CE: Three dimensional orientation of chondrocytic cilia in adult articular cartilage. Trans. ORS, New Orleans 11:448 Feb,1986.

Winter PM, Miller JN: Anesthesiology. Sci. Am. 252:124-131 1985.

Woo SLY, Kuei SC, AMiel D, Gomez MA, Hayes WC, White FC, Akeson WH: The effect of prolonged physical training on the properties of long bone: A study of Wolff's Law. J. Bone Joint Surg. 63A:780-787 1981.

Yamada KM: Cell surface interactions with extracellular materials. Ann. Rev. Biochem. 52:761-99 1983.

Yeh C-K, Rodan GA: Tensile forces enhance prostaglandin E synthesis in osteoblastic cells grown on collagen ribbons. Calcif. Tissue Int. 36:S67-S71 1984.